The Role of pH, Self-Association, and Lipid Binding in Vinculin Tail Structure and Function

Sean M. Palmer

A dissertation submitted to the faculty of the University of North Carolina at Chapel Hill in partial fulfillment of the for the degree of Doctor of Philosophy in the Department of Biochemistry and Biophysics

Chapel Hill
2008

Approved by:
Dr. Sharon L. Campbell, Advisor
Dr. Nikolay Dokholyan
Dr. Brian Kuhlman
Dr. Andrew Lee
Dr. Michael Schaller

Abstract

The Role of pH, Self-Association, and Lipid Binding in Vinculin Tail Structure and Function

(Under the direction of Dr. Sharon L. Campbell)

Vinculin is a highly conserved cytoskeletal protein that localized to sites of cell adhesion and is involved in linking the actin cytoskeleton to the cell membrane. Loss of normal vinculin function has been associated with cancer phenotypes, cardiovascular disease, and lethal errors in embryogenesis. Vinculin is composed of a 90 kDa head domain (Vh) and a 21 kDa tail domain (Vt) connected by a flexible "neck" region. Vh and Vt form auto-inhibitory interactions in its inactive state. Conformational changes in these domains have been proposed to be important for vinculin activation, freeing domains to bind to a variety of ligands involved in cell adhesion processes.

My work has focused on the vinculin tail domain. I have assigned the majority of the backbone $^{1}H_{N}$, ^{15}N, $^{13}C_{\alpha}$, ^{13}CO, and side chain $^{13}C_{\beta}$ NMR resonances of Vt (Biological Magnetic Resonance Data Bank, accession number 15653). These assignments have proven useful for investigating the effects of ligand binding, pH and Vt self-association.

The tail domain of vinculin has been reported to undergo a pH dependent conformational change between pH 5.5 and 7.5. However, we found no indication of a significant alteration in Vt conformation in this pH range by both circular dichroism and NMR. Although, Vt was reported to self-associate at pH 5.5 while remaining monomeric at

pH 7.0, results from analytical ultracentrifugation indicate that Vt self-associates at both pH values, albeit with weak affinity (K_d > 100 μM).

The binding of acidic phospholipids by Vt has been proposed to play a role in vinculin activation and focal adhesion turnover. We observe a marked affinity of Vt for phosphatidylinositol 4,5-bisphosphate (PIP_2), but no significant binding to phosphatidylethanolamine (PE), phosphatidylcholine (PC), phosphatidylserine (PS), or phosphatidylinositol (PI) in the context of mixed lipid vesicles. A significant increase in PIP_2 binding was observed with multiple mutant forms of Vt, expected to alter the conformation or flexibility of the N-terminal strap of Vt, suggesting that a rearrangement of this N-terminal strap may be required for PIP_2 binding. Additionally, we find that the hydrophobic hairpin at the C-terminus of Vt is not critical for lipid insertion, as previously proposed.

This work is dedicated to my loving and supportive wife, Heather, and to my family and friends. Their love, support, and encouragement were more valuable to me than they may understand, and made this achievement possible.

Acknowledgments

This work would not have been possible without the help and support of a number of individuals. I would first like to express my sincere appreciation to Dr. Sharon Campbell for to opportunity to carry out this research. Her expertise, insight, and guidance were critical in this endeavor, and I have been honored to have her as a mentor. I would also like to thank the members of my dissertation committee, Dr. Nikolay Dokholyan, Dr. Brian Kuhlman, Dr. Andrew Lee, and Dr. Michael Schaller, for their support, encouragement, and suggestions. I would also like to acknowledge the help and support of the current and former members of the Campbell Laboratory, colleagues in the Department of Biochemistry and Biophysics, and members of the UNC community.

Table of Contents

Page

List of Figures……...……xi

List of Abbreviations and Symbols…….xii

Chapter:

I. Introduction……1

A. Vinculin……....1

B. The Role of Vinculin in Development, Cell Motility, Cell Survival, and Cancer……...……...……..2

C. The Role of Vinculin in Cardiovascular Function…….……..2

D. Vinculin Domains and Their Ligands……..4

E. Vinculin Structure and Auto-inhibition……..…….4

F. Vinculin Activation……..5

G. The Tail Domain of Vinculin and its Ligands…….6

1. Vinculin Tail Structure……...……6

2. Actin Interactions……...…….8

3. Lipid Interactions…….…….10

4. Paxillin Interactions……..12

5. Vinculin Tail Phosphorylation……..……14

6. Vinculin Tail Self-Association……..…15

H. Literature Cited……..……19

II. Backbone ^{1}H, ^{13}C, and ^{15}N NMR Assignments of the Tail Domain of Vinculin…….…….…….24

A. Introduction……...…….24

B. Materials and Method……...…….25

1. Expression and Purification……...…25

2. Nuclear Magnetic Resonance Spectroscopy…….26

C. Assignments and Deposition…….…….26

D. Literature Cited……..……29

III. The Role of pH and Histidine 906…….……..30

A. Introduction…….…….……..30

B. Materials and Methods……..…….32

1. Protein Expression and Purification……..32

2. Nuclear Magnetic Resonance Assignments……..33

3. NMR Samples……..…….34

4. NMR Spectroscopy……..…….34

5. Circular Dichroism…….…….……..35

6. Analytical Ultracentrifugation……...…….……..35

C. Results……36

1. Mutation of Histidine 906 to Alanine does not significantly alter Vt structure……..36

2. The conformation of Vt is largely unaltered between pH 5.5 and 7.5……..38

3. Vinculin Tail Self-Association……...……..39

D. Discussion……..40

E. Literature Cited…….…….52

IV. Vinculin Tail and Lipid Binding……..55

A. Introduction……...…….55

B. Materials and Methods……...57

1. Protein expression and purification……..57

2. Lipid Co-sedimentation……..……..58

3. NMR Samples and Spectroscopy……..……59

4. Circular Dichroism……...…….60

C. Results……...…….60

1. The Vinculin Tail Domain Shows Specificity for PIP_2 Containing Vesicles……...…….60

2. Vt demonstrates loss of tertiary structure in lipid micelles and loses specificity for PIP_2…….……61

3. Vt C-terminal residues stabilize its tertiary fold……..…….63

4. The Role of the N-terminal Strap in PIP_2 binding……...…….65

D. Discussion……..67

E. Literature Cited……..77

V. Conclusions……...…….81

A. Introduction……..……..81

B. Backbone ^{1}H, ^{13}C, and ^{15}N NMR Assignments of the Tail Domain of Vinculin…….……83

1. Summary of Results……..83

2. Implications……..…….83

3. Current and Future Directions……..83

C. The Role of pH and Histidine 906 in Vinculin Tail Conformation……..…….85

1. Summary of Results……..……85

2. Implications…….……...……85

3. Current and Future Directions……..……87

D. Vinculin Tail and Lipid Binding……...…….89

1. Summary of Results……..……...…….89

2. Implications……..…….……...…….90

3. Current and Future Directions…….…….92

E. Literature Cited……..94

List of Figures

Page

Figure 1.1: The Structure of Full Length Vinculin……...……..17

Figure 1.2: Structural Features of Vinculin Tail……...…….18

Figure 2.1: Backbone NMR Assignments of Vinculin Tail…….…..28

Figure 3.1: Circular Dichroism of Wild-type Vt and Vt H906A……...……46

Figure 3.2: NMR HSQC Spectra of Vt H906A…….….47

Figure 3.3: NMR Chemical Shift Perturbations in Vt H906A……..……..…..…….48

Figure 3.4: Circular Dichroism of Wild-type Vt and Vt H906A at pH 5.5 and 7.5……...49

Figure 3.5: NMR Chemical Shift Perturbations Between pH 5.5 and 7.5……...…..50

Figure 3.6: Analytical Ultracentrifugation of Vinculin Tail…….…….51

Figure 4.1: Co-sedimentation of Vt with PIP_2 Containing Vesicles……..……70

Figure 4.2: Co-sedimentation of Vt with PI and PS Containing Vesicles…….…….71

Figure 4.3: Vt in the presence of DPC Micelles……...……..72

Figure 4.4: Circular Dichroism and HSQC Spectra of VtΔC……...……..73

Figure 4.5: NMR HSQC Spectra of VtΔC5 and VtΔC7……74

Figure 4.6: Interactions of the N-terminal Strap of Vt……...……75

Figure 4.7: Co-sedimentation of Mutant Forms of Vt with PIP_2 Containing Vesicles…..76

List of Abbreviations and Symbols

2D	Two Dimensional
3D	Three Dimensional
Arp 2/3	Actin-related protein complex
AUC	Analytical Ultracentrifuge
BME	β-mercaptoethanol
BMRB	Biological Magnetic Resonance Data Bank
CD	Circular Dichroism
cDNA	Complementary Deoxyribonucleic Acid
D_2O	Deuterium Oxide
DNA	Deoxyribonucleic Acid
DPC	Dodecylphosphocholine
DTT	Dithiothreitol
ε	Molar extinction coefficient
ECM	Extracellular Matrix
EDTA	Ethylenediaminetetraacetic Acid
ERK	Extracellular signal-regulated kinase
F-actin	Filamentous actin
FAK	Focal Adhesion Kinase
GdmCl	Guanidinium Chloride
HEPES	4-(2-hydroxyethyl)-1-piperazineethanesulfonic acid
HSQC	Heteronuclear Single Quantum Coherence

IpaA	A *Shigella flexneri* virulence factor
IPTG	isopropyl β-D-1-thiogalactopyranoside
K_d	Dissociation constant
kDa	kilodalton
LD	Paxillin-Leucine and Aspartate Rich Motif
LIM	Protein domain named due to their discovery in Lin11, Isl-1 and Mec-3
LPPC	1-palmitoyl-2-hydroxy-sn-glycero-3-[phospho-RAC-(1-glycerol)]
MHz	Megahertz
MVt	MetaVinculin Tail
NMR	Nuclear Magnetic Resonance
NOESY	Nuclear Overhauser Enhancement Spectroscopy
PC	Phosphatidylcholine
PDB ID	Protein Data Bank Identification Number
PE	Phosphatidylethanolamine
PI	Phosphatidylinositol
PIP_2	Phosphatidylinositol 4,5-bisphosphate
PKCa	Protein Kinase C α
PPI	Phosphoinositide
ppm	Part Per Million
PS	Phosphatidylserine
SDS	Sodium Dodecyl Sulfate
SDS-PAGE	Sodium Dodecyl Sulfate Polyacrylamide Gel Electrophoresis
SUV	Small Unilamellar Vesicles

Tris	Tris(hydroxymethyl)aminomethane
UV	Ultraviolet
VASP	Vasodilator-stimulated Phosphoprotein
VBS	Vinculin Binding Site
Vh	Vinculin Head
Vt	Vinculin Tail
VtΔC	A mutant form of vinculin tail, lacking the C-terminal 15 residues (1052-1066)
VtΔC5	A mutant form of vinculin tail, lacking the C-terminal 5 residues (1062-1066)
VtΔC7	A mutant form of vinculin tail, lacking the C-terminal 7 residues (1060-1066)
VtΔN	A mutant form of vinculin tail, lacking the N-terminal 5 residues (879-883)

Chapter I.

Introduction

A. Vinculin

Vinculin is a ubiquitously expressed, abundant, and highly conserved 116 kDa protein that localizes to membrane-associated complexes and couples the actin cytoskeleton to the membrane at sites of cellular attachment. These sites of attachment include adherence junctions and focal adhesions which link cells to neighboring cells and cells to extracellular matrix (ECM), respectively[1]. A larger isoform of vinculin, called metavinculin, is found exclusively in smooth and cardiac muscle[2]. Both vinculin and metavinculin are found in costameres, protein complexes that link the force generating sacromeres to the cell membrane, and in cardiac muscle both isoforms are also localized to intercalated discs, a specialized linkage between adjacent cells[2, 3]. In all of these locations vinculin plays a role in connecting the actin cytoskeleton to the membrane and therefore located at primary sites of contractile force transmission. In addition to the obvious importance for muscle contraction, transmission of contractile forces is also critical for cell motility and migration. Not too surprising, vinculin plays an important role in processes that require regulated cell movement, including development and wound healing, as well as pathological processes including invasion and metastasis[4, 5]. Dynamic regulation of cell adhesions and actin cytoskeletal morphology is also important for processes involved in cell growth, differentiation, and cell death. Aberrant function or regulation of these processes contributes

to a number of human diseases, including cancer. Loss of normal vinculin function, in particular, has been associated with cancer phenotypes, cardiovascular disease, and lethal errors in embryogenesis[5-9].

B. The Role of Vinculin in Development, Cell Motility, Cell Survival, and Cancer

Cell adhesions, whether they are between adjacent cells or with the extracellular matrix (ECM), play a critical role in development and survival. Ordered cellular motility requires adhesive structures to be dynamic and precisely controlled. In addition, these sites of adhesion are also involved in the sensing and transduction of a multitude of signals both from the extracellular and intracellular environment. Vinculin plays an important role in the regulation and function of both focal adhesion and adherence junctions and, consequently, affects many cellular processes that are mediated by cellular attachment. Vinculin null mice die in early embryogenesis, with mice embryos exhibiting brain and heart defects[5]. Vinculin null cells also exhibit tumor suppressor properties, including: decreased focal adhesion, increased motility, resistance to apoptosis and anoikis, ability to grow in soft agar, and altered signaling through extracellular signal-regulated kinase (ERK)[4, 5, 7, 10-12]. Additional support for vinculin's role in tumor suppression comes from studies showing decreased vinculin protein levels that are correlated with highly metastatic, invasive cancers. Moreover, transfection of vinculin cDNA into tumor cells lines with decreased vinculin expression drastically reduces their tumorigenic ability[13], further solidifying vinculin's role as a tumor suppressor.

C. The Role of Vinculin in Cardiovascular Function

Although vinculin is a widely expressed protein, it is particularly abundant in muscle cells where it localizes to costameres, which link sacromeres to the cell membrane[3]. In contrast, a larger isoform of vinculin, metavinculin, is exclusively expressed in smooth and cardiac muscle and contains a 68 amino acid insertion in the tail domain[2, 14, 15]. Both isoforms are found in intercalated discs of cardiac tissue[2]. Although no ligand specific to the metavinculin insert has been found, there is some evidence suggesting that metavinculin possesses distinct properties. In addition to the tissue specific expression, metavinculin tail (MVt) promotes distinct F-actin organization from the vinculin tail domain (Vt). Both Vt and MVt bind F-actin, however Vt bundles F-actin into parallel filaments, while MVt generates "highly viscous F-actin webs"[15].

Vinculin null mice and nematodes both die in development with cardiac and muscle defects, respectively[5, 16]. While it is possible that these developmental abnormalities are due solely to defects in cell migration, it is also possible that vinculin has a specific developmental role in these tissues. Regardless of its role in development, both vinculin and metavinculin have been implicated in cardiovascular function, as separate mutations in each have been associated with human cardiomyopathy. A leucine to methionine mutation at position 277 in vinculin is believed to confer susceptibility to hypertrophic cardiomyopathy, while an arginine to tryptophan substitution at position 975 in metavinculin is associated with both hypertrophic and dilated cardiomyopathy[17, 18]. The metavinculin mutation (R975W) has also been shown to alter F-actin organization *in vitro* as cardiac myocyte samples containing the mutation have irregular and fragmented intercalated discs (structures involved in transmitting contractile force between cardiac myocytes)[19]. Even in the absence of mutations, samples taken from patients with obstructive hypertrophic cardiomyopathy and

aortic stenosis, show a consistent defect in vinculin/metavinculin expression in intercalated discs suggesting an important and distinct role for vinculin/metavinculin in cardiac tissue[8].

D. Vinculin Domains and Their Ligands

Early studies using electron microscopy and proteolytic cleavage approaches indicated that vinculin consists of three domains; a globular head domain (Vh), a flexible neck, and a tail domain (Vt)[20, 21]. Each of these domains has been shown to bind multiple ligands. The head domain has been shown to interact with talin, α-actinin, α-catenin, β-catenin, and the bacterial virulence factor IpaA. The neck domain interacts with vinexin, ponsin, the Arp 2/3 complex, and the vasodilator-stimulated phosphoprotein (VASP). The tail domain binds to F-actin, paxillin, protein kinase C-α (PKCα), acidic phospholipids and α-synemin (reviewed by Ziegler, *et al*., 2006)[22, 23].

E. Vinculin Structure and Auto-inhibition

Multiple crystal structures of vinculin have been solved, including the full length protein, isolated domains, and isolated domains in complex with ligands[24-29]. The full length crystal structure was published in 2004, showing that vinculin consists of a "bundle of bundles"[24]. The structure is comprised of 8 helical bundles that are organized into tandem pairs. Each of the first three tandem pairs (D1-D3) contains two four-helix bundles with one long helix connecting them. The fourth tandem pair contains two helical bundles (D4 and Vt) connected by a flexible linker. The head domain of vinculin (Vh) consists of D1-D3 which forms a clamp-like structure, with the tail domain (Vt) held in its center (Figure 1.1). Vt consists of a five-helix bundle fold. The isolated domain shows similar structural features

to Vt in the context of full length vinculin[24, 25]. Multiple sites of interaction between Vh and Vt occur, giving rise to a compact, auto-inhibitory complex. While the majority of contacts are observed between D1 and Vt, additional interactions occur between Vt and D3 and D4. The numerous interactions between Vh and Vt, give rise to a high affinity intramolecular interaction, with an estimated K_d of ~1 nM [24]. Activation of vinculin requires release of auto-inhibitory Vh and Vt interactions to expose binding sites for interactions with α-actinin, VASP, talin, F-actin, PKCα, acidic phospholipids, and the Arp2/3 complex[10, 30-35].

F. Vinculin Activation

The tight auto-inhibitory interaction between the head and tail domains of vinculin is possible due to three distinct interaction surfaces between Vh and Vt (D1-Vt, D3-Vt, D4-Vt)[24, 36]. The apparent affinity is further increased due to the intramolecular nature of the interaction (once separated Vt does not diffuse away from Vh). Notably, binding cell adhesion protein, talin, to the vinculin head domain has been proposed to disrupt auto-inhibitory Vh-Vt interactions to activate vinculin. However, a detailed characterization study of talin/Vh interactions, indicated that although talin can efficiently displace Vt from the isolated D1 fragment of Vh[29], talin binding alone, disrupts only a subset of interactions between Vt and Vh, and thus cannot release auto-inhibitory interactions in the context of the full length protein[36]. To date, no single native ligand has been found with sufficient affinity to compete with the Vh-Vt interaction, suggesting a combination of multiple ligands are needed to activate vinculin[37]. A combinatorial activation mechanism is supported by the ability of talin to successfully interact with full length vinculin in the presence of

actin[37]. Given the number of ligands that bind to both the head and tail domains of vinculin, it is possible that additional ligand pairs may also be capable of activating vinculin or that subsequent binding of additional ligands after activation could help maintain vinculin in an activated state. Additional ligands interacting with the head, neck, or tail could conceivably play such roles. Interestingly the *Shigella flexneri* virulence factor, IpaA, appears to activate vinculin in the absence of other ligands[37]. Although IpaA contains two vinculin-binding sites (VBS), their binding to vinculin is mutually exclusive. Crystal structures of D1 of vinculin with either IpaA VBS have been solved and appear to mimic the binding of vinculin-binding sites from talin and α-actinin[28]. IpaA-VBS has been reported to have at least 10-fold higher affinity for Vh-D1 relative to other VBSs, which may account for its ability to activate vinculin[28]. However, it cannot be ruled out that an additional interaction between IpaA and vinculin could be involved in disrupting the Vt-D3 and Vt-D4 interactions.

G. The Tail Domain of Vinculin and its Ligands

1. Vinculin Tail Structure

The crystal structure of Vt (residues 879-1066) was published in 1999, showing a bundle of five amphipathic helices[25]. The conformation of the isolated tail domain, solved at pH 5.5, is virtually identical to that seen in the auto-inhibited full length structure of vinculin, solved at pH 6.5 in 2004[24]. In the full length structure of vinculin, Vt is held by the clamp-like Vh. In the isolated crystal structure, however, the asymmetric unit contains two Vt molecules, forming a dimer with a hydrophobic interaction interface covering end of helix 4 and the beginning of helix 5. Some of this same interface is involved in the

interaction between Vt and the D1 domain of Vh in the auto-inhibited structure[24]. In addition to the main helical bundle of Vt, there are two structural features of interest; an N-terminal strap and C-terminal extension (Figure 1.2).

Residues 879-893 form the N-terminal strap, and adopt an extended conformation. In the crystal structure of the isolated tail domain, this strap is seen in multiple conformations, suggesting some conformational mobility. In the more ordered conformation, this N-terminal strap packs against helix 1 and 2. In the second conformation, only weak electron density was seen prior to residue 890, and crystal contacts were seen at the position the strap occupied in the first conformation. Due to a more ordered electron density and the lack of crystal contacts, the conformation with the strap packing against helix 1 and 2 was assumed to be a better model of the structure in solution[25]. In support of this idea, in the full length vinculin structure the N-terminal strap of Vt is seen in a very similar conformation, packed along helix 1 and 2. Residues F885 and D882 of the strap form interactions with the helix bundle, and are likely important to maintaining the extended conformation along the helix 1-2 interface. In both the isolated tail structure and the full length vinculin structure, the side chain of F885 packs in a hydrophobic crevice between helix 1 and 2, making interaction with H906 of helix 1. Interactions made by D882 vary some between crystal structures, but they include interactions with S914 and K924, located in the helix 1-2 loop and helix 2 respectively, and K1061 and Y1065, located in the C-terminal extension[24, 25].

The C-terminal extension of Vt consists of residues 1047-1066 and is located at the bottom of the helical bundle. Residues in this C-terminal extension form the bottom of the hydrophobic core, packing against helix 1, the helix 1-2 loop, and helix 5. In particular, L1056 inserts into a hydrophobic cavity while W1058 packs against W912 of the helix 1-2

loop and these interactions are thought to be important for the structural stability of Vt[25, 38]. The final C-terminal residues form a "hydrophobic hairpin" (TPWYQ) that emerges close to the N-terminal strap. It has been postulated that this hydrophobic hairpin is important for insertion into the membrane.

The crystal structure of Vt also aided in identifying two solvent-accessible surface features that have been postulated to be important for lipid binding; the "basic collar" and "basic ladder" (Figure 1.2)[25]. The basic collar consists of residues from helix 1, helix 5, and the C-terminal extension, including R910, K911, R1039, K1049, R1060, and K1061. These residues surround the hydrophobic hairpin, at the bottom of the helical bundle. The basic ladder consists of residues located along the length of helix 3 and at the base of the helical bundle, including K944, R945, K952, K956, R963, K966, K970, R978, R1008, and R1049.

2. Actin Interactions

The binding of actin is considered one of the primary functional consequences of vinculin activation. Indeed, despite findings that vinculin can interact with additional actin-binding proteins (i.e., Arp2/3, Vasp, etc), interactions between the vinculin tail domain and actin, provide a major link between focal adhesions and the actin cytoskeleton [39]. In addition to F-actin binding, vinculin also promotes cross-linking of actin bundles[40]. F-actin binding has been reported to induce Vt dimerization with dimerization important for Vt-induced F-actin bundling[41]. Binding of F-actin by Vt is blocked by the auto-inhibitory Vh-Vt interaction and full length vinculin neither binds or crosslinks F-actin in the absence additional ligands[32, 37]. Two isolated recombinant fragments of Vt were shown to bind to

F-actin[42], however, in the context of the crystal structure of Vt neither of these fragments correspond to a canonical actin binding site. Changes in protease sensitivity and tryptophan fluorescence upon F-actin association have been reported, providing evidence of a possible conformational change in Vt upon actin binding[25], further complicating clear identification of the binding site or sites.

Three-dimensional models of Vt, both bound to and crosslinking F-actin, were created using a combination of electron microscopy, image analysis and computational docking[43]. Crystal structures of Vt, alone and in the context of full length vinculin, were docked into 3D difference maps produced from images of F-actin decorated with Vt. However, in contrast to earlier observations[25], the docked protein models did not support a large scale conformational change in Vt upon binding F-actin, as a high correlation of the docked structure with the corresponding reconstructions was obtained with no major clashes observed between the docked proteins [43]. This model supports Vt binding to two separate actin monomers along the actin filament via two distinct sites. The upper interaction interface includes residues at the top of helices 2 and 3, along with residues contained in the N-terminal strap (883-890). The corresponding interface on actin is located at the bottom of subdomain 1, and contains a large hydrophobic pocket implicated in interactions with several actin binding proteins[43]. The lower F-actin/Vt interaction interface is more polar, is located at the base of helix 3, and includes residues close to the C-terminus. This Vt interface interacts with an acidic region at the top of subdomain 1 of a second actin monomer. Superimposition of the full length structure of vinculin with the tail domain in the actin bound model exhibits severe clashes between Vh and actin, consistent with the evidence that the Vh-Vt interaction must be released to facilitate actin binding[32, 43]. A

three-dimensional model of actin bundling by Vt was produced by computationally docking the F-actin-Vt model into tomographic reconstructions of Vt-crosslinked actin arrays. This model shows an asymmetric dimer with the C-terminal residues of one monomer (located at the bottom of the helical bundle) contacting the N-terminal strap along the side of the second monomer. However, as severe steric clashes are observed between the C-terminus of one monomer and the N-terminus of the other, it was speculated that either one or both of these regions of Vt may undergo a conformational change to promote F-actin bundling[43]. The overall 5-helix bundle of Vt is believed to remain largely unaltered by either F-actin binding or bundling. Currently, no specific point mutations in Vt have been identified that effectively block its F-actin binding and/or bundling activity. The production and characterization of such mutants would be beneficial in elucidating the activation, role, and function of vinculin *in vivo*.

3. Lipid Interactions

The tail domain of vinculin has been shown by multiple groups to bind acidic phospholipids[25, 31, 44, 45]. Among the various types of acidic phospholipids, Vt has been shown to have an increased affinity for phosphatidylinositol 4,5-bisphosphate (PIP_2), although the affinity and degree of specificity has varied in the literature (possibly due to varying methods used to assay binding)[24, 25, 31, 46, 47]. PIP_2 has been shown to be a key regulator of actin dynamics, adhesion-site turnover, and cell morphology[48, 49], and therefore is of particular interest as its interaction with Vt could explain some of vinculin's effects on cell motility and morphology. The interaction between Vt and lipids alters vinculin interaction with actin, talin, and PKCα. Moreover, in earlier studies, lipid binding

to vinculin was proposed to release interactions between Vh and Vt, thereby leading to vinculin activation[24, 31, 35, 46, 50]. However, subsequent work indicated that phospholipid binding to full length vinculin is significantly reduced relative to Vt, and that this interaction is unable release Vh-Vt interaction. Thus, phospholipid binding to vinculin, alone, does not lead to vinculin activation[31, 44]. Instead of a role of phospholipids in vinculin activation and localization to sites of adhesion, multiple reports have now suggested that vinculin-lipid interactions are important in regulating focal adhesion disassembly and turnover, a process critical to cell motility[38, 44].

Although the lipid binding to vinculin resides in the tail domain, multiple disparate sites have been proposed. Deletion mutagenesis, using a Vt fragment containing residues 916-970, suggested a binding site localized to helix 3 and 4[31]. However, as this fragment, comprised of helix 3 and 4, is markedly amphipathic and undergoes self-association, the isolated fragment may possess different (perhaps non-specific) phospholipid interactions. Once a structure of Vt became available, additional sites of possible lipid interaction were proposed. The C-terminus was postulated to be important for insertion into the lipid membrane, based on results obtained from a deletion mutant (VtΔC) lacking residues 1052-1066 that showed a significant decrease in lipid binding. Additionally, a “basic collar” and “basic ladder” were noted as possible sites of electrostatic interaction with the phospholipid headgroup[25]. The “basic collar” surrounds the C-terminal extension and includes residues from the bottom of helices 1 and 5 and within the C-terminus. The “basic ladder” contains a stretch of exposed basic residues covering the length of helix 3. A model for phospholipid binding to Vt was proposed by Liddington and co-workers, in which following insertion of the C-terminus, the helical bundle “unfurls” exposing helical hairpins which could interact

with the lipid membrane and possibly additional ligands[25]. Further research, however, indicated that deletion of 15 C-terminal residues in Vt, significantly destabilizes the Vt tertiary fold due to removal of a hydrophobic interactions between the C-terminus and the base of the helical bundle. Hence, the reduction in lipid binding to VtΔC is likely to result from large scale conformational/dynamic change in Vt[38]. Two remaining basic collar residues, K911 and K924 were also proposed as key determinants of PIP_2 binding [24, 38]. A separate study produced a "lipid binding deficient" variant of vinculin by introducing a series of mutations into the basic collar and basic ladder; mutation of 4 basic residues (K952, K956, R963, and K966) in the basic ladder and 2 residues (R1060 K1016) within the basic collar and contained in the C-terminal extension. Mutation of either group of residues alone led to only a partial loss in lipid binding[44]. However, the effects of these multiple mutations on ligand binding were not fully characterization. Moreover, no studies were conducted to determine whether mutations of 6 residues within Vt alters Vt structure. Given the 3D disposition of the basic ladder and collar, it is unlikely that vinculin binds both sites, unless more than one site of interaction occurs upon interaction with phospholipids. Hence, with multiple mutations in disparate surfaces of the protein, the complete picture of lipid binding remains unclear. It is also still unknown whether these mutations have effected the conformation of Vt causing confusion in data interpretation, as appears to have happened with VtΔC.

4. Paxillin Interactions

Paxillin is a 68 kDa cytoskeletal protein that is associated with focal adhesions and exhibits increased tyrosine phosphorylation following cell adhesion or transformation by the

Rous sarcoma virus[51, 52]. Paxillin was identified as a vinculin binding protein that associates with a C-terminal cleavage fragment of vinculin containing the tail domain[51]. The domain structure of paxillin consists of 5 leucine-rich 'LD' motifs and 4 double zinc finger LIM domains. Paxillin is believed to function as a molecular scaffold, with both the LD and LIM domains participating in protein-protein interactions [53, 54]. Three of the LD motifs, LD1, LD2, and LD4, were shown to bind to the tail domain of vinculin[55]. Deletion mutagenesis studies suggested that paxillin binds to a Vt fragment comprising residues 979-1000[56]. Paxillin binding was assessed by an 'overlay' assay, by first using denaturing SDS-gel electrophoresis of Vt or Vt fragments, followed by blotting on nitrocellulose filters prior to paxillin binding[25, 56]. It should be noted that this fragment contains the majority of helix 4 of Vt, which is markedly amphipathic. Thus, the conformation of this fragment in overlay binding assays could be significantly different from Vt in solution.

The physiological role of the vinculin-paxillin interaction is currently unclear. Intriguingly, both vinculin and focal adhesion kinase (FAK) bind to the LD2 and LD4 domains of paxillin, suggesting that both of these cell adhesion proteins may compete for paxillin binding. This idea is further supported by findings that alterations in vinculin expression can modulate FAK-paxillin interactions and the activity of extracellular signal-regulated kinase (ERK), leading to changes in cell motility and survival[7]. However, no clear *in vivo* evidence currently exists, that supports a direct interaction between vinculin and paxillin, due at least in part to a lack of characterized, specific mutations to block the interaction. Further complicating this matter, recent evidence indicates that vinculin overexpression induces the robust recruitment of paxillin to focal adhesions, and this recruitment occurs independent of the vinculin tail domain[39]. Although care must be taken

in the interpretation of protein overexpression experiments, this would appear to suggest that, in addition to possible direct interactions with Vt, vinculin either possesses additional paxillin interactions or vinculin is capable of modulating the subcellular localization of paxillin indirectly. As there is no evidence suggesting a secondary paxillin binding site, the latter appears more likely. However, either circumstance may complicate interpretation of data concerning the physiological role of a vinculin-paxillin interaction.

5. Vinculin Tail Phosphorylation

Vinculin is phosphorylated as a result of various stimuli, including calcium, phorbol esters, and leukotriene D(4)[57-59]. In the case of calcium stimulation, phosphorylation of vinculin is observed in connection with both platelet stimulation and formation of tight junctions[59, 60]. Src kinases and protein kinase C-α (PKCα) are both capable of phosphorylating vinculin, although a direct functional role for phosphorylation by either kinase is still not understood[35, 61-63].

During cell spreading, PKCα has been shown to interact with vinculin *in vivo* via crosslinking and pulldown experiments, and two serine residues in Vt, S1033 and S1045, have been shown to be phosphorylated by PKCα *in vitro*. The *in vitro* phosphorylation of Vt by PKCα was promoted by the addition of acidic phospholipids, leading to the speculation that binding of phospholipids may help release of the Vh-Vt complex allowing phosporylation[35].

Two residues phosphorylated by Src have been identified, one in Vh and the other in Vt. The Src phosphorylation site in Vt is the sole tyrosine in the domain, Y1065, which is the second to last residue from the C-terminus. It has been suggested that phosphorylation of

Y1065 could inhibit the Vh-Vt interaction without affecting actin-binding[63]. Cells that contain a vinculin mutant with both Src phosphorylation sites (Y100F/Y1065F) mutated exhibited decreased cell spreading relative to wild-type vinculin, indicating a physiological role for Src phosphorylation[63].

6. Vinculin Tail Self-Association

There is some disagreement in the field concerning self-association of vinculin. Early work, using a variety of methods including overlay assays, infrared attenuated total reflection spectroscopy, and electron microscopy, suggested vinculin was capable of self-association. Electron microscopy implicated the tail domain as the strongest point of interaction[2, 20, 64-66]. It should be noted, however, that most of the methods used in these experiments involved either 1) vinculin interacting with a surface or 2) conditions where additional ligands may be present, which raises the question of whether surface or ligand induced conformational changes could have occurred. The tail domain of vinculin has been shown to dimerize in the presence of actin or acidic phospholipids, but was reported to be a monomer in solution[41, 43, 67]. The crystal structure of Vt was also solved as a dimer, although this dimer structure was distinct from the model of actin induced dimerization[25, 43]. The crystallographic dimer involves a hydrophobic surface at the top of helices 4 and 5, a surface also involved in the Vh(D1)-Vt interaction. While the actin induced Vt dimer is thought to be important for the F-actin bundling activity of vinculin, it is unknown whether the crystal dimer is physiologically relevant. However, based on the exposed hydrophobic nature of the crystallographic dimer interface, which is freed when Vt is separated from Vh, it is not

unreasonable to speculate that this site may be involved in some type of interaction, following the release of the Vh-Vt interaction.

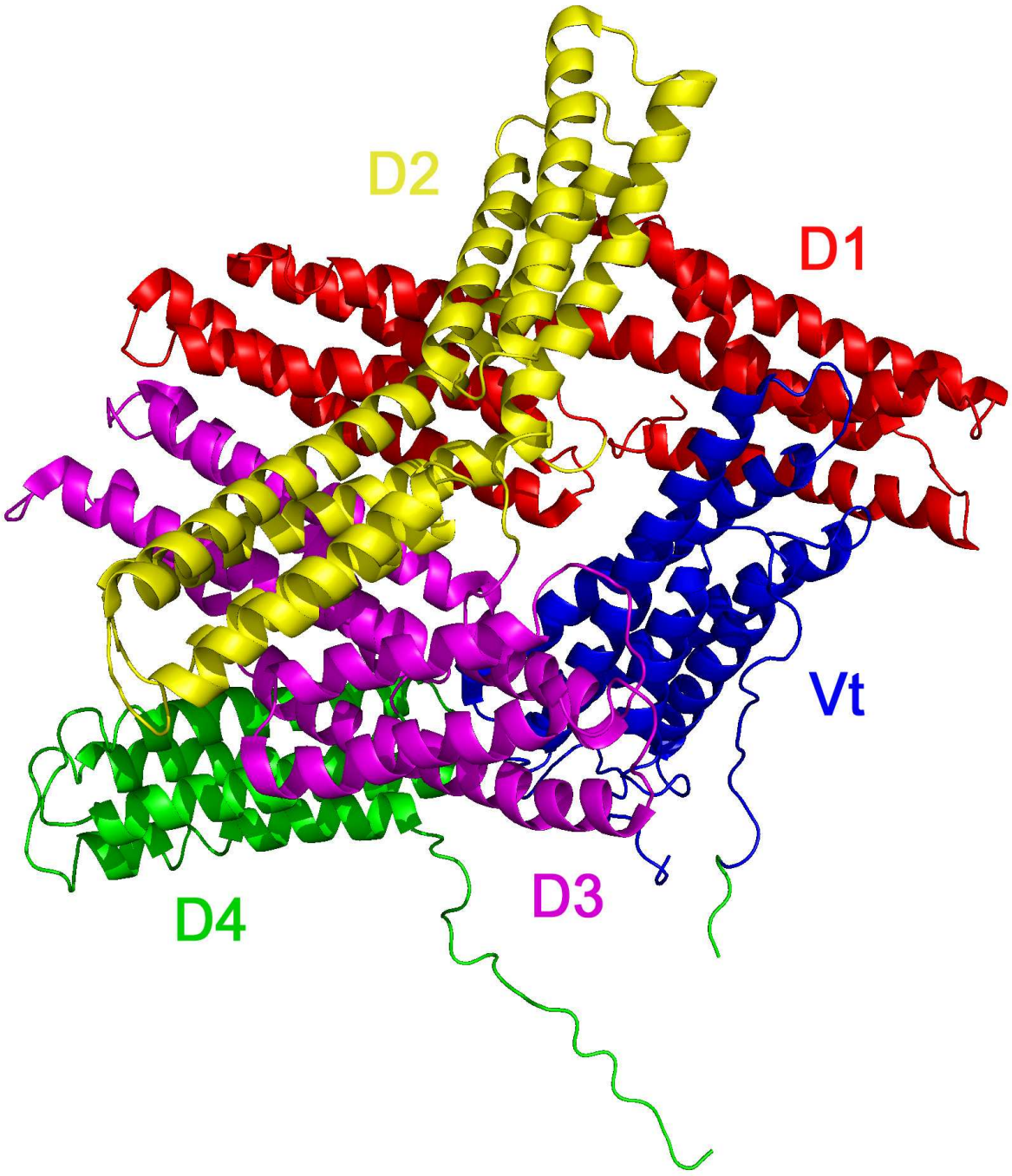

Figure 1.1: The full length crystal structure of vinculin (PDB ID 1ST6) is comprised of 8 helical bundles that are organized into tandem pairs. The first three tandem pairs (D1 colored red, D2 colored yellow, and D3 colored magenta) contains two four-helix bundles with one long helix connecting them and make up the head domain of vinculin (Vh). The "neck" domain, comprising D4 and a flexible linker, is colored green. The tail domain (Vt) is colored blue, and is held by the clamp-like head domain.

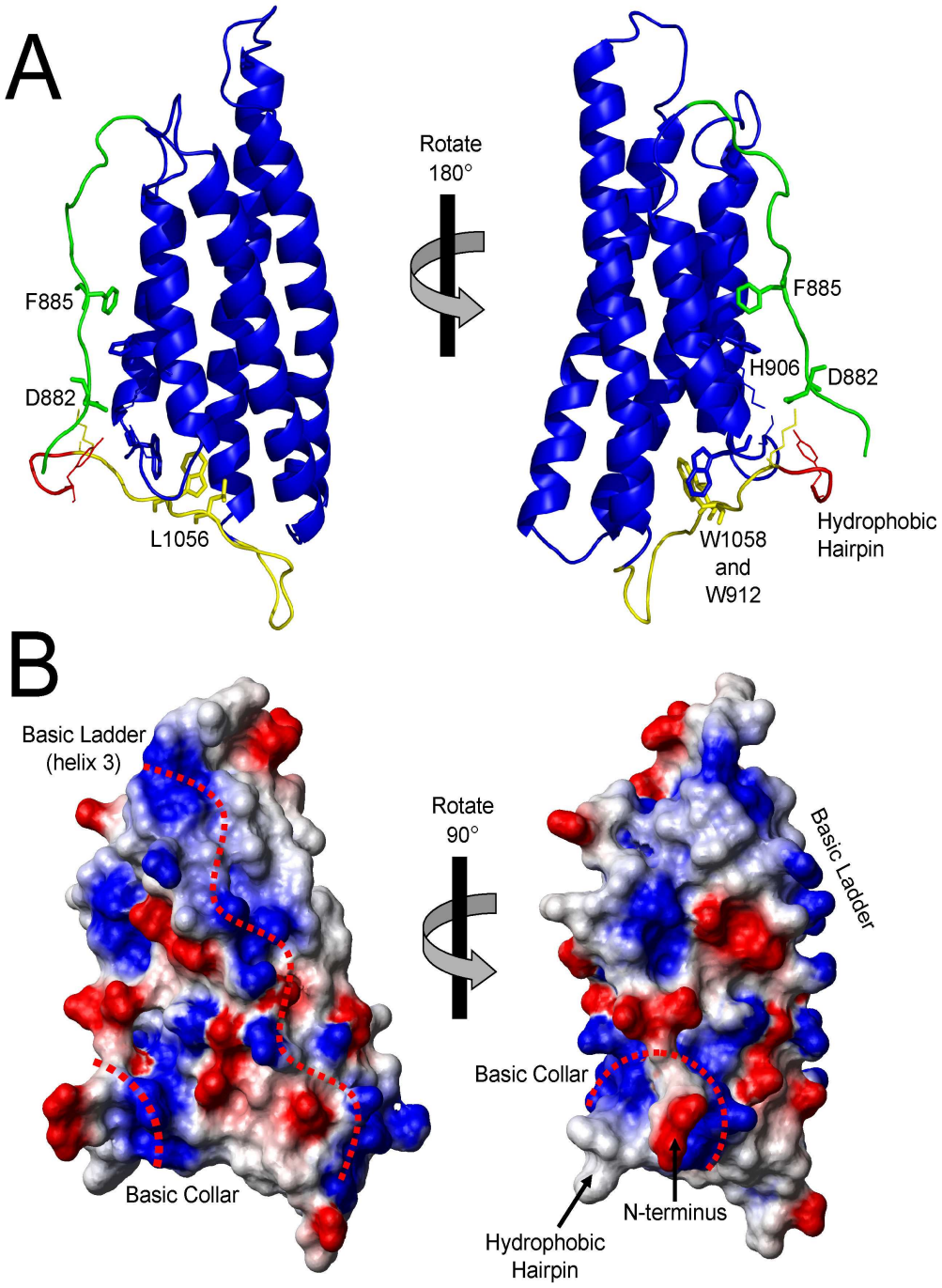

Figure 1.2: The tail domain of vinculin (residues 879-1066) is composed of a bundle of five amphipathic helices, with an N-terminal strap and C-terminal extension. The structures represented here are taken from the full length vinculin structure (PDB ID 1ST6). A) The N-terminal strap and C-terminal extension of Vt are highlighted in green and yellow respectively. The hydrophobic hairpin in the C-terminus is highlighted in red. Major interactions between the termini and the helical bundle are labeled, including L1056 and W1058 in the C-terminus, and D882 and F885 in the N-terminal strap. B) The basic ladder and basic collar are highlighted on the molecular surface, colored by electrostatic potential. The first structure in both A) and B) are depicted in roughly the same orientation.

H. Literature Cited

1. Geiger, B., et al., *Vinculin, an intracellular protein localized at specialized sites where microfilament bundles terminate at cell membranes.* Proc Natl Acad Sci U S A, 1980. **77**(7): p. 4127-31.

2. Belkin, A.M., et al., *Diversity of vinculin/meta-vinculin in human tissues and cultivated cells. Expression of muscle specific variants of vinculin in human aorta smooth muscle cells.* J Biol Chem, 1988. **263**(14): p. 6631-5.

3. Pardo, J.V., J.D. Siliciano, and S.W. Craig, *A vinculin-containing cortical lattice in skeletal muscle: transverse lattice elements ("costameres") mark sites of attachment between myofibrils and sarcolemma.* Proc Natl Acad Sci U S A, 1983. **80**(4): p. 1008-12.

4. Rodriguez Fernandez, J.L., et al., *Suppression of vinculin expression by antisense transfection confers changes in cell morphology, motility, and anchorage-dependent growth of 3T3 cells.* J Cell Biol, 1993. **122**(6): p. 1285-94.

5. Xu, W., H. Baribault, and E.D. Adamson, *Vinculin knockout results in heart and brain defects during embryonic development.* Development, 1998. **125**(2): p. 327-37.

6. Coll, J.L., et al., *Targeted disruption of vinculin genes in F9 and embryonic stem cells changes cell morphology, adhesion, and locomotion.* Proc Natl Acad Sci USA, 1995. **92**(20): p. 9161-5.

7. Subauste, M.C., et al., *Vinculin modulation of paxillin-FAK interactions regulates ERK to control survival and motility.* J Cell Biol, 2004. **165**(3): p. 371-81.

8. Vasile, V.C., et al., *Obstructive hypertrophic cardiomyopathy is associated with reduced expression of vinculin in the intercalated disc.* Biochem Biophys Res Commun, 2006. **349**(2): p. 709-15.

9. Zemljic-Harpf, A.E., et al., *Heterozygous inactivation of the vinculin gene predisposes to stress-induced cardiomyopathy.* Am J Pathol, 2004. **165**(3): p. 1033-44.

10. DeMali, K.A., C.A. Barlow, and K. Burridge, *Recruitment of the Arp2/3 complex to vinculin: coupling membrane protrusion to matrix adhesion.* J Cell Biol, 2002. **159**(5): p. 881-91.

11. Goldmann, W.H. and D.E. Ingber, *Intact vinculin protein is required for control of cell shape, cell mechanics, and rac-dependent lamellipodia formation.* Biochem Biophys Res Commun, 2002. **290**(2): p. 749-55.

12. Xu, W., J.L. Coll, and E.D. Adamson, *Rescue of the mutant phenotype by reexpression of full-length vinculin in null F9 cells; effects on cell locomotion by domain deleted vinculin.* J Cell Sci, 1998. **111 (Pt 11)**: p. 1535-44.

13. Rodriguez Fernandez, J.L., et al., *Suppression of tumorigenicity in transformed cells after transfection with vinculin cDNA.* J Cell Biol, 1992. **119**(2): p. 427-38.

14. Glukhova, M.A., et al., *Meta-vinculin distribution in adult human tissues and cultured cells.* FEBS Lett, 1986. **207**(1): p. 139-41.

15. Rudiger, M., et al., *Differential actin organization by vinculin isoforms: implications for cell type-specific microfilament anchorage.* FEBS Lett, 1998. **431**(1): p. 49-54.

16. Barstead, R.J. and R.H. Waterston, *Vinculin is essential for muscle function in the nematode.* J Cell Biol, 1991. **114**(4): p. 715-24.

17. Vasile, V.C., et al., *A missense mutation in a ubiquitously expressed protein, vinculin, confers susceptibility to hypertrophic cardiomyopathy.* Biochem Biophys Res Commun, 2006. **345**(3): p. 998-1003.

18. Vasile, V.C., et al., *Identification of a metavinculin missense mutation, R975W, associated with both hypertrophic and dilated cardiomyopathy.* Mol Genet Metab, 2006. **87**(2): p. 169-74.

19. Olson, T.M., et al., *Metavinculin mutations alter actin interaction in dilated cardiomyopathy.* Circulation, 2002. **105**(4): p. 431-7.

20. Molony, L. and K. Burridge, *Molecular shape and self-association of vinculin and metavinculin.* J Cell Biochem, 1985. **29**(1): p. 31-6.

21. Winkler, J., H. Lunsdorf, and B.M. Jockusch, *The ultrastructure of chicken gizzard vinculin as visualized by high-resolution electron microscopy.* J Struct Biol, 1996. **116**(2): p. 270-7.

22. Sun, N., et al., *Human alpha-synemin interacts directly with vinculin and metavinculin.* Biochem J, 2008. **409**(3): p. 657-67.

23. Ziegler, W.H., R.C. Liddington, and D.R. Critchley, *The structure and regulation of vinculin.* Trends Cell Biol, 2006. **16**(9): p. 453-60.

24. Bakolitsa, C., et al., *Structural basis for vinculin activation at sites of cell adhesion.* Nature, 2004. **430**(6999): p. 583-6.

25. Bakolitsa, C., et al., *Crystal structure of the vinculin tail suggests a pathway for activation.* Cell, 1999. **99**(6): p. 603-13.

26. Borgon, R.A., et al., *Crystal structure of human vinculin.* Structure (Camb), 2004. **12**(7): p. 1189-97.

27. Izard, T., et al., *Vinculin activation by talin through helical bundle conversion.* Nature, 2004. **427**(6970): p. 171-175.

28. Izard, T., G. Tran Van Nhieu, and P.R. Bois, *Shigella applies molecular mimicry to subvert vinculin and invade host cells.* J Cell Biol, 2006. **175**(3): p. 465-75.

29. Izard, T. and C. Vonrhein, *Structural basis for amplifying vinculin activation by talin.* J Biol Chem, 2004.

30. Johnson, R.P. and S.W. Craig, *An intramolecular association between the head and tail domains of vinculin modulates talin binding.* J Biol Chem, 1994. **269**(17): p. 12611-9.

31. Johnson, R.P. and S.W. Craig, *The carboxy-terminal tail domain of vinculin contains a cryptic binding site for acidic phospholipids.* Biochem Biophys Res Commun, 1995. **210**(1): p. 159-64.

32. Johnson, R.P. and S.W. Craig, *F-actin binding site masked by the intramolecular association of vinculin head and tail domains.* Nature, 1995. **373**(6511): p. 261-4.

33. Miller, G.J., S.D. Dunn, and E.H. Ball, *Interaction of the N- and C-terminal domains of vinculin. Characterization and mapping studies.* J Biol Chem, 2001. **276**(15): p. 11729-34.

34. Weekes, J., S.T. Barry, and D.R. Critchley, *Acidic phospholipids inhibit the intramolecular association between the N- and C-terminal regions of vinculin, exposing actin-binding and protein kinase C phosphorylation sites.* Biochem J, 1996. **314**(Pt 3): p. 827-32.

35. Ziegler, W.H., et al., *A lipid-regulated docking site on vinculin for protein kinase C.* J Biol Chem, 2002. **277**(9): p. 7396-404.

36. Cohen, D.M., et al., *Two distinct head-tail interfaces cooperate to suppress activation of vinculin by talin.* J Biol Chem, 2005. **280**(17): p. 17109-17.

37. Chen, H., D.M. Choudhury, and S.W. Craig, *Coincidence of actin filaments and talin is required to activate vinculin.* J Biol Chem, 2006. **281**(52): p. 40389-98.

38. Saunders, R.M., et al., *Role of vinculin in regulating focal adhesion turnover.* Eur J Cell Biol, 2006. **85**(6): p. 487-500.

39. Humphries, J.D., et al., *Vinculin controls focal adhesion formation by direct interactions with talin and actin.* J Cell Biol, 2007. **179**(5): p. 1043-57.

40. Jockusch, B.M. and G. Isenberg, *Interaction of alpha-actinin and vinculin with actin: opposite effects on filament network formation.* Proc Natl Acad Sci U S A, 1981. **78**(5): p. 3005-9.

41. Johnson, R.P. and S.W. Craig, *Actin activates a cryptic dimerization potential of the vinculin tail domain.* J Biol Chem, 2000. **275**(1): p. 95-105.

42. Huttelmaier, S., et al., *Characterization of two F-actin-binding and oligomerization sites in the cell-contact protein vinculin.* Eur J Biochem, 1997. **247**(3): p. 1136-42.

43. Janssen, M.E., et al., *Three-dimensional structure of vinculin bound to actin filaments.* Mol Cell, 2006. **21**(2): p. 271-81.

44. Chandrasekar, I., et al., *Vinculin acts as a sensor in lipid regulation of adhesion-site turnover.* J Cell Sci, 2005. **118**(Pt 7): p. 1461-72.

45. Fukami, K., et al., *alpha-Actinin and vinculin are PIP2-binding proteins involved in signaling by tyrosine kinase.* J Biol Chem, 1994. **269**(2): p. 1518-22.

46. Gilmore, A.P. and K. Burridge, *Regulation of vinculin binding to talin and actin by phosphatidyl- inositol-4-5-bisphosphate.* Nature, 1996. **381**(6582): p. 531-5.

47. Johnson, R.P., et al., *A conserved motif in the tail domain of vinculin mediates association with and insertion into acidic phospholipid bilayers.* Biochemistry, 1998. **37**(28): p. 10211-22.

48. Sechi, A.S. and J. Wehland, *The actin cytoskeleton and plasma membrane connection: PtdIns(4,5)P(2) influences cytoskeletal protein activity at the plasma membrane.* J Cell Sci, 2000. **113 Pt 21**: p. 3685-95.

49. Yin, H.L. and P.A. Janmey, *Phosphoinositide regulation of the actin cytoskeleton.* Annu Rev Physiol, 2003. **65**: p. 761-89.

50. Steimle, P.A., et al., *Polyphosphoinositides inhibit the interaction of vinculin with actin filaments.* J Biol Chem, 1999. **274**(26): p. 18414-20.

51. Turner, C.E., J.R. Glenney, Jr., and K. Burridge, *Paxillin: a new vinculin-binding protein present in focal adhesions.* J Cell Biol, 1990. **111**(3): p. 1059-68.

52. Burridge, K., C.E. Turner, and L.H. Romer, *Tyrosine phosphorylation of paxillin and pp125FAK accompanies cell adhesion to extracellular matrix: a role in cytoskeletal assembly.* J Cell Biol, 1992. **119**(4): p. 893-903.

53. Tumbarello, D.A., M.C. Brown, and C.E. Turner, *The paxillin LD motifs.* FEBS Lett, 2002. **513**(1): p. 114-8.

54. Dawid, I.B., J.J. Breen, and R. Toyama, *LIM domains: multiple roles as adapters and functional modifiers in protein interactions.* Trends Genet, 1998. **14**(4): p. 156-62.

55. Turner, C.E., et al., *Paxillin LD4 motif binds PAK and PIX through a novel 95-kD ankyrin repeat, ARF-GAP protein: A role in cytoskeletal remodeling.* J Cell Biol, 1999. **145**(4): p. 851-63.

56. Wood, C.K., et al., *Characterisation of the paxillin-binding site and the C-terminal focal adhesion targeting sequence in vinculin.* J Cell Sci, 1994. **107**(Pt 2): p. 709-17.

57. Massoumi, R. and A. Sjolander, *Leukotriene D(4) affects localisation of vinculin in intestinal epithelial cells via distinct tyrosine kinase and protein kinase C controlled events.* J Cell Sci, 2001. **114**(Pt 10): p. 1925-34.

58. Werth, D.K. and I. Pastan, *Vinculin phosphorylation in response to calcium and phorbol esters in intact cells.* J Biol Chem, 1984. **259**(8): p. 5264-70.

59. Vostal, J.G. and N.R. Shulman, *Vinculin is a major platelet protein that undergoes Ca(2+)-dependent tyrosine phosphorylation.* Biochem J, 1993. **294 (Pt 3)**: p. 675-80.

60. Perez-Moreno, M., et al., *Vinculin but not alpha-actinin is a target of PKC phosphorylation during junctional assembly induced by calcium.* J Cell Sci, 1998. **111 (Pt 23)**: p. 3563-71.

61. Ito, S., et al., *Vinculin phosphorylation by the src kinase. Interaction of vinculin with phospholipid vesicles.* J Biol Chem, 1983. **258**(23): p. 14626-31.

62. Sefton, B.M., et al., *Vinculin: a cytoskeletal target of the transforming protein of Rous sarcoma virus.* Cell, 1981. **24**(1): p. 165-74.

63. Zhang, Z., et al., *The phosphorylation of vinculin on tyrosine residues 100 and 1065, mediated by SRC kinases, affects cell spreading.* Mol Biol Cell, 2004. **15**(9): p. 4234-47.

64. Fringeli, U.P., et al., *Structure-activity relationship in vinculin: an IR/attenuated total reflection spectroscopic and film balance study.* Proc Natl Acad Sci U S A, 1986. **83**(5): p. 1315-9.

65. Otto, J.J., *Detection of vinculin-binding proteins with an 125I-vinculin gel overlay technique.* J Cell Biol, 1983. **97**(4): p. 1283-7.

66. Wilkins, J.A., K.Y. Chen, and S. Lin, *Detection of high molecular weight vinculin binding proteins in muscle and nonmuscle tissues with an electroblot-overlay technique.* Biochem Biophys Res Commun, 1983. **116**(3): p. 1026-32.

67. Huttelmaier, S., et al., *The interaction of the cell-contact proteins VASP and vinculin is regulated by phosphatidylinositol-4,5-bisphosphate.* Curr Biol, 1998. **8**(9): p. 479-88.

Chapter II.

Backbone ^{1}H, ^{13}C, and ^{15}N NMR Assignments of the Tail Domain of Vinculin

A. Introduction

Vinculin is a 116 kDa highly conserved cytoskeletal protein that localizes to both cell-matrix and cell-cell contacts and plays an important role in the linkage between transmembrane receptors (integrins or cadherins) and the actin cytoskeleton [1]. Vinculin is composed of an N-terminal head domain (Vh), a flexible neck domain, and a C-terminal tail domain (Vt). Each domain contains binding sites for multiple ligands. In addition to an important auto-inhibitory interaction with Vh, Vt binds F-actin, paxillin, and acidic phospholipids. However, these interactions are at least partially occluded in the intact protein due to auto-inhibitory interactions with Vh. The activation of vinculin requires release of the head/tail interaction, and is thought to require combinatorial binding of ligands to both Vh and Vt [2].

Vinculin is essential in development, as vinculin null embryos die early in embryogenesis [3]. Cells lacking vinculin are highly metastatic, highly motile, and resistant to apoptosis and anoikis, suggesting that vinculin functions as a tumor suppressor protein. The C-terminus of vinculin appears to play a critical role here, as a C-terminal fragment containing Vt, was shown to restore both apoptosis and anoikis in vinculin null cells [4]. In addition to cancer, deregulation of vinculin contributes to other disease states, as mutations in

the vinculin gene have been linked to both hypertrophic and dilated cardiomyopathy, while decreased expression of vinculin is correlated with a predisposition to stress-induced cardiomyopathy [5, 6]. In order to elucidate the role of vinculin in both physiological and pathophysiological states, a detailed understanding of its activation, function, and ligand interactions is needed.

B. Methods and Experiments

1. *Expression and Purification*

Escherichia coli strain BL21(DE3) was transformed by electroporation with a pET15b vector (Novagen) containing the tail domain of vinculin (*G. gallus*, 879-1066), as previously described [7]. Uniformly ^{15}N or $^{13}C/^{15}N$ isotopically enriched Vt was grown in M9 minimal media containing 1 g/L $^{15}NH_4Cl$, 2 g/L $^{13}C_6$-glucose (Spectra) in H_2O. Perdeuterated Vt was grown in M9 minimal media containing 1 g/L $^{15}NH_4Cl$, 2 g/L $^{2}H_7$-$^{13}C_6$-glucose (Spectra) in 99% D_2O. Bacterial cultures were grown at 37°C until reaching an optical density of 0.6, at which point Vt expression was induced by the addition of 0.25 mM IPTG and grown for 4-5 hours. The bacteria were harvested by centrifugation and resuspended in lysis buffer (20 mM Tris, pH 7.5, 150 mM NaCl, 5 mM Imidizole, 0.1% β-mercaptoethanol) and lysed by sonication. Vt was initially purified using by affinity separation using Ni-NTA Agarose beads (Qiagen). Following elution from the Ni-NTA beads, Vt was exchanged into thrombin cleavage buffer (20 mM Tris, pH 7.5, 500 mM NaCl, 2.5 mM $CaCl_2$, 0.1% BME) by dialysis. The 6-His tag was cleaved by thrombin and removed by dialysis in the same buffer. Vt was then further purified by cation-exchange chromatography using a HiPrep 16/10 SP XL column (GE Healthcare Life Sciences) with a

0.05-1 M NaCl gradient at pH 7.5. In some cases insoluble Vt was refolded and purified by resuspending cell pellets in 6M guanidinium chloride (GdmCl) prior to sonication. Vt was bound to Ni-NTA beads under denaturing conditions and refolded by removal of the GdmCl through dialysis. After refolding, thrombin cleavage and cation-exchange chromatography was performed as described above. Perdeuterated Vt was purified under denaturing conditions to ensure the back-exchange of amide protons to ^{1}H.

2. *Nuclear Magnetic Resonance Spectroscopy*

NMR spectra of Vt were collected at 37°C on Varian Inova 600, 700, and 800 MHz spectrometers. Select spectra were collected on Varian Inova 700 and 800 MHz spectrometers equipped with cryogenically cooled probe heads. The NMR buffer contained 10 mM K_2HPO_4, 50 mM NaCl, 0.01% NaN_3, 2 mM DTT at pH 5.5, in 90% H_2O and 10% D_2O. Backbone assignments were determined using ^{1}H-^{15}N HSQC, HNCO, HN(CA)CO, HNCA, HNCACB, HN(CA)CB, HN(CO)CA, and HN(COCA)CB experiments. Assignments were also verified where possible by HN-HN NOESY cross peaks obtained from 3D ^{15}N-edited NOESY data. NMR data was processed using NMRPipe/NMRDraw [8] and analyzed using NMRView [9].

C. Assignments and Deposition

The Vt domain employed for this study, comprises residues 879-1066 of full length vinculin, and was crystallized as a dimer with the two monomer units packed in an 'orthogonal' arrangement, each containing an anti-parallel five helix bundle fold [7].

Consistent with previous observations of Vt dimerization, our NMR, analytical ultracentrifugation, isothermal titration calorimetry, and fluorescence anisotropy studies all indicated that Vt is significantly dimeric at the concentrations used for NMR (0.3 mM). Standard 3D triple resonance NMR data on Vt showed poor magnetization transfer efficiency, consistent with a 43 kDa dimer at these concentrations. Perdeuteration of Vt improved efficiency of magnetization transfer in triple resonance NMR experiments, making sequential assignment possible. However, concentrations were limited to 0.3 mM. At higher Vt concentrations, magnetization transfer decreased significantly suggesting further oligomerization likely occurs. We were able to determine sequence specific assignments for 84.24% of the non-proline ^{15}N and amide proton resonances. We were also able to obtain 86.7%, 88.83%, and 82.98% of the ^{13}CO, $^{13}C_{\alpha}$, and $^{13}C_{\beta}$ resonances assignments, respectively. The majority of the unassigned residues fall in one region of the protein between residues 897 and 919. This region appears to be in intermediate exchange on the NMR time scale with backbone resonances not detectable. In the crystal structure of Vt [7], this region packs against the N-terminus which is seen in multiple conformations, possibly explaining the observed exchange broadening. Despite deuteration, complete side chain assignments could not be obtained due to poor magnetization transfer efficiency. Vt NMR assignments have been deposited in the BMRB with accession number 15653.

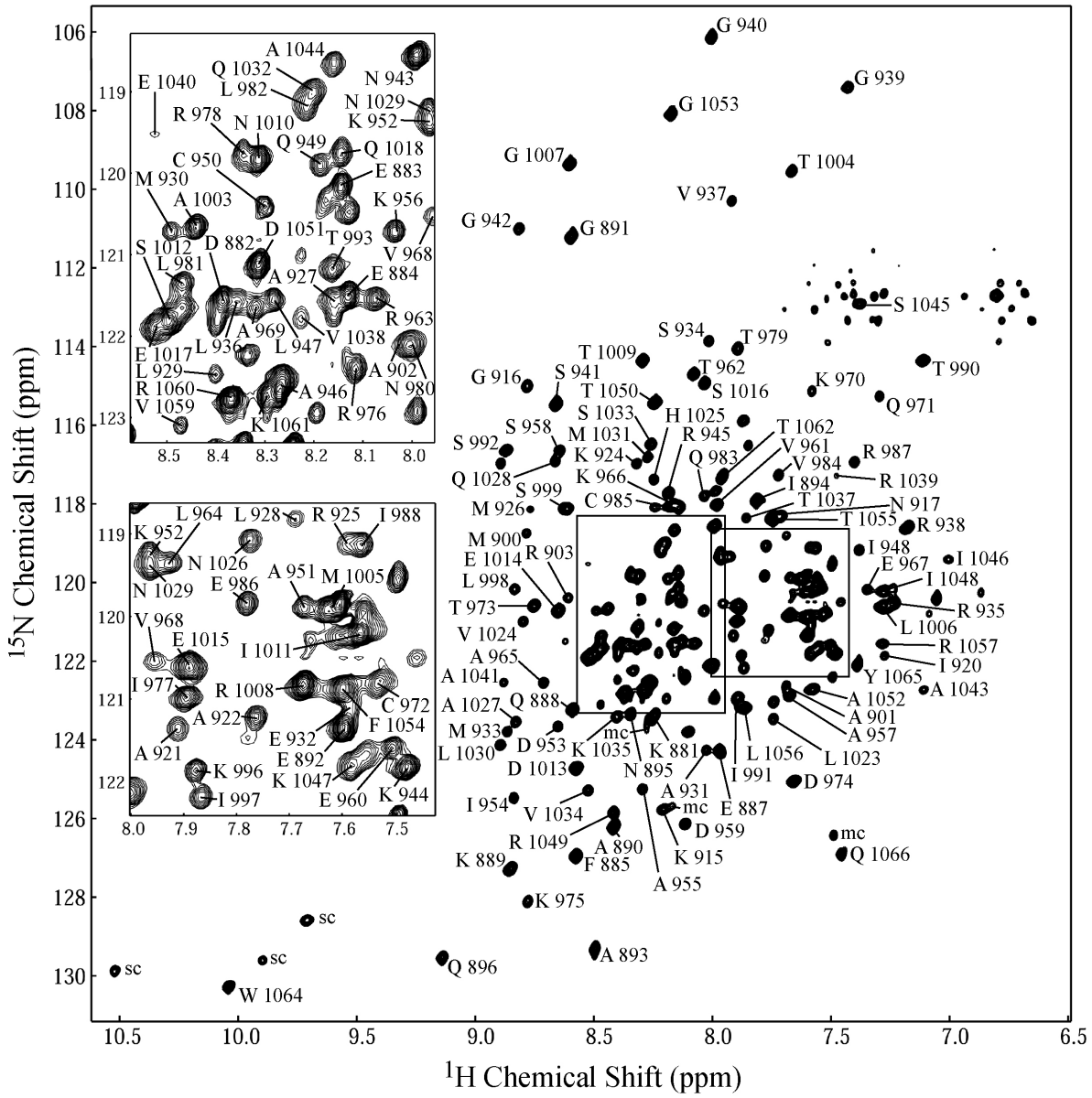

Figure 2.1: 2D ^{1}H-^{15}N HSQC spectrum of uniformly [^{2}H,^{15}N,^{13}C]-labeled Vt collected on a Varian Inova 700 MHz spectrometer at 37 ºC. The sample contained 0.3 mM Vt, 10 mM K_2HPO_4, 50 mM NaCl, 0.01% NaN_3, and 2 mM DTT at pH 5.5 in 90% H_2O and 10% D_2O. NMR resonance assignments are numbered according to the full length *G. gallus* vinculin protein sequence. To improve clarity, some side chain resonances are labeled with "sc". For resonances which appear in multiple conformations, peaks associated with the minor conformation are labeled with "mc".

D. Literature Cited

1. Jockusch, B.M. and M. Rudiger, *Crosstalk between cell adhesion molecules: vinculin as a paradigm for regulation by conformation.* Trends Cell Biol, 1996. **6**(8): p. 311-5.

2. Chen, H., D.M. Choudhury, and S.W. Craig, *Coincidence of actin filaments and talin is required to activate vinculin.* J Biol Chem, 2006. **281**(52): p. 40389-98.

3. Xu, W., H. Baribault, and E.D. Adamson, *Vinculin knockout results in heart and brain defects during embryonic development.* Development, 1998. **125**(2): p. 327-37.

4. Subauste, M.C., et al., *Vinculin modulation of paxillin-FAK interactions regulates ERK to control survival and motility.* J Cell Biol, 2004. **165**(3): p. 371-81.

5. Vasile, V.C., et al., *Identification of a metavinculin missense mutation, R975W, associated with both hypertrophic and dilated cardiomyopathy.* Mol Genet Metab, 2006. **87**(2): p. 169-74.

6. Zemljic-Harpf, A.E., et al., *Heterozygous inactivation of the vinculin gene predisposes to stress-induced cardiomyopathy.* Am J Pathol, 2004. **165**(3): p. 1033-44.

7. Bakolitsa, C., et al., *Crystal structure of the vinculin tail suggests a pathway for activation.* Cell, 1999. **99**(6): p. 603-13.

8. Delaglio, F., et al., *NMRPipe: a multidimensional spectral processing system based on UNIX pipes.* J Biomol NMR, 1995. **6**(3): p. 277-93.

9. Johnson, B.A. and R.A. Blevins, *NMR View: A computer program for the visualization and analysis of NMR data.* J Biomol NMR, 1994. **4**(5): p. 603-614.

Chapter III.

The Role of pH and Histidine 906

A. Introduction

Contacts between cells (cell-cell) and with the extracellular matrix (cell-matrix) regulate a wide variety of critical cellular processes including cell growth, migration, differentiation, and cell death[1-3]. Aberrant regulation of these processes contributes to a number of human diseases, including cancer[4]. The highly conserved cytoskeletal protein, vinculin, is found in both cell-cell and cell-matrix contacts [5], is essential for embryogenesis[6], and plays an important role in regulating cell morphology and migration[7]. Vinculin is a large, approximately 116 kDa protein consisting of an amino-terminal "head" domain (~ 90 kDa) and a carboxy-terminal "tail" domain (~ 21 kDa) connected by a flexible hinge region. The vinculin tail (Vt) domain forms auto-inhibitory contacts with the vinculin head (Vh) domain and binds several ligands including F-actin, paxillin, PKCα and acidic phospholipids [8-15]. Auto-inhibitory contacts between the head and tail domain are believed to downregulate vinculin function by preventing the interaction of multiple ligands [11-13, 16, 17]. On the flip side, vinculin activation requires release of auto-inhibitory contacts. Current models of vinculin activation have proposed that a combinatorial input of multiple ligands is necessary to release interactions between the head and tail domain. For example, acidic phospholipid or F-actin binding to the tail domain, when coupled with talin association with the head domain are believed to modulate vinculin

activity [18-21]. The binding of these ligands is believed to induce conformational changes in both the head and tail domains causing disruption of auto-inhibitory contacts [18, 19, 22, 23]. One study suggested that a single histidine residue (H906) in the vinculin tail domain (Vt) is critical for both a pH- and lipid-dependent conformational change in Vt, which in turn, can modulate vinculin head/tail interactions [24].

Several crystal structures of vinculin are now available [18, 19, 22, 25]. The Vt domain was solved at pH 5.0, and found to possess an anti-parallel, five helix bundle fold. The tail domain adopts a similar structure in the context of the full length protein, despite differences in the pH at which the structures were solved. In addition to the helix bundle fold, Vt contains an N-terminal "strap" (residues 879 to 893) that exists in an extended conformation and forms interactions with residues along the helix 1-2 face and the C-terminus. In particular, F885 in the strap packs against the H906 side chain in helix 1, and D882 of the strap forms electrostratic interactions with S914, K924, K1061, and Y1065 (located in the loop between helices 1 and 2, helix 2, and the C-terminus respectively). In the isolated Vt domain solved at pH 5.0, the strap is observed in multiple conformations, suggesting conformational mobility.

Histidine 906 has been implicated in both pH and lipid-induced Vt conformational changes, which in turn affect auto-inhibitory contacts between the head and tail domain[24]. To better characterize the role of H906 in pH dependent Vt conformational changes, we investigated whether the protonation state of H906 influences Vt structure using NMR and CD spectroscopy. Although a previous CD study indicated that protonation/deprotonation of H906 promotes a change in Vt conformation[24], results obtained from our NMR and CD studies do not support a large scale conformational change in Vt over a pH range from 5.5 to

7. 5. Mutation of H906 to alanine cause localized chemical shift perturbations in helices 1 and 2 and the N-terminal strap, consistent with perturbation of the F885/H906 interaction resulting in release of the strap from the helix 1-2 interface. However, loss of this contact does not appear to cause a large scale conformational change in the Vt five helix bundle fold. As H906 has also been implicated in pH-dependent Vt self-association[24], we employed NMR and analytical ultracentrifugation (AUC) approaches to investigate whether Vt undergoes pH-dependent self-association. The isolated Vt domain was crystallized as a dimer at pH 5.0 with the site of dimerization located in the upper portions of helices 4 and 5[19]. Our NMR data support Vt self-association in the solution state, with the dimerization interface consistent with that observed by crystallography. However, in contrast to a previous report[24], our AUC and NMR results indicate that Vt does not undergo a monomer to dimer transition between pH 5.5 and pH 7.5. Thus, our overall results indicate that Vt does not undergo a pH-dependent change in structure, and retains the ability to self-associate between pH 5.5 and pH 7.5.

B. Materials and Methods

1. *Protein expression and purification*

The tail domain of vinculin (Vt) comprising residues 879-1066 of chicken vinculin (98.9% identity with human vinculin) was expressed with a N-terminal His-tag[19]. The Vt construct was transformed into *E. coli* strain BL21(DE3), and expression of Vt induced upon addition of 0.25 mM IPTG at 37°C. Cells were grown for 5 hrs and lysed by sonication in a buffer containing 20 mM Tris, pH 7.5, 150 mM NaCl, 5 mM Imidizole, 0.1% β-mercaptoethanol (BME). Soluble protein was separated by centrifugation for 1 hour at

25,000g. Vt was initially purified by affinity separation using Ni-NTA Agarose beads (Qiagen). The bound protein was washed and eluted with lysis buffers containing 60 mM and 500 mM Imidizole, respectively. The eluted protein was dialyzed into Thrombin cleavage buffer (20 mM Tris, pH 7.5, 500 mM NaCl, 2.5 mM $CaCl_2$, 0.1% BME) and the His-tag was cleaved by incubation with thrombin (~1 unit per 5 mg protein) overnight at 37° C. Thrombin was then removed by dialysis in the same buffer. Vt was then further purified by cation-exchange chromatography (HiPrep 16/10 SP XL column from GE Healthcare Life Sciences) in a buffer containing 20 mM Tris (pH 7.5), 2.5 mM ethylenediaminetetraacetic acid (EDTA), and 0.1% BME with a 0.05-1 M NaCl gradient. In some cases insoluble Vt was refolded and purified by resuspending cell pellets in 6M guanidinium chloride (GdmCl) prior to sonication. GdmCl-treated Vt was purified using a similar procedure as for soluble Vt, except that purification using Ni-NTA Agarose beads was carried out under denaturing conditions. Vt was subsequently refolded by removal of the GdmCl by dialysis in a buffer containing 20 mM Tris, pH 7.5, 500 mM NaCl, 0.1% BME. The His-tag was removed and Vt further purified by cation-exchange chromatography, using the procedures described above for the natively folded protein. ^{1}H-^{15}N HSQC spectra were acquired on ^{15}N-enriched refolded Vt and natively folded Vt, to verify similar spectral features and proper refolding. The Vt mutant, Vt H906A, was expressed and purified using procedures described above for wild-type Vt.

2. *Nuclear Magnetic Resonance Assignments*

The nuclear magnetic resonance (NMR) assignments for the majority of the backbone $^{1}H_N$, ^{15}N, $^{13}C_\alpha$, ^{13}CO, and side chain $^{13}C_\beta$ resonances were determined for wild-type Vt. The

assignments and experimental details have been deposited in the Biological Magnetic Resonance Data Bank (http://www.bmrb.wisc.edu/), accession number 15653. In brief, NMR assignments were determined using a standard series of triple resonance experiments (^{1}H-^{15}N HSQC, HNCO, HN(CA)CO, HNCA, HNCACB, HN(CA)CB, HN(CO)CA, and HN(COCA)CB)[26] on (^{2}H, ^{13}C, ^{15}N)-enriched Vt in a buffer containing 10 mM K_2HPO_4, 50 mM NaCl, 0.01% NaN_3, 2 mM dithiothreitol (DTT) at pH 5.5, in 90% H_2O and 10% D_2O. NMR resonance assignments for Vt H906A were determined using the wild-type assignments as a starting point, and were confirmed from HNCO, HNCA, and HN(CA)CB spectra on (^{13}C, ^{15}N)-enriched labeled Vt H906A.

3. *NMR Samples*

Bacteria containing the Vt construct[19] were grown in minimal media containing 1g/L ^{15}N-NH_4Cl (Spectra Stable Isotopes). Vt protein was expressed and purified as described above and exchanged into NMR buffer (10 mM Potassium Phosphate, 50 mM NaCl, 2mM DTT, 0.1% NaN_3 and 10% D_2O) using an Amicon Ultra centrifugal filter device (10000-dalton molecular weight cutoff, Millipore). Protein concentration was determined by UV absorbance (280 nm, $\varepsilon = 17990\ M^{-1}\ cm^{-1}$).

4. *NMR Spectroscopy*

NMR experiments were conducted on a Varian INOVA 700 MHz spectrometer at 37° C. ^{1}H-^{15}N HSQC spectra were collected on uniformly ^{15}N-enriched wild-type and Vt H906A in NMR buffer (10 mM Potassium Phosphate, 50 mM NaCl, 2 mM DTT, 0.1% NaN_3 and 10% D_2O). The data was processed with NMRPipe[27] and analyzed with NMRView[28].

^{1}H-^{15}N HSQC spectra were collected over a pH range from 5.5 to 7.5 on 150 µM wild-type Vt and Vt H906A protein samples. Weighted chemical shifts were calculated using the following equation:

$$weighted\ chemical\ shift = \sqrt{(^{1}H\ chemical\ shift)^{2} + \frac{(^{15}N\ chemical\ shift)^{2}}{6}}$$

5. *Circular Dichroism*

All circular dichroism (CD) data were collected using an Applied Photophysics Pistar-180 spectrometer. The CD buffer contained 10 mM Potassium Phosphate, 50 mM Na_2SO_4, 1 mM DTT, at either pH 5.5 or 7.5 and 25° C. Near UV (ultraviolet) CD spectra (350-250 nm) were collected using 450 µM protein samples. Far UV CD spectra (260-190 nm) were collected using 5 µM protein samples. In both cases, spectra were recorded in 0.5 nm steps, averaging over 100,000 samplings per step. A smoothing function using a three point window was applied to all spectra.

6. *Analytical Ultracentrifugation*

Sedimentation equilibrium experiments were performed using a Beckman Optima XL-I analytical ultracentrifuge equipped with absorbance optics. A Ti50 8-hole rotor was used with six-sectored centerpieces. Wild-type Vt and Vt H906A, each at three different concentrations (150 µM, 300 µM, and 450 µM), were analyzed at both pH 5.5 and pH 7.5 in a buffer containing 10 mM Potassium Phosphate, 50 mM NaCl, and 2 mM DTT. Samples were spun at 20° C, at 19,000 rpm for 18 hours, and absorbance scans were recorded every 2

hours. Due to high absorbance at 280 nm, data were collected at 305 nm (absorbance of all samples was between 0.2 and 0.95). Equilibrium was assumed to have been reached when the difference between two consecutive absorbance profiles was zero. The meniscus-depletion method was used to determine absorbance offsets after centrifugation of the samples at 40,000 rpm for 6 h[29]. Data were analyzed with Beckman XL-A/XL-I Analysis Software Version 4.0, and fit to a monomer/dimer model using a partial specific volume of 0.736.

C. Results

The tail domain of vinculin (Vt) has been reported to undergo an H906-dependent conformational change as a function of pH and acidic phospholipid binding[24]. Intriguingly, H906 has also been linked to pH dependent Vt self-association[24]. Based on these findings, it was speculated that H906 plays a key role in the conformational dynamic properties of Vt and thus in the regulation of vinculin function. To this end, we have employed NMR, CD, and AUC approaches to better characterize the role of H906 in pH- and lipid-dependent Vt conformational changes.

1. *Mutation of Histidine 906 to Alanine does not significantly alter Vt structure*

As mutations have the potential to alter protein structure and therefore significantly change the interpretation of experimental results, we employed CD and NMR spectroscopy to determine whether mutation of histidine 906 to alanine alters the conformation of Vt. Circular dichroism (CD) spectroscopy can be used to probe both secondary and tertiary structural alterations in proteins[30]. Far-UV (190-250 nm) CD is sensitive to the

conformation of the peptide bond and therefore secondary structure of proteins and is often used to estimate the percent of secondary structure (i.e., α-helix or β-sheet) present. Near-UV (250-350 nm) CD can be used to detect aromatic side chain packing interactions in proteins, and is thus a useful probe of tertiary structure[30]. We obtained virtually identical near and far-UV CD spectra for both wild-type Vt and the Vt H906A variant at pH 7.5 (Figure 3.1), indicating that both the overall helical content and the tertiary packing of aromatic residues in Vt are not significantly altered by mutation of histidine 906 to alanine.

However, as near and far-UV CD provide information on the average of all chromophores that absorb at the wavelength of interest in the molecular population, it is not possible to obtain residue specific information. To more specifically characterize site specific spectral perturbations in Vt resulting from mutation of H906, we employed multidimensional heteronuclear Nuclear Magnetic Resonance (NMR) spectroscopy. Uniformly ^{15}N-enriched wild-type Vt and the H906A Vt proteins were expressed and purified as described in Methods, and 2D NMR heteronuclear correlation spectra collected. ^{1}H-^{15}N Heteronuclear Single Quantum Coherence (HSQC) spectra detect signals for protons attached to ^{15}N nuclei, and can provide a residue specific probe for each NH pair in wild-type and H906A Vt. The NH resonance is sensitive to changes in its electrochemical environment. By analyzing the chemical shift and/or intensity change in NH resonances corresponding to each residue, perturbations resulting from the mutation (Vt H906A) can be assessed. As is shown in Figure 3.2, the majority of residues in Vt are unaffected by the mutation. A small subset of NH resonances exhibit chemical shift changes greater than 0.1 ppm (13), and four additional NH resonances exhibit significant loss of intensity. The residues associated with these NH resonances are proximal to the site of mutation (H906) in

the three dimensional structure, and are displayed in Figure 3.3. NH resonances associated with residues that exhibit changes in either chemical shift or intensity almost all localize to the N-terminal strap of Vt and the surface of helices 1 and 2 that contact the strap. In crystal structures of Vt and full length vinculin, H906 packs against the side chain of the N-terminal strap residue, F885. It is likely that this interaction is disrupted by mutation of the histidine aromatic side chain, resulting in loss of contacts between the strap and helix 1, consistent with the chemical perturbations observed at these sites.

2. *The conformation of Vt is largely unaltered between pH 5.5 and 7.5*

It was previously reported that Vt undergoes a pH dependent conformational change. However, this study employed far-UV CD, which is sensitive only to secondary structure[24]. To assess the effects of pH changes on the secondary and tertiary structure of Vt, both near and far-UV CD spectra were acquired on wild type Vt and Vt H906A at pH 5.5 and 7.5. Inspection of Figure 3.4, shows virtually identical near and far-UV CD spectra at pH 5.5 and 7.5 for both Vt and Vt H906A, suggesting that neither the secondary or tertiary structure of Vt or Vt H906A differs between pH 5.5 and pH 7.5. As noted previously, CD does not provide residue specific information. To complement CD analyses, NMR studies were conducted.

^{1}H-^{15}N HSQC spectra were collected at pH values ranging from 5.5 to 7.5 for both Vt and Vt H906A. The chemical shift perturbations for all detectable resonances were analyzed with the results are shown in Figure 3.5. For both wild-type and H906A Vt, the largest chemical shift change was observed for the H1025 NH resonance. Almost all other significant perturbations (> 0.15 ppm) were from residues close to H1025, while the vast

majority of resonances showed no significant perturbation (< 0.1 ppm). Thus, our NMR and CD data indicate that the neither the conformation of wild-type Vt or Vt H906A is significantly altered between pH 5.5 and 7.5. Based on the small and localized nature of the chemical shifts around H1025, it is likely that these chemical shift perturbations simply represent the protonation/deprotonation of the histidine side chain rather than a localized conformational change. We could not detect and therefore assign NH resonances near to and including H906 (904-914), presumably due to broadening of these resonances by conformational exchange on the intermediate NMR time scale. However, our findings that the NH resonances corresponding to E884, K924, A927, L928, which are proximal to this site, do not significantly change as a function of pH, indicates that either H906 does not titrate over this pH range due to interactions with the strap or that deprotonation of this side chain does not cause a large scale conformational change in the helix bundle.

3. *Vinculin Tail Self-Association*

Evidence for vinculin tail domain dimerization and oligomerization has been observed in both the presence and absence of F-actin and acidic phospholipids[19, 24, 31, 32]. As noted earlier, the vinculin tail domain was crystallized at pH 5.0 as a dimer[19]. Moreover, studies by Miller et al (2001) indicate that Vt undergoes pH-dependent self-association with H906 playing a critical role. To better characterize Vt self-association and the role of H906 in the pH dependence, we have conducted analytical ultracentrifugation (AUC) studies.

The self-association of wild-type Vt and Vt H906A was analyzed by AUC at pH 5.5 and pH 7.5. All data was fit to a monomer/dimer model of self-association. Apparent K_d

values and a representative monomer/dimer fit are reported in Figure 3.6. Interestingly, Miller et al (2001) reported that Vt was monomeric at pH 7.0, but self-associated at pH 5.5 as determined by gel filtration chromatography[24]. However, our AUC data indicates that Vt is capable of self-association at both pH 5.5 and 7.5, with a K_d of 243 and 134 μM, respectively. Moreover, we observed a decrease in the dissociation constant at pH 7.5 relative to pH 5.5, which is reverse of the trend reported by Miller et al[24]. A decrease in self-association was observed with Vt H906A at both pH 5.5 and pH 7.5 relative to wild-type Vt, however all apparent K_d values were >100 μM, suggesting this self-association may not be biologically relevant.

D. Discussion

Ligand binding to both the vinculin head and tail domain has been reported to induce conformational changes in vinculin that modulate its function[19, 22, 32, 33]. In particular, binding of F-actin and acidic phospholipids to the tail domain has been reported to cause both a change in conformation and oligomerization state[19, 32]. Studies reported by Miller and Ball (2001) supported a H906-dependent conformational change in Vt in response to pH changes and acidic phospholipid binding [24]. In addition, the protonation state of H906 was reported to modulate Vt self-association. To better understand the molecular basis for the role of H906 in pH–dependent Vt conformation and dimerization, we conducted a series of biophysical studies on Vt and a Vt H906A variant.

H906 was previously proposed as a critical residue in lipid and pH-dependent Vt conformational changes[24], based on far-UV CD studies of wild-type Vt and Vt H906A. As far UV CD (190-250 nm) is sensitive only to secondary structure, we were interested in

further characterizing whether mutation of H906 to alanine affects the tertiary structure of Vt. We conducted near-UV CD (250-350 nm) on wild-type Vt and the H906A variant, as near-UV CD spectra are sensitive to differences in packing interactions associated with aromatic amino acids and therefore tertiary structure. Interestingly, we found both the near and far UV CD spectra of Vt and Vt H906A were similar at pH 7.5 (Figure 3.1). These results indicate that, within the resolution of CD, that mutation of histidine 906 to alanine does not alter the secondary or tertiary fold of Vt at pH 7.5. We also conducted Nuclear Magnetic Resonance (NMR) studies, as NMR spectroscopy can report on site specific differences in the chemical environment of residues within wild-type and Vt H906A. For these studies, ^{1}H-^{15}N HSQC spectra were collected on ^{15}N-enriched wild-type Vt and Vt H906A to analyze chemical shift differences in the amide ^{15}N and proton resonances for Vt and Vt H906A. We found that the majority of the amide proton resonances in Vt H906A are not significantly changed from wild-type Vt, indicating that the overall conformation is not altered by the mutation (Figure 3.2), consistent with CD data. Of the resonances that do exhibit chemical shift changes, the changes are small and localized to the site of mutation. In addition, as NMR chemical shifts are very sensitive to surrounding chemical environment, changes in chemical shifts do not necessarily represent conformational changes. For residues in the immediate vicinity of H906, the removal of the histidine side chain is likely to alter the chemical shift associated with neighboring residues even in the absence of a conformational change. The additional chemical shift changes seen are tenably explained upon inspection of the known crystal structure. In the crystal structures of both Vt and full length vinculin, histidine 906 is located in helix 1 and the histidine side chain extends away from the helical bundle and interacts with the side chain of phenylalanine 885 in the N-terminal strap of

Vt[18, 19]. The N-terminal strap is held in an extended conformation along the interface of helices 1 and 2, mainly via interactions involving F885 and D882. Interactions between the side chains of F885 and H906 are likely to stabilize contacts with the helix 1-2 interface and the extended conformation of the strap. Intriguingly, in the crystal structure of Vt, the strap is observed in two distinct conformations, suggesting conformational flexibility[19]. Disruption of the interaction between H906 and F885 is likely to promote increased conformational flexibility in the strap, though additional interactions between residues in the strap and the helical bundle should still restrain the conformation of the strap to some degree. Mutation of histidine 906 to alanine should increase the conformational flexibility of the N-terminal strap, allowing increased sampling of alternate strap conformations, due to disruption of contacts between the N-terminal strap and the helical bundle. These conformations are likely also sampled in the wild-type structure although at lower frequency. The chemical shift changes observed for NH resonances associated with the strap and the surface of helices 1 and 2 between wild-type Vt and Vt H906A, are consistent with increased conformational flexibility of the strap. The lack of chemical shift changes in the remaining helices of the bundle suggest that there are not significant changes in helices 1 and 2, as structural alterations in these helices are likely to perturb the chemical environment of the other helices within the helical bundle.

CD studies by Miller and Ball (2001) concluded that although the conformation of Vt and Vt H906A are similar at pH 7.0, differences were observed at pH 5.5. A change in the far UV CD spectrum of wild-type Vt between pH 5.5 and 7.0 was interpreted as a pH-dependent conformational change. In this previous study, far UV CD spectra of Vt H906A, but not wild-type Vt, was reported to be similar at both pH 7.0 and pH 5.5, suggesting that

H906 was critical for a pH dependent conformational change in Vt[24]. To further characterize this reported conformational change, we conducted both near and far UV CD of both wild-type Vt and Vt H906A at pH 7.5 and pH 5.5. However, comparison of CD spectra for both Vt and Vt H906A, showed no significant spectral differences at either pH 7.5 or pH 5.5 (Figure 3.4). Thus, our CD results do not support a pH dependent conformational change for either wild-type Vt or Vt H906A. As these results differed from findings of Miller and Ball, we sought to corroborate these data with additional NMR studies. For these studies, ^{1}H-^{15}N HSQC NMR spectra were collected at pH values between 5.5 and 7.5 for both ^{15}N-enriched wild-type Vt and Vt H906A. Heteronuclear 2D spectra as a function of pH provide residue specific probes of pH dependent changes. The only amino acid side chain that normally undergoes protonation/deprotonation over this pH range is that of histidine (δ1 proton), consistent with our observation that the histidine NH resonances show the largest changes in chemical shift. Vt has two native histidine residues, H906 and H1025. Histidine 1025 exhibits large chemical shift changes over the pH range studied, consistent with the titration of its side chain. Unfortunately, the NH resonance associated with H906 is not detected in our spectra, presumably due to chemical exchange on an intermediate time scale resulting in broadening. However, of all detectable residues, the only significant chemical shift changes are localized to H1025, consistent with the protonation/deprotonation of its side chain between pH 5.5 and 7.5. Although H906 could not be measured, residues within 3-4 amino acids from H906 and those closest in the three dimensional structure were detectable and showed small/insignificant chemical shift changes. The majority of NH resonances in Vt exhibit insignificant chemical shift changes between pH 5.5 and 7.5 (Figure 3.5). This is strong evidence that the conformation of Vt is not significantly altered by pH, consistent with

CD data. Additionally, the pH dependent chemical shift changes observed in HSQC spectra of both Vt and Vt H906A are virtually identical, indicating that mutation of H906 does not alter pH-dependent spectral changes observed for Vt.

Vinculin tail self-association has been reported under a variety of different conditions, by a number of groups[8, 19, 24, 31, 32]. In one report[24], Vt was reported to exist in its monomeric state at pH 7.0, but self-associate at pH 5.5. In contrast, the Vt H906A variant was reported be insensitive to pH-dependent self-association. Based, on these findings, H906 was proposed to play an important role in Vt self-association. Interestingly, the crystal structure of Vt was solved as a dimer showing H906 to be distant from the site of dimerization, raising the question of how H906 could regulate this self-association. As self-association is likely critical for the F- actin bundling function of Vt[8, 31, 32], we were interested in further characterizing Vt self-association in solution. AUC and NMR studies were conducted to measure Vt self-association. Concentration dependent NMR spectral changes support the existence of the Vt dimer observed by crystallography, at both pH 7.5 and pH 5.5. The concentration dependence of the amide resonances in HSQC spectra were fit to a monomer dimer model and provided an approximate K_d between 200 and 300 µM at pH 5.5 (data not shown). As the high protein concentrations required by NMR and complications associated with interpretation of chemical shifts can lead to significant uncertainty in the determination of a K_d by NMR, we conducted AUC to better characterize Vt self-association. Initial AUC studies, monitored at 280 nm, with Vt samples between 10 and 40 µM did not exhibit evidence of self-association (data not shown), consistent with the approximate K_d obtained by NMR. AUC experiments at higher protein concentrations do show evidence of self-association for both wild-type Vt and Vt H906A (Figure 3.6). For

both wild-type Vt and Vt H906A, however, the apparent K_d determined by fitting to a monomer/dimer model was greater than is commonly observed for physiological interactions, suggesting the self-association in the absence of F-actin or acidic phospholipids may not be biologically relevant. It remains unclear if the weak self-association observed in solution is relevant to the self-association in the presence of F-actin. Although all apparent K_d measurements determined were >100 μM, the Vt H906A increase in the K_d for self-association. For both wild-type Vt and Vt H906A, there is also an increase in self-association at pH 7.5 relative to pH 5.5. In all cases, it should be noted that the apparent K_d determined by AUC may be complicated higher order oligomerization. While the AUC data was fit to a monomer/dimer model, it is possible that Vt self-association may involve higher order oligomerization, in which case the K_d's determined by a monomer/dimer fit may be inaccurate. Poor magnetization transfer efficiency in heteronuclear NMR experiments and some non-random residuals in monomer/dimer fits of AUC data both suggest some higher order oligomerization may occur, however the nature and extent of this oligomerization is unclear.

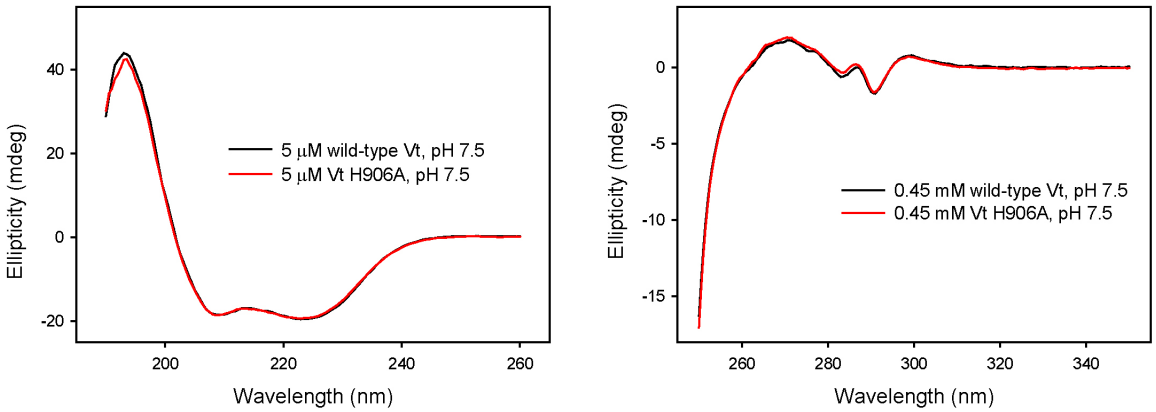

Figure 3.1: The circular dichroism (CD) spectra of wild-type Vt and Vt H906A were compared to assess potential changes in secondary and tertiary structure. Far ultraviolet (UV) CD, 190-260 nm, is sensitive to changes in the conformation of the peptide backbone and therefore secondary structure of proteins. Near UV CD, 250-350 nm, can detect aromatic side chain packing interactions in proteins, and is thus a useful probe of tertiary structure. The far and near UV spectra of Vt and Vt H906A are virtually identical at pH 7.5, suggesting that the mutation of histidine 906 to alanine in Vt does not alter either the secondary or tertiary structure over this pH range.

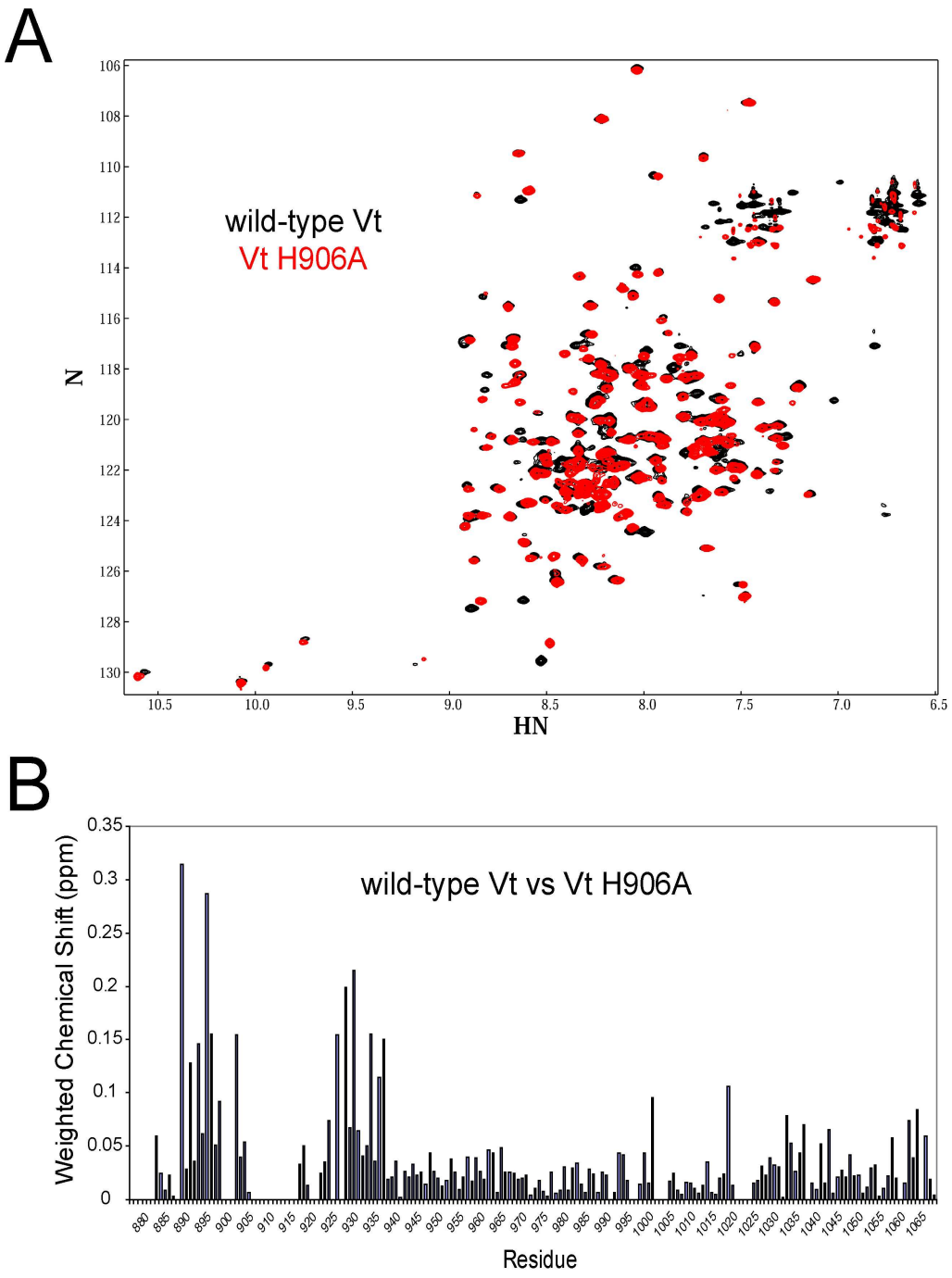

Figure 3.2: To specifically characterize site specific spectral perturbations in Vt resulting from mutation of H906, ^{1}H-^{15}N Heteronuclear Single Quantum Coherence (HSQC) spectra were collected on ^{15}N-enriched Vt and Vt H906A (0.15 mM protein, pH 5.5). As shown in A, minor chemical shift perturbations are observed primarily for backbone HN resonances associated with residues in the N-terminal strap and helix 1-2 interface, consistent with minimal changes in the overall fold of Vt. The weighted chemical shift changes for each residue are displayed in B. The majority of residues exhibit perturbations of < 0.05 ppm, with perturbations > 0.1 ppm localized to the N-terminal strap and the helix 1-2 interface (see Figure 3.3).

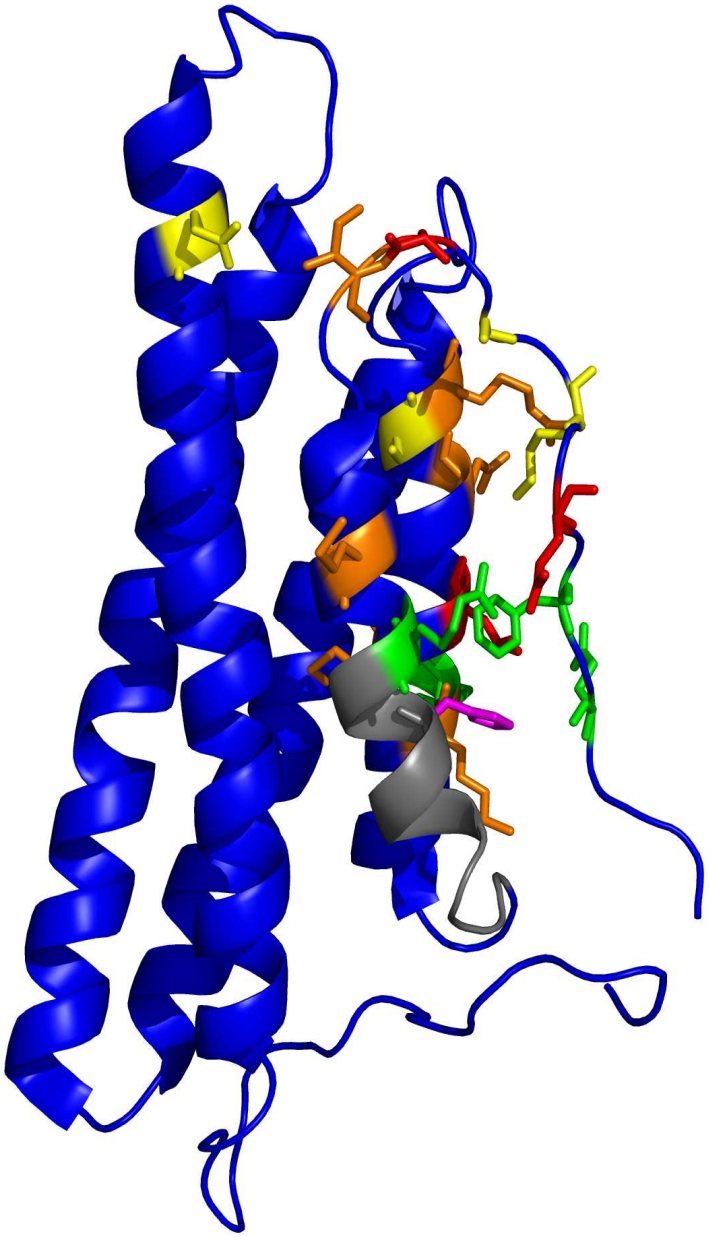

Figure 3.3: Residues exhibiting either chemical shift perturbations or significant changes in intensity due to mutation of H906 to alanine are highlighted on the structure of Vt (1ST6). The site of mutation (H906) is highlighted in magenta. Residues showing chemical shift changes > 0.2 ppm, between 0.15 and 0.2 ppm, and between 0.1 and 0.15 ppm are shown in red, orange, and yellow, respectively. Residues displayed in green exhibit significant changes in intensity or broadening of the associated NH resonances. The residues colored grey could not be measured in either wild-type Vt or Vt H906A, presumably due to broadening of the NH resonance due to chemical exchange between two or more conformers. Almost all residues whose NH resonances chemical shift or intensity perturbations relative to wild-type Vt, are localized to the N-terminal strap and the surface of helices 1 and 2 that are contacted by the strap. This is consistent with a localize change in the N-terminal strap of Vt, with the overall conformation of the helical bundle largely unaltered.

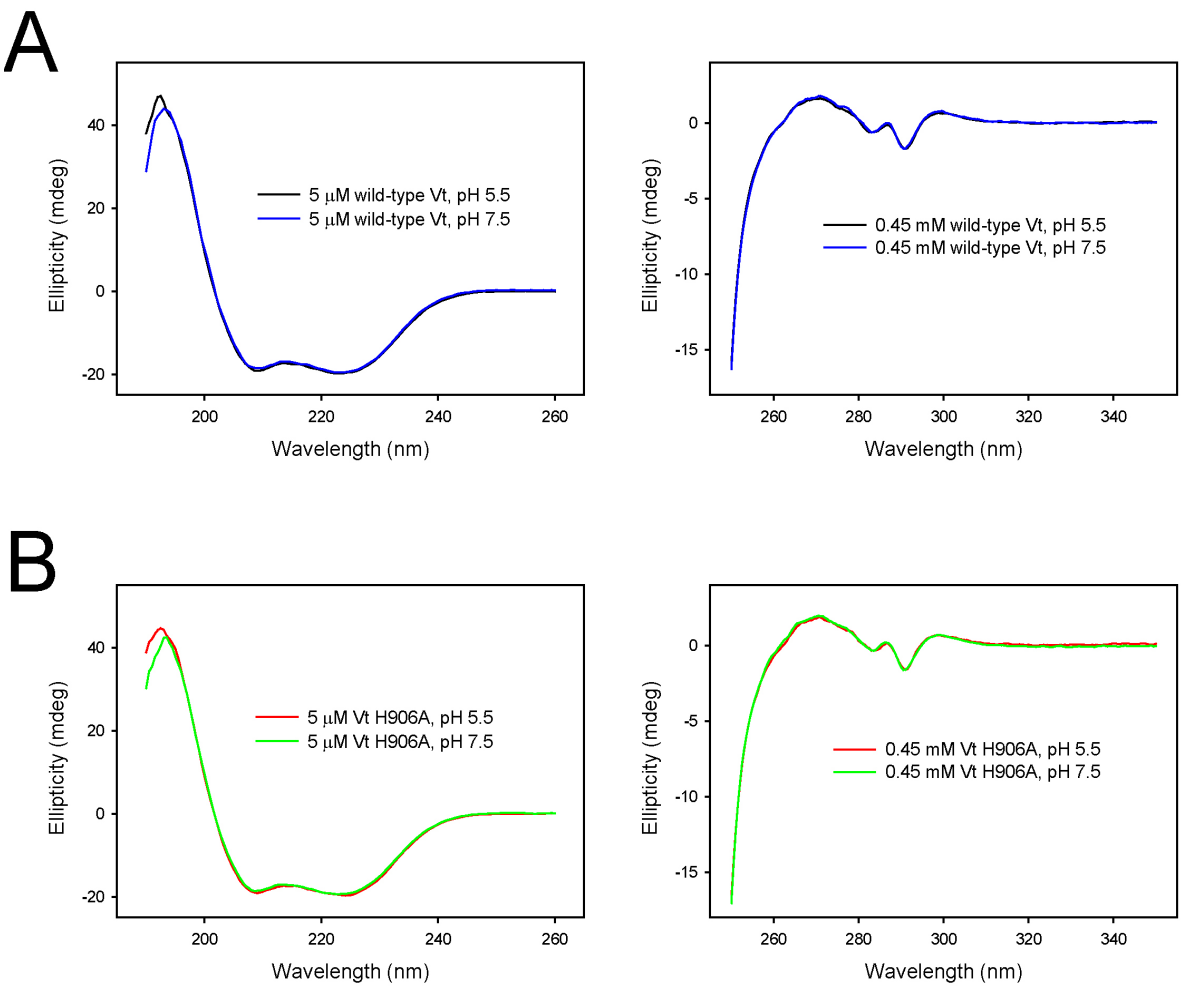

Figure 3.4: The far and near UV spectra of wild-type Vt and Vt H906A were compared at pH 5.5 and 7.5 to assess pH dependent conformational changes. Both wild-type Vt (A) and Vt H906A (B) exhibited no significant differences in either far or near UV CD spectra between pH 5.5 and 7.5, suggesting that there is no significant pH dependent conformational change for either wild-type Vt or Vt H906A across this pH range.

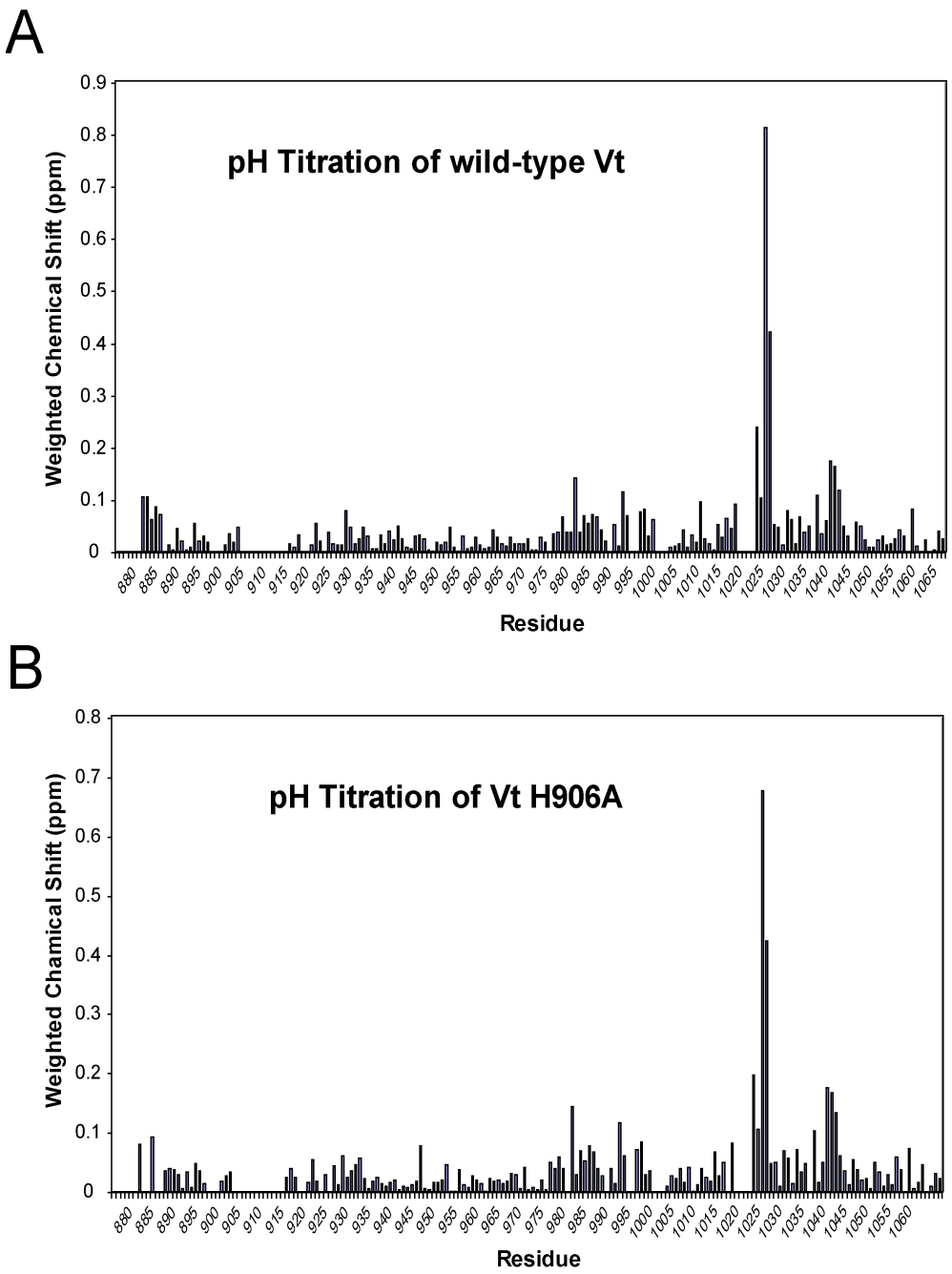

Figure 3.5: The weighted chemical shift changes in ^{1}H-^{15}N HSQC spectra of wild-type Vt (A) and Vt H906A (B) collected between pH 5.5 and 7.5. For both Vt and Vt H906A, the largest chemical shift changes measured correspond to H1025. The backbone HN resonance of H906 is not detectable, presumably due to chemical exchange on an intermediate time scale resulting in broadening. The majority of chemical shift changes are small (< 0.05 ppm), suggesting there is no overall conformational change in Vt between pH 5.5 and 7.5. The largest chemical shift changes are localized to H1025, consistent with titration of the histidine side chain over this pH range. Furthermore, the chemical shift changes observed for Vt H906A are nearly identical to wild-type Vt, suggesting that the protonation state of H906 does not play a role in pH dependent spectra changes observed between pH 5.5 and 7.5.

A

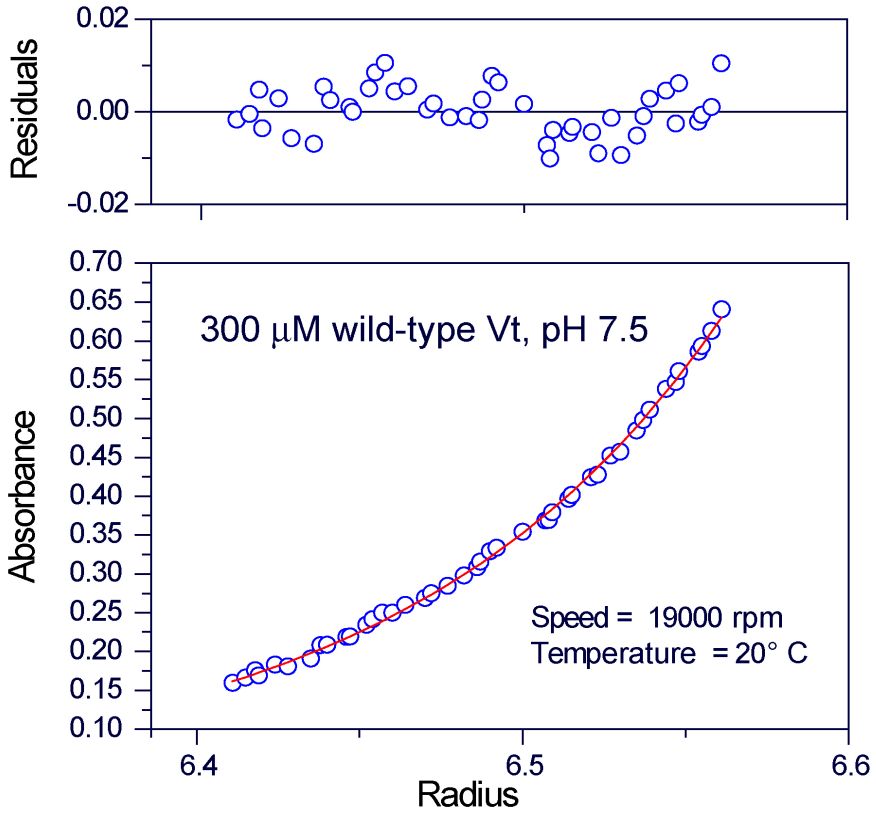

B

K_d (monomer/dimer model)

	pH 5.5	pH 7.5
wild-type Vt	240 ± 70 μM	130 ± 10 μM
Vt H906A	390 ± 110 μM	190 ± 30 μM

Figure 3.6: Analytical ultracentrifugation (AUC) studies were conducted on both wild-type Vt and Vt H906A to quantify Vt self-association. Experiments were conducted at 150, 300, and 450 μM protein concentrations. Sedimentation equilibrium curves were fit to a monomer/dimer model, and a representative fit is shown in A. The K_d for self-association was observed to be lower at pH 7.5 relative to pH 5.5 for both Vt and Vt H906A, however in both cases the association was relatively weak, with K_d values > 100 μM. Dissociation constants determined for monomer/dimer fits are shown in B.

E. Literature Cited

1. Berrier, A.L. and K.M. Yamada, *Cell-matrix adhesion.* J Cell Physiol, 2007. **213**(3): p. 565-73.

2. Danen, E.H. and A. Sonnenberg, *Integrins in regulation of tissue development and function.* J Pathol, 2003. **201**(4): p. 632-41.

3. Delon, I. and N.H. Brown, *Integrins and the actin cytoskeleton.* Curr Opin Cell Biol, 2007. **19**(1): p. 43-50.

4. Kedrin, D., et al., *Cell motility and cytoskeletal regulation in invasion and metastasis.* J Mammary Gland Biol Neoplasia, 2007. **12**(2-3): p. 143-52.

5. Geiger, B., et al., *Vinculin, an intracellular protein localized at specialized sites where microfilament bundles terminate at cell membranes.* Proc Natl Acad Sci U S A, 1980. **77**(7): p. 4127-31.

6. Xu, W., H. Baribault, and E.D. Adamson, *Vinculin knockout results in heart and brain defects during embryonic development.* Development, 1998. **125**(2): p. 327-37.

7. Coll, J.L., et al., *Targeted disruption of vinculin genes in F9 and embryonic stem cells changes cell morphology, adhesion, and locomotion.* Proc Natl Acad Sci USA, 1995. **92**(20): p. 9161-5.

8. Huttelmaier, S., et al., *Characterization of two F-actin-binding and oligomerization sites in the cell-contact protein vinculin.* Eur J Biochem, 1997. **247**(3): p. 1136-42.

9. Menkel, A.R., et al., *Characterization of an F-actin-binding domain in the cytoskeletal protein vinculin.* J Cell Biol, 1994. **126**(5): p. 1231-40.

10. Wood, C.K., et al., *Characterisation of the paxillin-binding site and the C-terminal focal adhesion targeting sequence in vinculin.* J Cell Sci, 1994. **107 (Pt 2)**: p. 709-17.

11. Johnson, R.P. and S.W. Craig, *An intramolecular association between the head and tail domains of vinculin modulates talin binding.* J Biol Chem, 1994. **269**(17): p. 12611-9.

12. Johnson, R.P. and S.W. Craig, *The carboxy-terminal tail domain of vinculin contains a cryptic binding site for acidic phospholipids.* Biochem Biophys Res Commun, 1995. **210**(1): p. 159-64.

13. DeMali, K.A., C.A. Barlow, and K. Burridge, *Recruitment of the Arp2/3 complex to vinculin: coupling membrane protrusion to matrix adhesion.* J Cell Biol, 2002. **159**(5): p. 881-91.

14. Johnson, R.P., et al., *A conserved motif in the tail domain of vinculin mediates association with and insertion into acidic phospholipid bilayers.* Biochemistry, 1998. **37**(28): p. 10211-22.

15. Ziegler, W.H., et al., *A lipid-regulated docking site on vinculin for protein kinase C.* J Biol Chem, 2002. **277**(9): p. 7396-404.

16. Weekes, J., S.T. Barry, and D.R. Critchley, *Acidic phospholipids inhibit the intramolecular association between the N- and C-terminal regions of vinculin, exposing actin-binding and protein kinase C phosphorylation sites.* Biochem J, 1996. **314 (Pt 3)**: p. 827-32.

17. Miller, G.J., S.D. Dunn, and E.H. Ball, *Interaction of the N- and C-terminal domains of vinculin. Characterization and mapping studies.* J Biol Chem, 2001. **276**(15): p. 11729-34.

18. Bakolitsa, C., et al., *Structural basis for vinculin activation at sites of cell adhesion.* Nature, 2004. **430**(6999): p. 583-6.

19. Bakolitsa, C., et al., *Crystal structure of the vinculin tail suggests a pathway for activation.* Cell, 1999. **99**(6): p. 603-13.

20. Chen, H., D.M. Choudhury, and S.W. Craig, *Coincidence of actin filaments and talin is required to activate vinculin.* J Biol Chem, 2006. **281**(52): p. 40389-98.

21. Cohen, D.M., et al., *Two distinct head-tail interfaces cooperate to suppress activation of vinculin by talin.* J Biol Chem, 2005. **280**(17): p. 17109-17.

22. Izard, T., et al., *Vinculin activation by talin through helical bundle conversion.* Nature, 2004. **427**(6970): p. 171-175.

23. Kelly, D.F., et al., *Structure of the alpha-actinin-vinculin head domain complex determined by cryo-electron microscopy.* J Mol Biol, 2006. **357**(2): p. 562-73.

24. Miller, G.J. and E.H. Ball, *Conformational change in the vinculin C-terminal depends on a critical histidine residue (His-906).* J Biol Chem, 2001. **276**(31): p. 28829-34.

25. Borgon, R.A., et al., *Crystal structure of human vinculin.* Structure (Camb), 2004. **12**(7): p. 1189-97.

26. Cavanagh, J., *Protein NMR spectroscopy: principles and practice*. 2nd ed. 2007, Amsterdam; Boston: Academic Press. p.

27. Delaglio, F., et al., *NMRPipe: a multidimensional spectral processing system based on UNIX pipes.* J Biomol NMR, 1995. **6**(3): p. 277-93.

28. Johnson, B.A. and R.A. Blevins, *NMR View: A computer program for the visualization and analysis of NMR data.* Journal of Biomolecular NMR, 1994. **4**(5): p. 603-614.

29. Yphantis, D.A., *Equilibrium Ultracentrifugation Of Dilute Solutions.* Biochemistry, 1964. **3**: p. 297-317.

30. Kelly, S.M., T.J. Jess, and N.C. Price, *How to study proteins by circular dichroism.* Biochimica et Biophysica Acta (BBA) - Proteins & Proteomics, 2005. **1751**(2): p. 119.

31. Janssen, M.E., et al., *Three-dimensional structure of vinculin bound to actin filaments.* Mol Cell, 2006. **21**(2): p. 271-81.

32. Johnson, R.P. and S.W. Craig, *Actin activates a cryptic dimerization potential of the vinculin tail domain.* J Biol Chem, 2000. **275**(1): p. 95-105.

33. Izard, T. and C. Vonrhein, *Structural basis for amplifying vinculin activation by talin.* J Biol Chem, 2004.

Chapter IV.

Vinculin Tail and Lipid Binding

A. Introduction

Vinculin is a highly conserved cytoskeletal protein which localizes to points of cell adhesion and is involved in linking the actin cytoskeleton to the cell membrane[1]. Sites of adhesion in which vinculin is enriched include focal adhesions (cell-extracellular matrix), adherence junctions (cell-cell), costameres in muscle cells, and intercalated discs in cardiac cells[1-3]. At these sites, vinculin is believed to play an important role in cell adhesion processes involving regulation of the actin cytoskeleton. Moreover, vinculin has been linked to pathways that control cell growth, differentiation, motility, and survival[4-7]. Vinculin is also critical for proper development in model organisms[6, 8] and its loss in cells leads to increased motility, invasiveness, and resistance to apoptosis[5, 9, 10]. Decreased vinculin expression and mutations have also been associated with human cardiomyopathies[11-14].

Vinculin is a 116 kDa cytoskeletal protein, and early studies by electron microscopy and proteolytic cleavage determined it to be made up of a globular head domain (Vh), a flexible neck, and a tail domain (Vt)[15, 16]. The full length structure of vinculin has been solved by X-ray crystallography, and has been described as a "bundle of bundles"[17]. Vh is composed of 6 helical bundles organized into 3 tandem pairs of bundles while Vt is composed of a single helical bundle. The head and tail domain interact to form a closed, auto-inhibited conformation with Vt held "pincer-like" by Vh[17]. Vinculin binds a number

cytoskeletal and adhesion proteins including actin, talin, α-actinin, α-catenin, β-catenin, vinexin, ponsin, actin-related protein complex (Arp 2/3), vasodilator-stimulated phosphoprotein (VASP), and paxillin. However, many of these interactions are at least partially masked in the intact, unstimulated protein due to the auto-inhibitory interactions between the head and tail domains[18]. Vinculin has also shown to bind acidic phospholipids through its tail domain, and this interaction also appears to be regulated by head/tail interactions[19-21], with lipid binding proposed to play a role in vinculin activation and focal adhesion turnover[17, 19, 22, 23]. Although vinculin has been shown to bind acidic phospholipids, including phosphatidylserine (PS), phosphatidylinositol (PI), and phosphatidylinositol 4,5-bisphosphate (PIP_2), the relative affinity for various acidic phospholipids and phosphoinositides (PPIs) has not been reported. The inositol ring of PPIs can be phosphorylated at three separate positions (not including the phosphodiester linkage at position 1), allowing for a number of PPIs with distinct functions. Three families of phosphoinositol phosphate kinases are involved in the production, interconversion, and regulation of PPIs[24, 25]. PPIs, including PIP_2, have been shown to be regulated both spatially and temporally at sites of actin assembly and cytoskeletal remodeling[26-29]. Although a number of structurally conserved PPI and PIP_2 binding motifs have been identified[30-32], none have been found within the vinculin tail domain. Structural studies of Vt identified three features proposed to play a role in binding of acidic lipids; a C-terminal extension containing a “hydrophobic hairpin”, a “basic collar” of lysine and arginine residues surrounding the hydrophobic hairpin, and a “basic ladder” of exposed basic residues along the length of helix 3. A series of vinculin mutagenesis studies have been conducted to pinpoint the site of lipid binding to Vt. However, the data is somewhat difficult to interpret,

as the number, location and effectiveness of the mutations vary. Although some of the phospholipid defective variants have been characterized to determine whether the mutation(s) effect other ligand binding interactions (i.e., Vh, actin), the structural effects of these mutations are largely unknown. Thus, the exact site and mode of phospholipid binding is still unclear. In order to better characterize phospholipid binding interactions with the vinculin tail domain (Vt), we have examined the relative ability of various acidic phospholipids to associate with the vinculin tail domain using lipid co-sedimentation assays, and performed biophysical characterization and lipid binding studies on various Vt mutants.

B. Materials and Methods

1. *Protein expression and purification*

Vinculin tail (Vt) constructs containing residues 879-1066 (generously provided by Dr. Robert Liddington) and 884-1066 of chicken vinculin in the pET15b vector (Novagen) have been described previously[19, 21]. Mutant forms of Vt were produced using the QuikChange Site-Directed Mutagenesis Kit (Stratagene) and verified by DNA sequencing. Vectors were transformed into *E. coli* strain BL21(DE3) and cells were grown at 37°C to an optical density of 0.6 (600 nm). Vt expression initiated by addition of 0.25 mM isopropyl β-D-1-thiogalactopyranoside (IPTG) and cells were grown for a further 5 hrs and harvested by centrifugation. Vinculin was expressed at high level and purified from both the soluble and insoluble fraction. Cell pellets were resuspended in a lysis buffer containing 20 mM Tris, pH 7.5, 150 mM NaCl, 5 mM Imidizole, 0.1% β-mercaptoethanol (BME) and lysed by sonication. Vinculin, expressed in the soluble fraction was separated from the particulate fraction by centrifugation for 1 hour at 25,000 g. The fraction containing soluble Vt, was

purified by affinity separation using Ni-NTA agarose beads (Qiagen). Vt was washed and eluted from the beads using lysis buffer containing 60 mM and 500 mM Imidizole, respectively, and then dialyzed into Thrombin cleavage buffer (20 mM Tris, pH 7.5, 500 mM NaCl, 2.5 mM $CaCl_2$, 0.1% BME). The His-tag was cleaved by thrombin (~1 unit per 5 mg protein) overnight at 37° C. Cation-exchange chromatography (HiPrep 16/10 SP XL column from GE Healthcare Life Sciences) was used to further purify Vt, using a 0.05-1 M NaCl gradient in a buffer containing 20 mM Tris (pH 7.5), 2.5 mM ethylenediaminetetraacetic acid (EDTA), and 0.1% BME.

To purify Vt from the insoluble fraction, cell pellets were resuspended in 6 M guanidinium chloride (GdmCl) prior to sonication. A protocol similar to that used for soluble Vt was employed except that purification from Ni-NTA agarose beads was carried out under denaturing conditions. Following elution, GdmCl was removed and Vt refolded by dialysis in a buffer containing 20 mM Tris, pH 7.5, 500 mM NaCl, and 0.1% BME. Thrombin cleavage to remove the His-tag and further cation-exchange chromatography was identical to the procedure for the natively folded protein. Proper refolding was verified by comparison of ^{1}H-^{15}N HSQC spectra acquired on refolded and natively folded Vt (both ^{15}N enriched).

2. *Lipid Co-sedimentation*

Lipid binding to Vt was assessed by co-sedimentation with small, unilamellar vesicles (SUV). The binding of phosphatidylinositol (PI) and phosphatidylserine (PS) were assessed in lipid vesicles containing 60% phosphatidylethanolamine (PE), 40% phosphatidylcholine (PC) by weight, with either PI or PS replacing PE at the concentration indicated. The

binding of phosphatidylinositol 4,5-bisphosphate (PIP_2) was assessed using vesicles containing 60% PE, 20% PC, and either 20% PS by weight, with PIP_2 replacing PS at the concentration indicated. For example, experiments testing the role of 10% PIP_2 employed vesicles composed of 60% PC, 20% PE, 10% PS, and 10% PIP_2. Vesicles were produced by combining the appropriate lipids suspended in chloroform, to producing a sample containing 250 µg total lipid. The mixture was dried using a SpeedVac and then resuspended in 90 µL of buffer containing 40 mM 4-(2-hydroxyethyl)-1-piperazineethanesulfonic acid (HEPES), 150 mM NaCl, and 2 mM dithiothreitol (DTT), pH 7.4. Resuspension and production of the SUVs was accomplished by brief sonication with a probe tip sonicator. 10 µL of 100 µM protein (in an identical buffer) was added to each vesicle sample, producing a final volume of 100 µL and a final protein concentration of 10 µM. Samples were nutated at 4° C for 1 hour, then centrifuged at 100,000 g for 1 hour. The supernatant was removed and the pellet resuspended in buffer containing 0.1% sodium dodecyl sulfate (SDS), 25 mM glycine, and 25 mM TRIS, pH 8.3. Supernatant and pellet samples were analyzed by SDS polyacrylamide gel electrophoresis (SDS-PAGE). Gels were stained with coomassie, scanned, and protein levels quantified using ImageJ software[33].

3. *NMR Samples and Spectroscopy*

Bacterial expressed ^{15}N-labeled Vt protein was produced for nuclear magnetic resonance spectroscopy (NMR) studies by growth in M9 minimal media containing 1g/L ^{15}N-NH_4Cl (Spectra Stable Isotopes). NMR samples were exchanged into NMR buffer (10 mM Potassium Phosphate, 50 mM NaCl, 2 mM DTT, 0.1% NaN_3 and 10% D_2O at the indicated pH) using an Amicon Ultra centrifugal filter device (10000-dalton molecular

weight cutoff, Millipore). ^{1}H-^{15}N Heteronuclear Single Quantum Coherence (HSQC) spectra were collected on a Varian INOVA 700 MHz spectrometer at 37° C. NMR data processing and analysis was performed using NMRPipe[34] and NMRView[35].

4. *Circular Dichroism*

Circular dichroism (CD) spectra were collected at both near-ultraviolet (350-250 nm) and far-ultraviolet (260-190 nm) spectral regions. All spectra were collected at 25 °C in a buffer contained 10 mM Potassium Phosphate, 50 mM Na_2SO_4, and 1 mM DTT, pH 7.5 using an Applied Photophysics Pistar-180 spectrometer. Protein concentrations were 0.45 mM and 5 µM for near-UV and far-UV respectively.

C. Results

1. *The Vinculin Tail Domain Shows Specificity for PIP_2 Containing Vesicles* Although the tail domain of vinculin has been reported to bind acidic phospholipids and phosphatidylinositol 4,5-bisphosphate (PIP_2), the methods used to assess acidic phospholipid binding have varied significantly, making comparison of separate reports on lipid binding difficult[17, 19, 21, 22, 36, 37]. To clarify the affinity and specificity of Vt for PIP_2, we performed co-sedimentation experiments with mixed PE, PC, and PS vesicles, examining the effect of increasing PIP_2 concentration. Although Vt has previously been shown to bind to pure PS vesicles[21], we found that under physiologically relevant lipid and salt concentrations, no significant binding of Vt to PS containing vesicles was observed. In the absence of PIP_2, little co-sedimentation of Vt with mixed lipid vesicles containing 60% PC, 20% PE, and 20% PS vesicles was observed, in 150 mM NaCl (Figure 4.1). Upon the

addition of PIP_2 however, a clear concentration dependent co-sedimentation was observed, indicating that Vt specifically recognizes PIP_2.

The vinculin tail domain has also been reported to interact with pure phosphatidylinositol (PI) and phosphatidylserine (PS) vesicles. To ascertain the relative affinity of Vt for PI, PS, and PIP_2, Vt association was observed in mixed lipid vesicles containing each of these lipids. As shown in figure 4.2, Vt does not bind PI or PS significantly in the context of mixed lipid vesicles, and demonstrated a marked preference for PIP_2 over either PI or PS.

2. *Vt demonstrates loss of tertiary structure in lipid micelles and loses specificity for PIP_2*

As shown in figures 4.1 and 4.2, the vinculin tail domain shows enhanced association with PIP_2 in lipid co-sedimentation relative to PS and PI. In an effort to determine the site(s) of interaction between Vt with PIP_2, we employed circular dichroism (CD) and solution nuclear magnetic resonance (NMR) spectroscopy. In general, information derived from high resolution NMR decreases as the molecular size increases. Hence, we initiated studies of phospholipid interactions with Vt using micelles as opposed to larger vesicles. However, introduction of dodecylphosphocholine (DPC), at concentrations that promote micelle formation causes a collapse in Vt structure, as determined by both near-UV (ultraviolet) CD and ^{1}H-^{15}N heteronuclear 2D NMR.

Near-UV CD is sensitive to the tertiary packing of aromatic residues and therefore the tertiary structure of proteins. Far-UV CD is sensitive to the conformation of the peptide backbone and therefore the secondary structure of proteins. The far-UV CD of Vt exhibits only minor changes in the presence of 100 mM DPC indicating there is no significant change

in the secondary structure (Figure 4.3 A). The near-UV CD spectra, however, exhibits a significant los of signal, indicating a loss of tertiary structure (Figure 4.3 A).

The ^{1}H-^{15}N HSQC NMR spectra detect signals for protons attached to ^{15}N nuclei. The backbone NH of each amino acid (with the exception of proline) providing a residue specific probe sensitive to changes in its electrochemical environment. ^{1}H-^{15}N HSQC spectral dispersion arises from the unique environment of each distinct NH pair. Loss of a distinct, folded structure results in convergence of resonances toward random coil chemical shifts (centered at ~8.3 ppm). The significant loss of spectral dispersion seen in Vt in the presence of 100 mM DPC (Figure 4.3 B) is indicative of a significant loss in tertiary structure, in agreement with the near-UV CD. The residual dispersion seen also agrees with the persistence of helices suggested by far-UV CD.

Although Vt has been proposed to undergo a conformational change upon association with phospholipids[17], DPC micelles may act as a detergent causing unfolding of Vt. As Vt does not bind to PC containing vesicles, the interaction with DPC micelles may be non-specific. Adding to this possibility, a similar collapse in NMR chemical shift dispersion was observed in ^{1}H-^{15}N HSQC spectra of Vt in the presence of other micelles tested, including C-4 PIP_2 and 1-palmitoyl-2-hydroxy-sn-glycero-3-[phospho-RAC-(1-glycerol)] (LPPG) (data not shown).

Attempts to map the PIP_2 interaction site by NMR using the PIP_2 headgroup, D-myo-Inositol-1,4,5-triphosphate or a short chain (C8) derivative of PIP_2 were also unsuccessful (data not shown), as a clear, specific binding site was not observed. These results indicate that the head group alone does not have sufficient affinity for Vt to either bind specifically to Vt or promote a conformational change necessary for high affinity binding.

3. *Vt C-terminal residues stabilize its tertiary fold*

A C-terminal deletion Vt mutant reported to be deficient in lipid binding has been utilized in multiple studies[17, 19, 22, 23]. This mutant, VtΔC, lacks 15 C-terminal amino acids (1052-1066). The deletion of this fragment has been reported to decrease PIP_2 binding but does not significantly affect interaction with either actin or the head domain of vinculin[19, 23]. However, VtΔC shows increases susceptibility to protease degradation[19, 23] and alterations in one dimensional ^{1}H NMR spectra indicating loss of structure [23]. As residues in the C-terminus form tertiary interactions with other residues in the tail domain, the loss of these residues upon deletion could alter the structure and stability of Vt. In particular, the deletion results in removal of tryptophan 1058 (W1058) which packs against tryptophan 912 (W912) that is located at the bottom of helix 1, could alter Vt structure resulting in destabilization. Interestingly, both residues are conserved in all vinculins as well as α-catenin, a cell adhesion protein with high homology to vinculin[23, 38]. There is also an interaction of the C-terminus and the N-terminal strap of Vt seen in full length vinculin[17]. To better understand the role of the Vt C-terminus in lipid binding, we conducted NMR and CD analyses of the VtΔC variant. As reported previously, we found VtΔC to be significantly more susceptible to protease cleavage than wild-type Vt[19, 23]. The 2-D ^{1}H-^{15}N (NMR) spectra indicate that the C-terminal deletion results in significant loss of tertiary structure. As shown in Figure 4.4A, the ^{1}H-^{15}N HSQC spectra of wild-type Vt displays the spectral dispersion consistent with that of a well folded α-helical protein. In contrast, the ^{1}H-^{15}N spectrum of VtΔC exhibits increased overlap resulting from a collapse in chemical shift dispersion and an increase of resonances with random coil chemical shifts

(Figure 4.4 A). In addition, the majority of resonances exhibit chemical shift changes. These NMR data suggest loss of structural stability upon deletion of the C-terminal residues.

While the near UV CD (350-250 nm) of VtΔC could not be directly compared with wild-type Vt due to the removal two of the three tryptophan residues in the protein (Trp residues represent a majority of the near UV CD in proteins), far UV CD (260-190 nm) which is sensitive to the secondary structure of proteins, suggests that the helical content of wild-type Vt and VtΔC are nearly identical (Figure 4.4 B). Together, this data suggest that while the secondary structure of VtΔC is largely unaltered relative to wild-type Vt, its tertiary conformation and stability has been significantly altered.

Structural changes in VtΔC have been attributed at least in part to loss of W1058[23], however other residues present in the deleted C-terminal fragment have been suggested to be important for lipid binding. The "hydrophobic hairpin" (TPWYQ at the extreme C-terminus) has been postulated to be important for vinculin insertion into the membrane, and that R1057, R1060, and K1061 (part of the "basic collar") may be involved in binding acidic lipid headgroups[19, 22]. To elucidate the role of these residues in Vt structural integrity, we generated two new C-terminal deletion mutants, VtΔC5 and VtΔC7. VtΔC5 is a deletion which removes 5 amino acids from Vt that make up the hydrophobic hairpin (TPWYQ), whereas in VtΔC7, two additional amino acids are deleted, R1060 and K1061, which are part of the basic collar. As shown in Figure 4.5 A, the ^{1}H-^{15}N HSQC spectra of VtΔC5 is nearly identical to that of wild-type Vt, suggesting that the removal of these 5 amino acids has a minimal effect on the structure of the protein. In contrast, the ^{1}H-^{15}N HSQC spectra of VtΔC7 exhibits changes similar to those seen in VtΔC (chemical shift changes, increase in overlap, increase in resonances with random coil chemical shifts), although the comparative

spectra changes observed for VtΔC7 are not as significant as those observed for VtΔC (Figure 4.4 A and Figure 4.5 B). This NMR data indicates that R1060 and K1061 may play a role in maintaining the tertiary fold.

4. *The Role of the N-terminal Strap in PIP_2 binding*

A significant number of mutations have been made in Vt to assess their affect on lipid binding. In addition to the VtΔC deletion mutant, a variety of basic residues have been mutated, targeted predominately to residues in the the "basic collar" and "basic ladder"[17, 22, 23]. To elucidate lipid binding determinants in Vt, we characterized a series of mutants in both Vt (879-1066) as well as a shorter construct of Vt containing residues 884-1066[21]. For clarity, we will refer to the construct containing residues 884-1066 as VtΔN and the construct containing residues 879-1066 as wild-type Vt or simply Vt.

The N-terminus of Vt contains a "strap", which is found in an extended conformation along the interface of helices 1 and 2 in the crystal structure of full length vinculin[17]. The N-terminal strap is found in multiple conformations in the crystal structure of Vt, suggesting conformational flexibility. In the full length crystal structure, the N-terminal strap forms contacts with the main helical bundle through both phenylalanine 885 (F885) and aspartic acid 882 (D882). The side chain of F885 packs against the side chain of histidine 906 (H906) in helix 1, while D882 makes polar contacts with residues including S914 (helix 1-2 loop), K924 (helix 2), and K1061 and Y1065 in the C-terminus (Figure 4.6). Removal of 5 amino acids from the N-terminal strap of Vt (VtΔN) results in loss of D882, which makes multiple interactions with the helix bundle.and C-terminus

Intriguingly, we found the lipid binding capacity of VtΔN to be significantly different from wild-type Vt. While the lipid binding specificity of VtΔN was nearly identical to Vt (minimal binding to PS and PI, data not shown), the affinity for PIP_2 was considerably higher (Figure 4.7). As one of the points of interaction between the N-terminal strap and the helical bundle (D882) has been removed in VtΔN, we hypothesized that the enhancement observed in PIP_2 binding may be due to release or partial release of the strap. To test this hypothesis, we conducted lipid co-sedimentation assays on two mutants, Vt D882A and Vt H906A. Mutation of either of these residues should disrupt interactions with the N-terminal strap. In particular, mutation of H906 to alanine should disrupt packing with F885 while the aspartic acid to alanine mutation at 882 should disrupt polar contacts S914, K924, K1061, and Y1065. Results shown in figure 4.7, indicate that both mutants significantly increase the co-sedimentation of Vt with PIP_2 containing lipids, consistent with our hypothesis that release of the N-terminal strap increases PIP_2 binding.

As previously mentioned, we found that changes in the ^{1}H-^{15}N HSQC spectra of VtΔC are indicative of loss in structural relative to Vt, while VtΔC5, which removes only the hydrophobic hairpin at the C-terminus of Vt, shows similar NMR spectra to wild-type Vt indicating similar fold. As VtΔC5 does not appear to perturb the tertiary fold of Vt and is postulated to play a role in membrane insertion, we conducted lipid co-sedimentation experiments with VtΔC5. We found that similar to VtΔN, VtΔC5 significantly increases association with PIP_2 containing vesicles. Interestingly, in the crystal structure of vinculin, Y1065 (removed in VtΔC5) forms tertiary contacts with both D882 and S914 (which also appears to makes polar contact with D882), in the N-terminal strap and helix 1-2 loop, respectively, possibly linking the N and C-termini. Thus, the apparent increase in PIP_2

binding associated with the VtΔC5 mutant may results from the release of the contacts with D882, allowing for increased release of the N-terminal strap from the helical bundle.

D. Discussion

The regulation of the actin cytoskeleton, its connections to the cell membrane, and the linkage to neighboring cells or extra cellular matrix all play an integral part in many physiological and pathological processes. Cell processes including migration, differentiation, proliferation, and survival, along with larger scale processes such as tissue organization, wound healing, and tumorigenesis are all regulated in part by dynamic regulation of cell adhesions and the actin cytoskeleton[39-42]. Motility changes required for many of theses processes involves dynamic creation, stabilization, and turnover of sites of adhesion[43, 44], with vinculin playing an important role[5, 22, 23, 45, 46]. The activation and function of vinculin has been shown to be spatially and temporally regulated in cells, and vinculin has been associated with the strengthening of adhesions[47, 48]. Intriguingly, interactions with lipids play a role in the regulation of adhesion site turnover[22, 23]. The lipid binding function of vinculin is localized to the tail domain (Vt), which had been reported to bind to acidic phospholipids, including PS, PI, and PIP_2[20, 21]. Of these, PIP_2 is of particular interest as it is known to be an important regulator of the actin cytoskeleton[32]. As many of the reports of Vt lipid binding were in the context of pure lipid vesicles, we were interested in assessing binding in more physiological mixed lipid vesicles. We found that Vt does not bind significantly to vesicles containing PE, PC, and PS, while demonstrating a significant concentration dependent binding to PIP_2 containing vesicles (Figure 4.1). Although Vt has been shown to bind pure PI and PS vesicles, we observed only minimal co-sedimentation

with mixed lipid vesicles containing PI or PS (Figure 4.2). Local concentrations of PIP_2 are controlled by both synthesis and sequestration, and regulated by signaling pathways known to affect the actin cytoskeleton such as the Rho and Rac families of GTPases[31]. The selective affinity of vinculin for PIP_2 suggests this interaction may be a link in the regulation of actin cytoskeletal dynamics.

Our lipid co-sedimentation assays indicated that Vt exhibits marked affinity for PIP_2, but does not specifically associate with vesicles containing PE, PC, and PS. It is of interest to note that while vinculin does not appear to specifically bind phosphatidylcholine (PC), we see interactions with dodecylphosphocholine (DPC) micelles. In fact our CD and NMR data support loss of tertiary structure and lipid specificity upon association with micelles (Figure 4.3). These observations suggest that Vt may interact with lipid micelles acting as a detergent to unfold Vt. Therefore, micelles may not mimic physiological lipid interactions.

How PIP_2 interacts with Vt to modulate vinculin function remains unclear. Vinculin does not contain motifs known PIP_2 binding motifs[30], and mutation and deletions reported to block lipid binding have not identified a clear site of binding[17, 19-23]. Supporting the observations of Saunders, *et al* [23], our data supports a loss in structural stability associated with the C-terminal deletion mutant VtΔC (Figure 4.4). Hence, loss of lipid binding may result from an altered tertiary structure. In contrast, removal of the hydrophobic hairpin results in enhanced PIP_2 association and does not appear to alter Vt structure. Moreover, our results indicate that removal of the hydrophobic hairpin (TPWYQ) is not critical for lipid insertion, as previously proposed[19]. Removal of an additional two amino acids from the C-terminus, VtΔC7, causes spectral perturbations that may be indicative of a structural change, albeit not as extensive as those observed for VtΔC (Figure 4.5). These results indicate that

perturbations of contacts between the basic collar residues, R1060 and K1061, and both the bottom of helix 1 and the N-terminal strap, may alter Vt structure, which should be noted when interpreting the lipid binding data of Vt variants containing mutations at these positions.

Intriguingly, analysis of lipid binding data on multiple Vt mutants (VtΔN, D882A, and H906A), indicates that perturbation of interactions with the N-terminal strap of Vt enhances PIP_2 association (Figure 4.6 and 4.7). It is possible that the release of this strap may expose a surface important for lipid binding, allowing for the formation of a lipid binding surface not present in the closed conformation, or more readily allow a conformational change required for lipid binding. It is intriguing to speculate that residues in the basic collar (K911 and K924) become more accessible for interaction with PIP_2 upon release of the N-terminal strap, as these residues have been proposed to be important for PIP_2 association[17, 23]. It has also been reported that a rearrangement in the N-terminal strap of Vt may be required for F-actin binding[49], and that PIP_2 inhibits interactions of vinculin with F-actin[36, 50]. Rearrangement of the N-terminal strap of Vt may be a common requirement for the binding of either PIP_2 or F-actin, with both ligands sharing a mutually exclusive, overlapping site of interaction. This would be consistent with the hypothesis that PIP_2 binding may displace vinculin from F-actin, allowing focal adhesion turnover as has been proposed[22, 23].

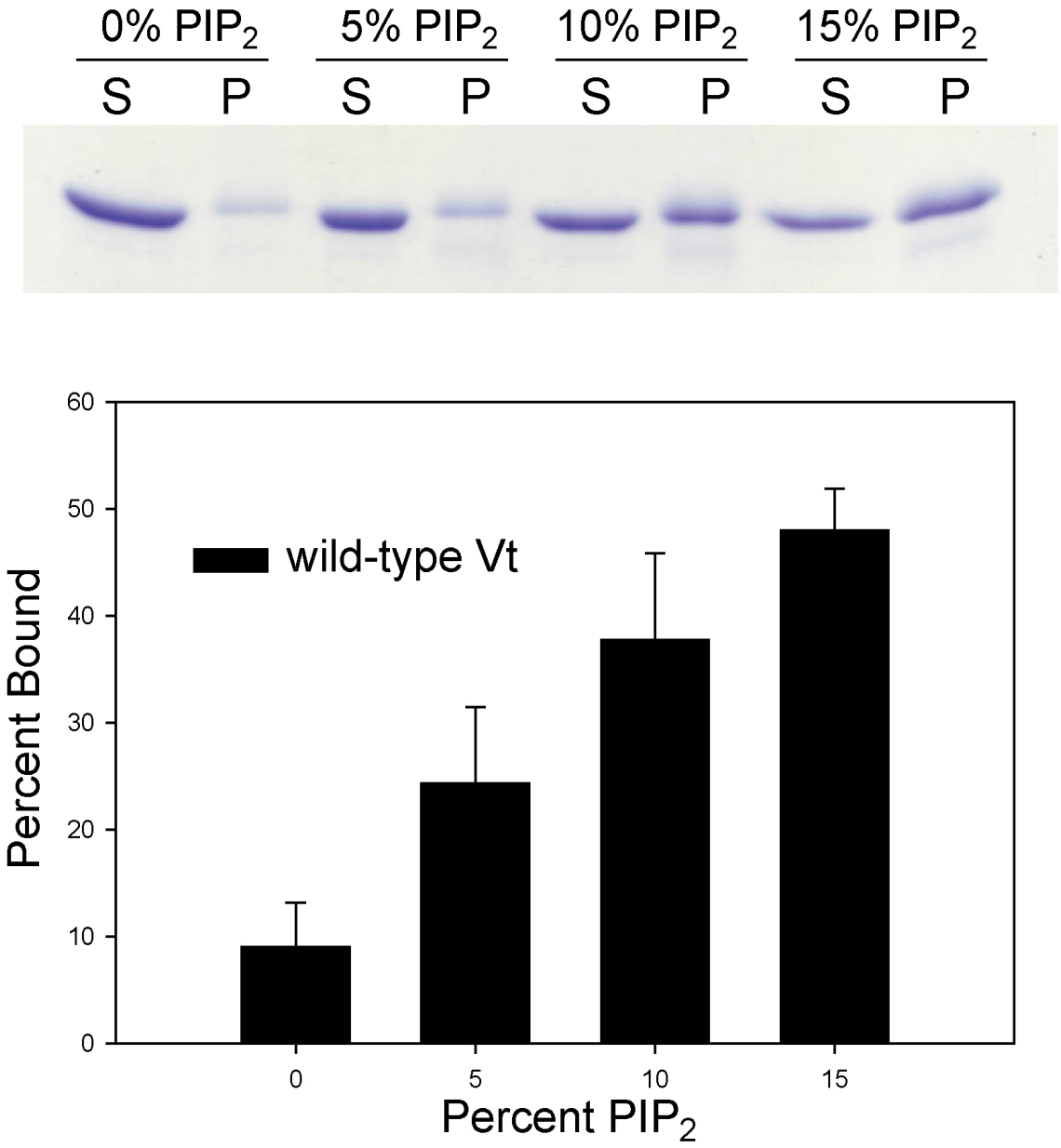

Figure 4.1: The lipid binding of wild-type Vt was examined by co-sedimentation studies with lipid vesicles containing 60% phosphatidylethanolamine (PE), 20% phosphatidylcholine (PC), and either 20% phosphatidylserine (PS) by weight or with phosphatidylinositol 4,5-bisphosphate (PIP_2) at concentrations that replace PS. Soluble (S) and pellet (P) fractions were analyzed by SDS polyacrylamide gel electrophoresis (stained with coomassie), and a representative gel is shown in A. Gels were scanned and the amount of protein in each fraction quantified using ImageJ software. Wild-type Vt shows minimal binding to vesicles containing 60% PE, 20% PC and 20% PS (displayed as 0% PIP_2), while exhibiting increasing association as PIP_2 concentrations are increased (B), suggesting a specific affinity for PIP_2.

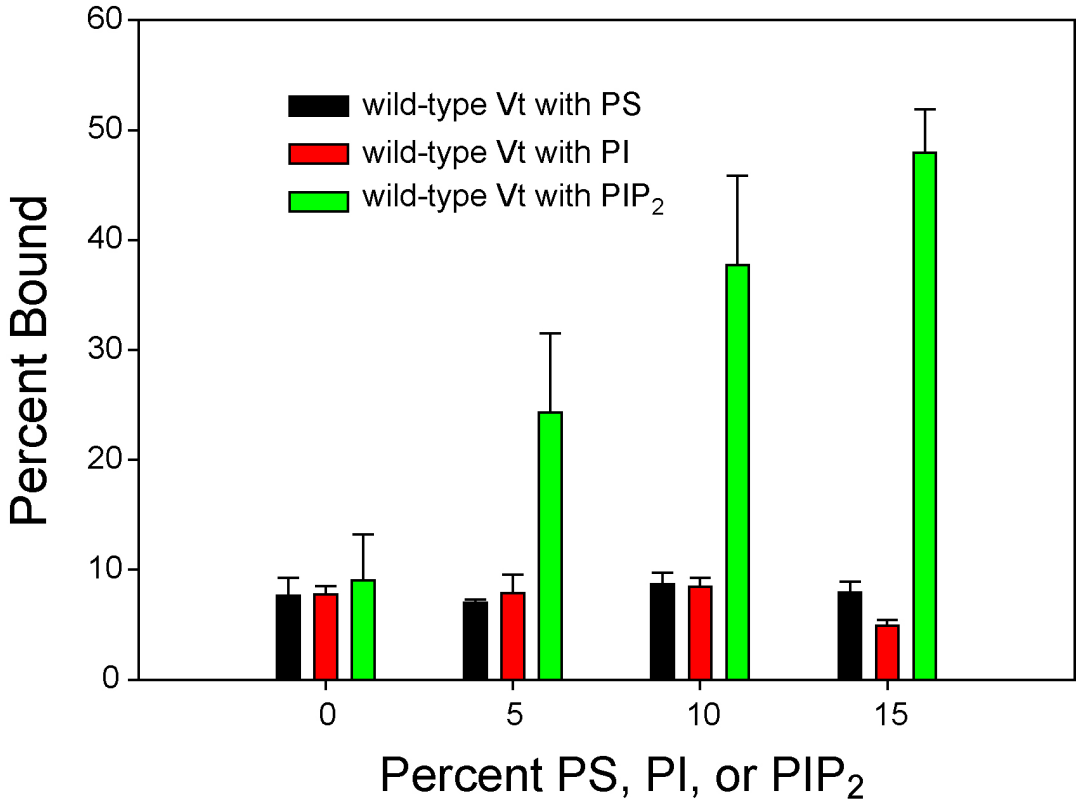

Figure 4.2: To compare the affinity of Vt for PS, PI, and PIP_2, co-sedimentation studies with mixed lipid vesicles containing PE, PC, and either PS and PI. Binding of PS and PI was minimal at concentrations up to 15%.

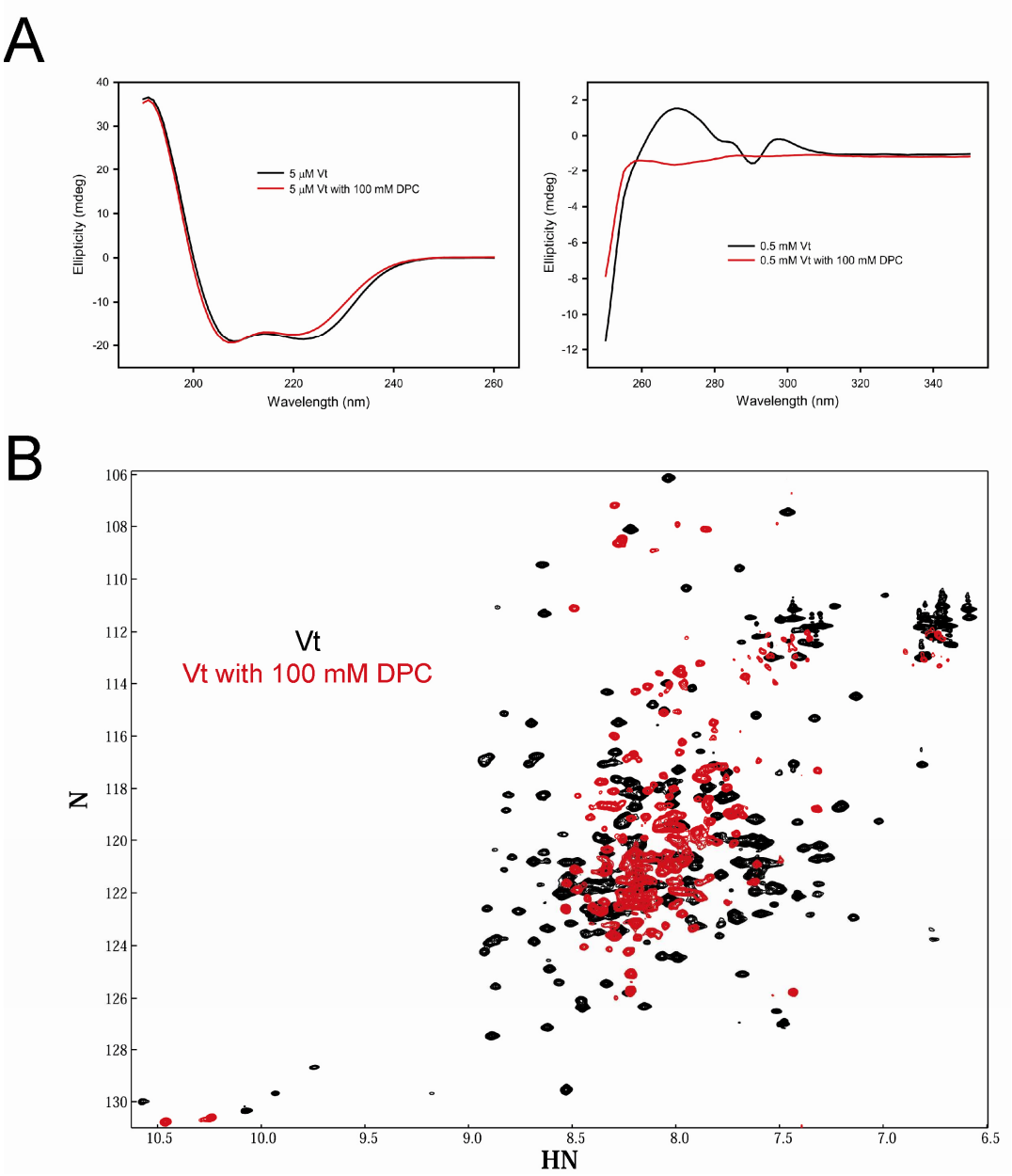

Figure 4.3: The structural effect of association with dodecylphosphocholine (DPC) micelles was assessed by CD and NMR. While the far UV CD of Vt in the presence of 100 mM DPC shows only minor alteration, the near UV CD is drastically reduced (A). This is consistent with a minor change in secondary structure in Vt due to interactions with DPC, but a significant change in tertiary structure. This is further supported by NMR studies. ^{1}H-^{15}N HSQC NMR spectra were collected on 0.15 mM Vt at pH 5.5, both alone and in the presence of 100 mM DPC (B). The loss of spectral dispersion and the increase in resonances with chemical shifts close to the random coil values (~8.3 ppm) suggest that Vt losses significant tertiary structure upon association with DPC micelles. As vinculin does not appear to specifically bind phosphatidylcholine (PC), interactions with dodecylphosphocholine (DPC) micelles are likely non-specific. In addition, Vt showed similar structural perturbation with all lipid micelles tested, suggesting that lipid micelles may act as a detergent, unfolding Vt.

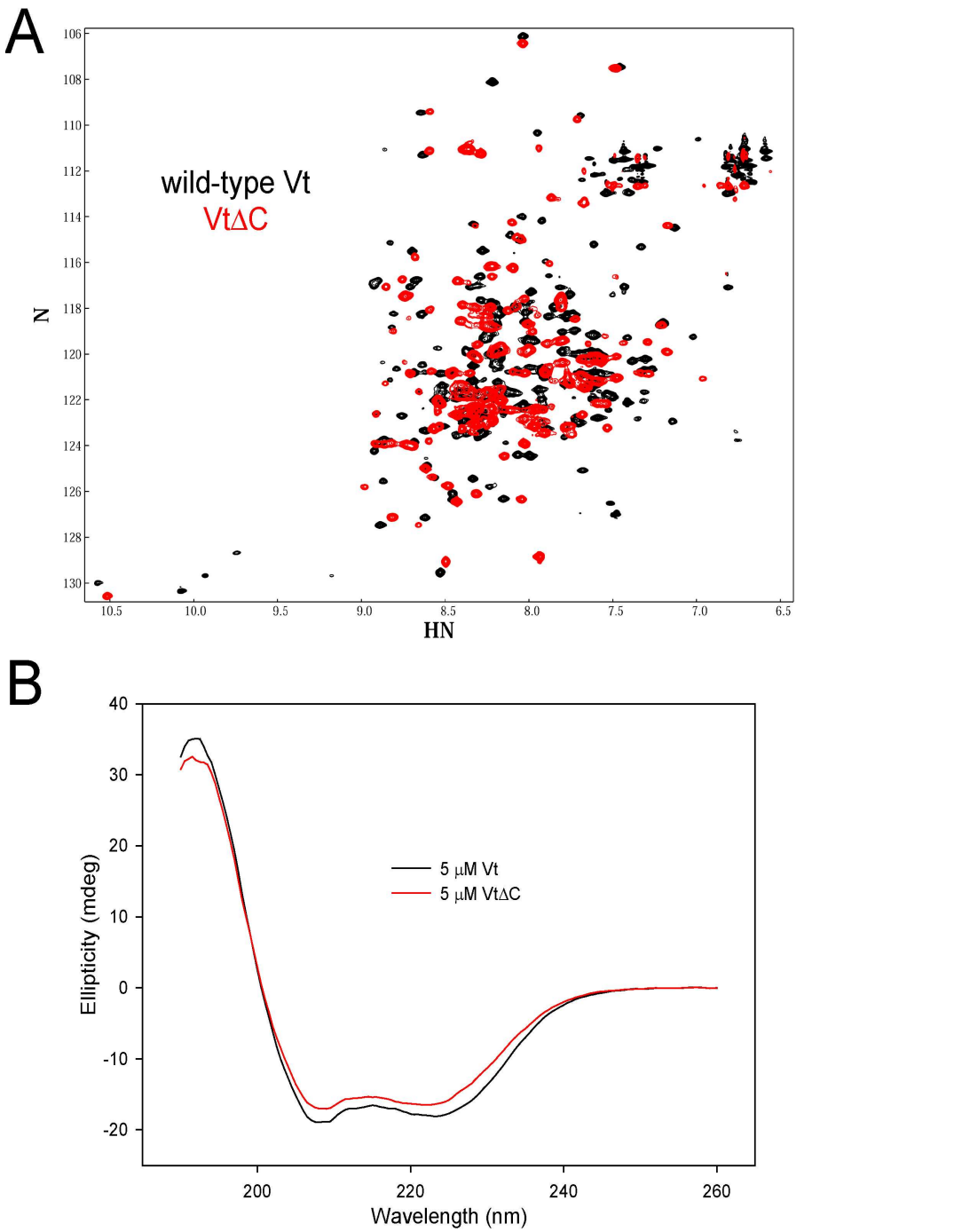

Figure 4.4: The deletion mutant, VtΔC, lacking the 15 C-terminal residues of Vt has been reported to be deficient in lipid binding. In order to assess possible structural perturbations due to this deletion, we conducted NMR and CD studies of VtΔC. The ^{1}H-^{15}N spectrum of VtΔC exhibits increased overlap resulting from a collapse in chemical shift dispersion and an increase of resonances with random coil chemical shifts (~8.3 ppm) (A). This is consistent with a loss of structural stability due to the C-terminal deletion. The far UV CD of VtΔC shows minor changes relative to wild-type Vt (B), suggesting only small alterations in the overall helical content.

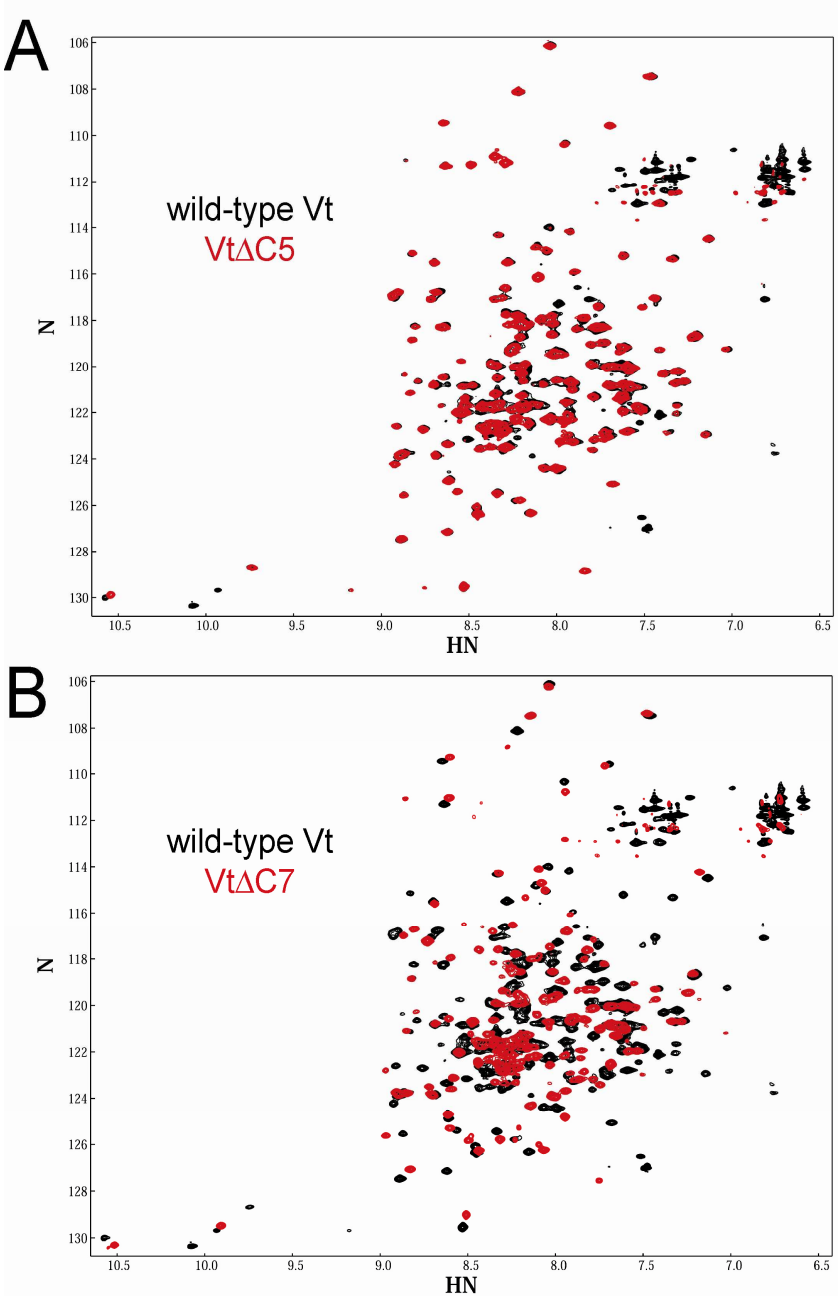

Figure 4.5: To assess the role the hydrophobic hairpin and C-terminal basic collar residues in Vt structure, two deletion mutant (VtΔC5 and VtΔC7) were created. VtΔC5 removes only the hydrophobic hairpin (the final five C-terminal residues), while VtΔC7 removes an additional two residues that are part of the basic collar (R1060 and K1061). As seen in A, the ^{1}H-^{15}N HSQC spectra of VtΔC5 is nearly identical to that of wild-type Vt, consistent with the deletion of the hydrophobic hairpin causing minimal changes to the structure of Vt. In contrast, the ^{1}H-^{15}N HSQC spectra of VtΔC7 shows exhibits changes similar to those seen in VtΔC (Figure 4.4), although not as drastic. The changes seen in the spectra of VtΔC are consistent with the deletion of R1060 and K1061 causing a loss in tertiary stability, suggesting these residues play a role in the tertiary stability of Vt.

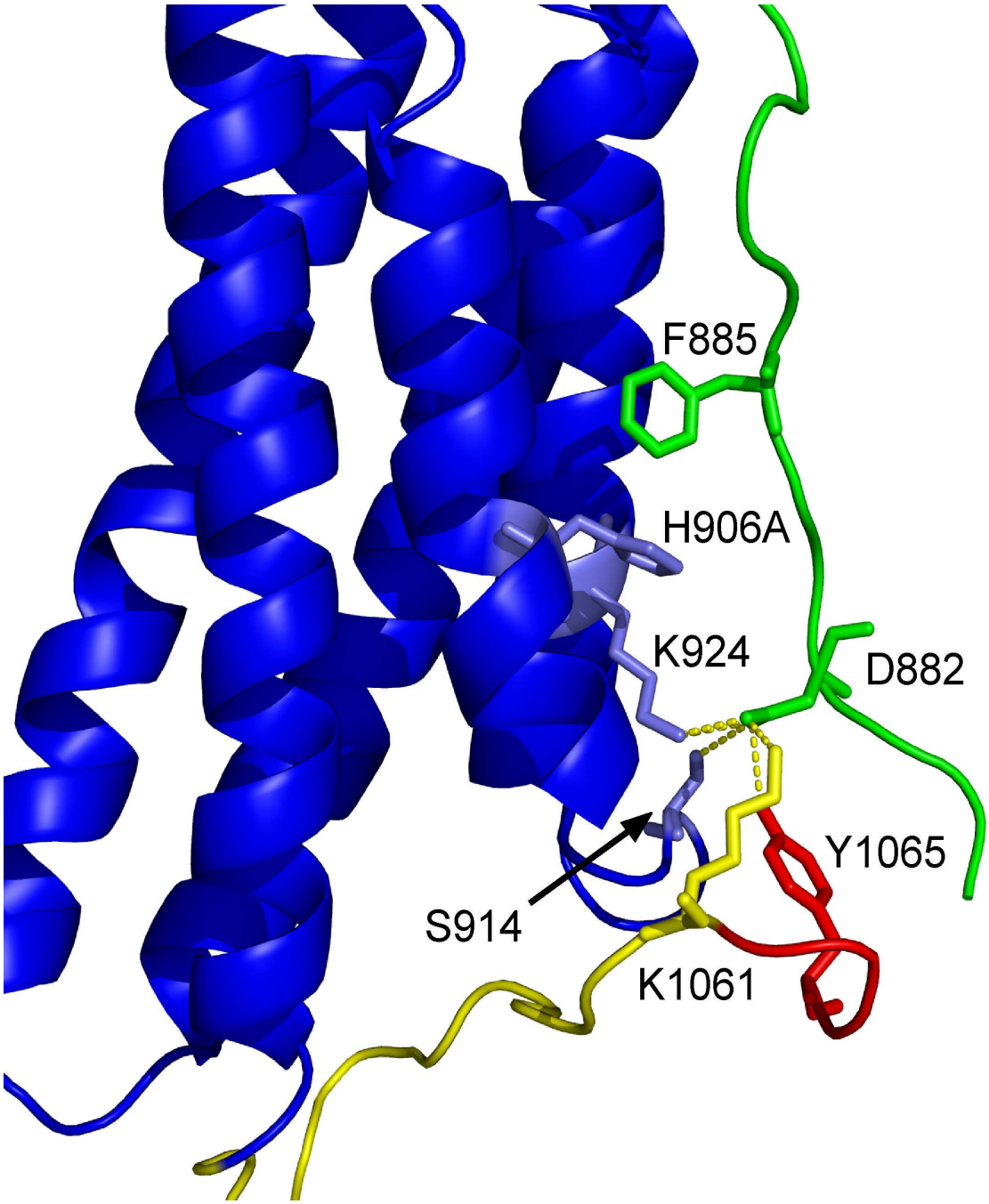

Figure 4.6: The structure of Vt (from 1ST6), highlighting the interactions of the N-terminal strap of Vt with the helix 1-2 interface and the C-terminus. The N-terminal strap of Vt is depicted in green, while the C-terminus is shown in yellow (with the hydrophobic hairpin shown in red). Two significant residues (F885 and D882) of the strap make interactions likely to stabilize the extended conformation of the strap, which packs against the helix 1-2 interface. F885 of the N-terminal strap packs against H906 of helix 1, while D882 makes polar interactions with S914 (helix 1-2 loop), K924 (helix 2), and K1061 and Y1065 in the C-terminus.

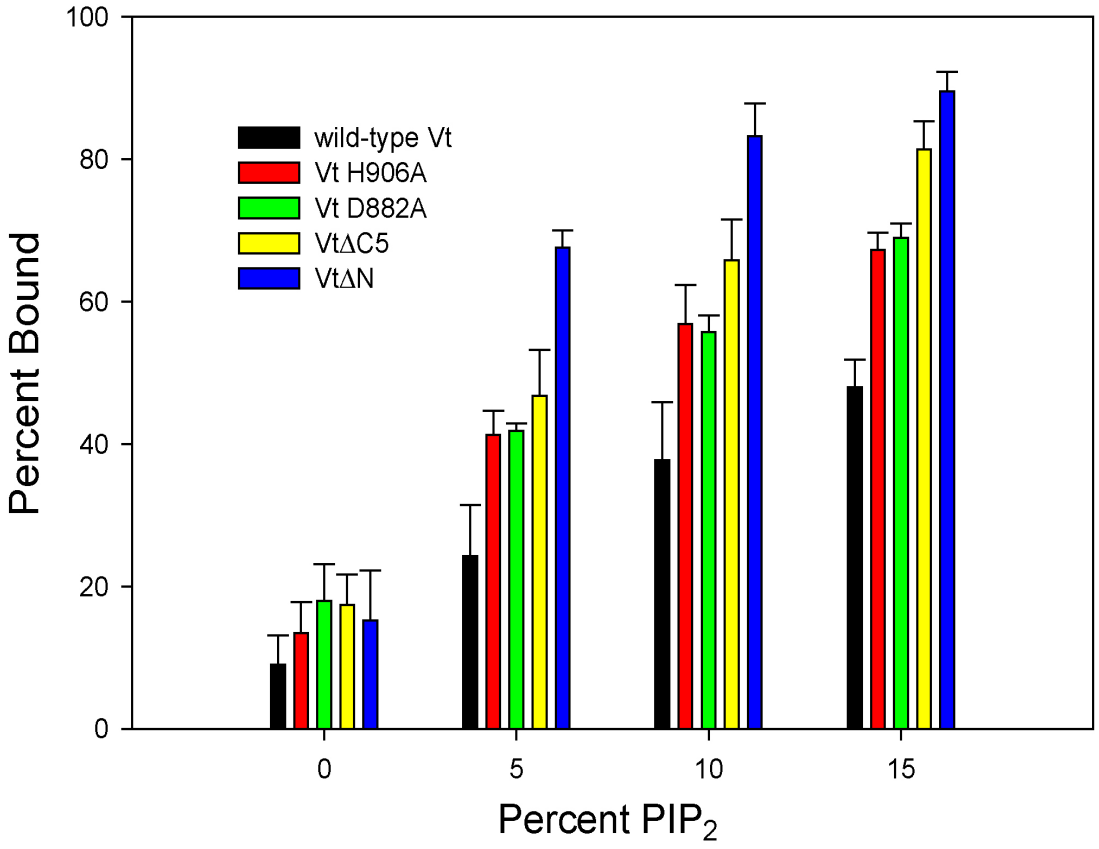

Figure 4.7: While wild-type Vt exhibits a PIP_2 dependent association with lipid vesicles, a number of mutant forms of Vt show marked increase in PIP_2 affinity. Of these, VtΔN, Vt D882A, and Vt H906A are all likely to allow for increased release of the N-terminal strap from its conformation packed along the helix 1-2 interface. Both VtΔN and Vt D882A remove D882, which makes polar interactions with residues in the helix 1-2 interface and the C-terminus. Vt H906A should disrupt the packing of F885. The increase in PIP_2 binding seen with these mutants is consistent with the hypothesis that a conformational change in the N-terminal strap of Vt facilitates high affinity lipid binding. VtΔC5 also exhibits increased association with PIP_2 containing vesicles, and either could also effect the conformation of the N-terminal strap (through loss of interactions with D882), or its removal may expose an occluded surface to allow lipid binding. For details of the structural interactions of D882, F885, H906A, and residues in the helix 1-2 interface and the C-terminus, see Figure 4.6.

E. Literature Cited

1. Geiger, B., et al., *Vinculin, an intracellular protein localized at specialized sites where microfilament bundles terminate at cell membranes.* Proc Natl Acad Sci U S A, 1980. **77**(7): p. 4127-31.

2. Belkin, A.M., et al., *Diversity of vinculin/meta-vinculin in human tissues and cultivated cells. Expression of muscle specific variants of vinculin in human aorta smooth muscle cells.* J Biol Chem, 1988. **263**(14): p. 6631-5.

3. Pardo, J.V., J.D. Siliciano, and S.W. Craig, *A vinculin-containing cortical lattice in skeletal muscle: transverse lattice elements ("costameres") mark sites of attachment between myofibrils and sarcolemma.* Proc Natl Acad Sci U S A, 1983. **80**(4): p. 1008-12.

4. Coll, J.L., et al., *Targeted disruption of vinculin genes in F9 and embryonic stem cells changes cell morphology, adhesion, and locomotion.* Proc Natl Acad Sci USA, 1995. **92**(20): p. 9161-5.

5. Subauste, M.C., et al., *Vinculin modulation of paxillin-FAK interactions regulates ERK to control survival and motility.* J Cell Biol, 2004. **165**(3): p. 371-81.

6. Xu, W., H. Baribault, and E.D. Adamson, *Vinculin knockout results in heart and brain defects during embryonic development.* Development, 1998. **125**(2): p. 327-37.

7. Xu, W., J.L. Coll, and E.D. Adamson, *Rescue of the mutant phenotype by reexpression of full-length vinculin in null F9 cells; effects on cell locomotion by domain deleted vinculin.* J Cell Sci, 1998. **111 (Pt 11)**: p. 1535-44.

8. Barstead, R.J. and R.H. Waterston, *Vinculin is essential for muscle function in the nematode.* J Cell Biol, 1991. **114**(4): p. 715-24.

9. Rodriguez Fernandez, J.L., et al., *Suppression of vinculin expression by antisense transfection confers changes in cell morphology, motility, and anchorage-dependent growth of 3T3 cells.* J Cell Biol, 1993. **122**(6): p. 1285-94.

10. Rodriguez Fernandez, J.L., et al., *Suppression of tumorigenicity in transformed cells after transfection with vinculin cDNA.* J Cell Biol, 1992. **119**(2): p. 427-38.

11. Vasile, V.C., et al., *Identification of a metavinculin missense mutation, R975W, associated with both hypertrophic and dilated cardiomyopathy.* Mol Genet Metab, 2006. **87**(2): p. 169-74.

12. Zemljic-Harpf, A.E., et al., *Heterozygous inactivation of the vinculin gene predisposes to stress-induced cardiomyopathy.* Am J Pathol, 2004. **165**(3): p. 1033-44.

13. Vasile, V.C., et al., *Obstructive hypertrophic cardiomyopathy is associated with reduced expression of vinculin in the intercalated disc.* Biochem Biophys Res Commun, 2006. **349**(2): p. 709-15.

14. Vasile, V.C., et al., *A missense mutation in a ubiquitously expressed protein, vinculin, confers susceptibility to hypertrophic cardiomyopathy.* Biochem Biophys Res Commun, 2006. **345**(3): p. 998-1003.

15. Molony, L. and K. Burridge, *Molecular shape and self-association of vinculin and metavinculin.* J Cell Biochem, 1985. **29**(1): p. 31-6.

16. Winkler, J., H. Lunsdorf, and B.M. Jockusch, *The ultrastructure of chicken gizzard vinculin as visualized by high-resolution electron microscopy.* J Struct Biol, 1996. **116**(2): p. 270-7.

17. Bakolitsa, C., et al., *Structural basis for vinculin activation at sites of cell adhesion.* Nature, 2004. **430**(6999): p. 583-6.

18. Ziegler, W.H., R.C. Liddington, and D.R. Critchley, *The structure and regulation of vinculin.* Trends Cell Biol, 2006. **16**(9): p. 453-60.

19. Bakolitsa, C., et al., *Crystal structure of the vinculin tail suggests a pathway for activation.* Cell, 1999. **99**(6): p. 603-13.

20. Johnson, R.P. and S.W. Craig, *The carboxy-terminal tail domain of vinculin contains a cryptic binding site for acidic phospholipids.* Biochem Biophys Res Commun, 1995. **210**(1): p. 159-64.

21. Johnson, R.P., et al., *A conserved motif in the tail domain of vinculin mediates association with and insertion into acidic phospholipid bilayers.* Biochemistry, 1998. **37**(28): p. 10211-22.

22. Chandrasekar, I., et al., *Vinculin acts as a sensor in lipid regulation of adhesion-site turnover.* J Cell Sci, 2005. **118**(Pt 7): p. 1461-72.

23. Saunders, R.M., et al., *Role of vinculin in regulating focal adhesion turnover.* Eur J Cell Biol, 2006. **85**(6): p. 487-500.

24. Kanaho, Y. and T. Suzuki, *Phosphoinositide kinases as enzymes that produce versatile signaling lipids, phosphoinositides.* J Biochem, 2002. **131**(4): p. 503-9.

25. Takenawa, T. and T. Itoh, *Phosphoinositides, key molecules for regulation of actin cytoskeletal organization and membrane traffic from the plasma membrane.* Biochim Biophys Acta, 2001. **1533**(3): p. 190-206.

26. Botelho, R.J., et al., *Localized biphasic changes in phosphatidylinositol-4,5-bisphosphate at sites of phagocytosis.* J Cell Biol, 2000. **151**(7): p. 1353-68.

27. Holz, R.W., et al., *A pleckstrin homology domain specific for phosphatidylinositol 4, 5-bisphosphate (PtdIns-4,5-P2) and fused to green fluorescent protein identifies plasma membrane PtdIns-4,5-P2 as being important in exocytosis.* J Biol Chem, 2000. **275**(23): p. 17878-85.

28. Honda, A., et al., *Phosphatidylinositol 4-phosphate 5-kinase alpha is a downstream effector of the small G protein ARF6 in membrane ruffle formation.* Cell, 1999. **99**(5): p. 521-32.

29. Stauffer, T.P., S. Ahn, and T. Meyer, *Receptor-induced transient reduction in plasma membrane PtdIns(4,5)P2 concentration monitored in living cells.* Curr Biol, 1998. **8**(6): p. 343-6.

30. Cullen, P.J., et al., *Modular phosphoinositide-binding domains--their role in signalling and membrane trafficking.* Curr Biol, 2001. **11**(21): p. R882-93.

31. McLaughlin, S., et al., *PIP(2) and proteins: interactions, organization, and information flow.* Annu Rev Biophys Biomol Struct, 2002. **31**: p. 151-75.

32. Yin, H.L. and P.A. Janmey, *Phosphoinositide regulation of the actin cytoskeleton.* Annu Rev Physiol, 2003. **65**: p. 761-89.

33. Rasband, W.S., *ImageJ, U. S. National Institutes of Health, Bethesda, Maryland, USA, http://rsb.info.nih.gov/ij/.* 1997-2007.

34. Delaglio, F., et al., *NMRPipe: a multidimensional spectral processing system based on UNIX pipes.* J Biomol NMR, 1995. **6**(3): p. 277-93.

35. Johnson, B.A. and R.A. Blevins, *NMR View: A computer program for the visualization and analysis of NMR data.* J Biomol NMR, 1994. **4**(5): p. 603-614.

36. Gilmore, A.P. and K. Burridge, *Regulation of vinculin binding to talin and actin by phosphatidyl- inositol-4-5-bisphosphate.* Nature, 1996. **381**(6582): p. 531-5.

37. Miller, G.J. and E.H. Ball, *Conformational change in the vinculin C-terminal depends on a critical histidine residue (His-906).* J Biol Chem, 2001. **276**(31): p. 28829-34.

38. Pokutta, S. and W.I. Weis, *Structure of the dimerization and beta-catenin-binding region of alpha-catenin.* Mol Cell, 2000. **5**(3): p. 533-43.

39. Berrier, A.L. and K.M. Yamada, *Cell-matrix adhesion.* J Cell Physiol, 2007. **213**(3): p. 565-73.

40. Danen, E.H. and A. Sonnenberg, *Integrins in regulation of tissue development and function.* J Pathol, 2003. **201**(4): p. 632-41.

41. Delon, I. and N.H. Brown, *Integrins and the actin cytoskeleton.* Curr Opin Cell Biol, 2007. **19**(1): p. 43-50.

42. Kedrin, D., et al., *Cell motility and cytoskeletal regulation in invasion and metastasis.* J Mammary Gland Biol Neoplasia, 2007. **12**(2-3): p. 143-52.

43. Moissoglu, K. and M.A. Schwartz, *Integrin signalling in directed cell migration.* Biol Cell, 2006. **98**(9): p. 547-55.

44. Ridley, A.J., et al., *Cell migration: integrating signals from front to back.* Science, 2003. **302**(5651): p. 1704-9.

45. Goldmann, W.H. and D.E. Ingber, *Intact vinculin protein is required for control of cell shape, cell mechanics, and rac-dependent lamellipodia formation.* Biochem Biophys Res Commun, 2002. **290**(2): p. 749-55.

46. Humphries, J.D., et al., *Vinculin controls focal adhesion formation by direct interactions with talin and actin.* J Cell Biol, 2007. **179**(5): p. 1043-57.

47. Chen, H., et al., *Spatial distribution and functional significance of activated vinculin in living cells.* J Cell Biol, 2005. **169**(3): p. 459-70.

48. Galbraith, C.G., K.M. Yamada, and M.P. Sheetz, *The relationship between force and focal complex development.* J Cell Biol, 2002. **159**(4): p. 695-705.

49. Janssen, M.E., et al., *Three-dimensional structure of vinculin bound to actin filaments.* Mol Cell, 2006. **21**(2): p. 271-81.

50. Steimle, P.A., et al., *Polyphosphoinositides inhibit the interaction of vinculin with actin filaments.* J Biol Chem, 1999. **274**(26): p. 18414-20.

Chapter V.

Conclusion

A. Introduction

Vinculin is a highly conserved and abundant cytoskeletal protein involved in linking the actin cytoskeleton to sites of adhesion[1]. Vinculin localizes to specialized multi-protein involved in various types of cellular adhesion, including adherence junctions (cell-cell adhesion), focal adhesions (cell-extracellular matrix adhesion), costameres (linkage between the force producing sacromeres and the cell membrane in muscle cells), and intercalated discs (specialized adhesions between adjacent cardiac cells)[1-4]. Vinculin is critical in development, as vinculin null mice die in early embryogenesis with heart and brain defects[5]. Vinculin has the properties of a tumor suppressor, and reduction in vinculin expression in cells results in increased motility, increases invasiveness, resistance to apoptosis and anoikis, and the ability to grow in soft agar[6-10]. In addition, transfection of vinculin cDNA into cancer cells lines causes a drastic suppression of tumorigenicity[11]. Vinculin also plays a role in cardiovascular health, and both mutations or reduction in vinculin expression has been linked to cardiomyopathies in human patients[12-14].

Vinculin is a 116 kDa protein consisting of three domains; a head domain (Vh), and flexible neck, and a tail domain (Vt). Each vinculin binds a number of ligands, including talin, α-actinin, α-catenin, β-catenin, and the bacterial virulence factor IpaA for the head domain, vinexin, ponsin, the Arp 2/3 complex, and the vasodilator-stimulated phosphoprotein

(VASP) for the neck domain, and F-actin, paxillin, protein kinase C-α (PKCα), and acidic phospholipids for the tail domain[15]. In addition, the head and tail domain interact, forming a closed, auto-inhibited conformation which must be released in order to bind many important ligands, including F-actin, talin, α-actinin, VASP, PKCα, the Arp2/3 complex, and acidic phospholipids[16-22]. Current models of vinculin activation and function suggest a combinatorial activation mechanism requiring the interaction of ligand on both the head and tail domains, and that the activation of vinculin is regulated both spatially and temporally[15, 23, 24]. Conformational changes in both the head and tail domain have also been proposed to play a critical role in vinculin function[25-33].

Despite significant research, both the physiological role and detail structural information about many of vinculin's ligand interactions is still unclear. Multiple proposed conformational changes in Vh and Vt are also not well understood. In order to elucidate the role of vinculin in both physiological and pathological processes including, development, cancer, and cardiovascular health, a details understanding of vinculin activation, ligand binding, and conformational changes is required. My doctoral dissertation has focused on increasing the understanding of conformation changes and ligand binding of the tail domain of vinculin. I have addressed the following topics:

- Backbone ^{1}H, ^{13}C, and ^{15}N NMR Assignments of the Tail Domain of Vinculin
- The Role of pH and Histidine 906 in Vinculin Tail Conformation
- Vinculin Tail and Lipid Binding

B. Backbone ^{1}H, ^{13}C, and ^{15}N NMR Assignments of the Tail Domain of Vinculin

1. *Summary of Results*

a) The majority of the backbone $^{1}H_{N}$, ^{15}N, $^{13}C_{\alpha}$, ^{13}CO, and side chain $^{13}C_{\beta}$ NMR resonance assignments of the tail domain of vinculin were determined.

2. *Implications*

Multidimensional nuclear magnetic resonance (NMR) spectroscopy can provide atom specific probes of the electrochemical environment of proteins in solution. This makes NMR uniquely suited to the study of protein structure, dynamics, and ligand binding. However, a prerequisite of atom specific studies of proteins by NMR is the assignment of the observed resonances. Assignment of the protein backbone NMR resonances provides residue specific probes sensitive to a variety of perturbations. Changes in the chemical shift and/or intensity of a resonance are signs of changes in the electrochemical environment of the corresponding amino acid, and can represent changes in protein conformation, dynamics, or alterations due to ligand binding.

The majority of the backbone $^{1}H_{N}$, ^{15}N, $^{13}C_{\alpha}$, ^{13}CO, and side chain $^{13}C_{\beta}$ NMR resonance assignment were determine for wild-type Vt at pH 5.5. Backbone amide proton assignments were extended to pH 7.5. The NMR resonance assignments for the backbone of Vt has allowed the residue specific analysis of the effect of pH, both point and deletion mutations, and ligand binding on the structure and conformation of Vt.

3. *Current and Future Directions*

The NMR resonance assignments of Vt, deposited in the Biological Magnetic Resonance Data Bank (BMRB), serve as a basis for current and future NMR studies of Vt. Current and future work in the Campbell lab that has and will benefit from the NMR resonance assignments of Vt may include:

- Assessing perturbations in Vt resulting from mutagenesis
- Mapping the site of interaction on Vt for the LD2 peptide of paxillin
- Further characterization of the Vt self-association of Vt, and its effect on F-actin bundling
- Determining the site of interaction of actin on Vt

In addition, as the assignments have been publicly deposited, they may also be used by additional research groups as a starting point for their own NMR studies of Vt.

While the majority of the ^{1}HN, ^{15}N, ^{13}Cα, ^{13}CO, and side chain ^{13}Cβ NMR resonance assignments of Vt have been determined, full backbone and side chain assignments has not been completed due to intrinsic difficulties with the system. Vt self-association, dynamics, and conformational exchange may have all contributed to making complete assignments impractical. If it is determined that further resonance assignments are required for future experiments, additional strategies could be used to determine additional assignments. These strategies may include selective mutagenesis to decrease self-association and selective isotopic labeling to decrease spectral overlap and possible resonance assignments. Additionally, if the question about structural or dynamic properties of Vt arise, more complete assignments may be possible with Vt variants which decrease self-association.

C. The Role of pH and Histidine 906 in Vinculin Tail Conformation

1. *Summary of Results*

a) Mutation of Histidine 906 to Alanine does not significantly alter Vt structure.

b) There is no significant conformational change in Vt between pH 5.5 and 7.5, and the effect of pH on Vt and the variant, Vt H906A, are virtually indistinguishable.

c) Vt self-associates at both pH 5.5 and 7.5, however the interaction is weak and may not be physiologically relevant.

2. *Implications*

The tail domain of vinculin was reported to undergo a H906-dependent conformational change as a function of pH and acidic phospholipid binding. In addition, H906 was reported to be important for Vt self-association at low pH 5.5[33]. These results suggested that H906 and its protonation state may play an important role in Vt conformational changes, which could play a part in vinculin activation and function.

In order to clarify the role of H906 in both pH and lipid dependent Vt conformational changes, we first assessed the effect of the histidine to alanine mutation at position 906 in Vt, as this variant, Vt H906A, was used in the studies implicating H906 in conformational changes in Vt[33]. We found no indication of a significant change in the overall conformation of Vt H906A, relative to wild-type Vt. Circular dichroism spectra, both at both near and far ultraviolet wavelengths (350-250 nm and 260-190 nm respectively), show no significant difference between wild-type Vt and Vt H906A. We also collected and compared

2 D ^{1}H-^{15}N Heteronuclear Single Quantum Coherence (HSQC) NMR spectra of wild-type Vt and Vt H906A. Comparison of the chemical shift and intensity changes associated with the HN resonances, indicate that the mutation of H906 to alanine may cause localized perturbation in the N-terminal strap, but the overall conformation of the helical bundle is unaltered. Although changes in HN resonances in HSQC spectra can not be conclusively interpreted in terms of specific changes in conformation, the spectral differences between wild-type Vt and Vt H906A are consistent with a change in the packing of the N-terminal strap of Vt. In the crystal structure of vinculin, this N-terminal strap is packed along the helix 1-2 interface in an extended conformation[25]. F885 in the N-terminal strap packs against H906 (in helix 1), and disruption of this interaction would likely alter the packing of the strap. Protonation of the H906 side chain could in theory disrupt the interaction with F885. To test this possibility, we assessed pH dependent changes in both CD and NMR spectra of Vt and Vt H906A.

In contradiction to the work of Miller *et al*, our data suggests that there is no significant conformational change in Vt between pH 5.5 and pH 7.5. Moreover, the localized spectral changes as a function of pH observed by NMR are virtually identical for Vt and Vt H906A, indicating that H906 does not play a critical role in any significant pH dependent effects. Furthermore, pH dependent chemical shift changes in the N-terminal strap and helix 1 and 2 for both wild-type Vt and Vt H906A are small (less than 0.05 ppm on average). This is consistent with the hypothesis that protonation of the side chain of H906, between pH 5.5 and 7.5, does not cause a significant conformational change in the N-terminal strap. By comparison, the chemical shift changes between wild-type Vt and Vt H906A are more

substantial (up to 0.3 ppm), suggesting that mutation of H906 to alanine perturbs interactions with the N-terminal strap more so, than does the protonation of the H906 side chain.

We also analyzed the self-association of both Vt and Vt H906A at pH 5.5 and 7.5. While Miller *et al* reported that Vt was monomeric at pH 7.5 but self-associated at low pH, we found that Vt self-association was present at both pH 5.5 and 7.5. Sedimentation equilibrium analytical ultracentrifugation (AUC) indicated that Vt self-association is greater at pH 7.5 than pH 5.5, however the interaction is weak (K_d >100 μM) at both pH values. Given K_d's determined by AUC, this self-association may not be physiologically significant. Vt H906A was also determined to self-associate at both pH 5.5 and 7.5, with a greater association at higher pH, as was observed with wild-type Vt. While the K_d for Vt H906A self-association was 190 ± 30 μM relative to 130 ± 10 μM for wild-type Vt at pH 7.5, it is not clear if this difference is significant.

3. *Current and Future Directions*

Our data suggests that there are no significant pH dependent conformation changes in Vt, and therefore pH is not likely to play a role in the Vinculin activation or function. With no link evident between ligand dependent conformational changes and pH, there is no data to suggest that pH changes over a physiologically relevant pH range play a role in modulating vinculin function, via either Vt-dependent ligand or self-association. As such, without additional data to suggest a role for pH dependent functional changes, further study of pH effects on Vt is not warranted. There are two remaining points of interest in this research; release of the N-terminal strap, and Vt self-association.

NMR spectral comparison of wild-type Vt and VtH906A HN resonances suggest that there is no significant alteration in the main helical bundle due to mutation of histidine 906 to alanine. There is, however, evidence to suggest that that the N-terminal strap may be altered due to loss of the interaction between H906 (in helix 1) and F885 (in the strap). This alteration in the N-terminal strap due to mutation of H906 is of particular interest as it appears to play a role in Vt/ligand interactions. In particular, Vt H906A and other mutant forms of Vt that appear to perturb interactions between the N-terminal strap and the helix 1-2 interface enhance Vt-PIP_2 association (see Chapter 4). Further characterization of the alterations in the N-terminal strap of these mutants (including H906A) may elucidate binding determinants and/or conformational changes associated with phospholipid binding. In addition, the N-terminal strap of Vt has been suggested to change conformation to accommodate F-actin binding, and possibly play a role in F-actin bundling[31]. The mutant characterized in these studies, Vt H906A, may be useful in elucidating the role of the N-terminal strap of Vt in F-actin binding and bundling.

We found that the Vt self-association occurs at both pH 5.5 and pH 7.5, with a small increase in affinity at pH 7.5. This is in contrast to previous work suggesting that that Vt self-association only at the lower pH[33]. The degree of self-association at either pH is weak (K_d > 100 μM). Despite the significant levels of vinculin found in cells and the possibility of increased localized concentration, this weak self-association may not be able to compete with other ligand interactions that may bind with higher affinity. For example, the Vh-Vt interaction has an estimated K_d of ~1 nM[25], and may inhibit Vt self-association. With the K_d of self-association >100 μM, this interaction may not be physiological relevant unless it is modulated by the binding of additional ligands. Self-association of Vt in the presence of

ligands is thought to be physiologically important. Vt has been reported to self-associate in the presence of both actin and phospholipids, with Vt dimerization postulated to be critical for F-actin bundling[31, 32, 34]. However, it is unclear whether the self-association observed in solution in the absence of ligands, is related to or distinct from ligand induced Vt self-association. The Vt dimer that promotes F-actin bundling may be either 1) a separate, cryptic site of self-association not accessible in the conformation present in solution, or 2) an allosteric enhancement of the ligand-free self-association site. Characterization of the ligand-free self-association observed in solution by NMR has suggested that the site of interaction is similar to the dimer interface identified in the crystal structure of Vt[26]. Characterization of mutations designed to disrupt this ligand-free self-association is underway, and these mutants may aid in understanding the role of Vt dimerization in F-actin binding and bundling.

D. Vinculin Tail and Lipid Binding

1. *Summary of Results*

a) Vt shows little affinity for mixed lipid vesicles containing 20% phosphatidylserine

b) A concentration dependent co-sedimentation of Vt with PIP_2 containing vesicles indicates specific recognition of PIP_2.

c) Although Vt has been reported to bind pure phosphatidylinositol (PI) vesicles, we find that that the affinity for PI containing vesicles is significantly reduced compared to PIP_2.

d) Vt demonstrates a loss of tertiary structure and lipid specificity in the presence of micelles, suggesting Vt interactions with micelles do not mimic physiological lipid interactions.

e) The C-terminal deletion mutant, VtΔC, shows a loss of tertiary structure, which may contribute to its loss of lipid binding. In addition to W1058 (proposed to be C-terminal residue important for tertiary structure[35]), R1060 and K1061 also appear important for maintaining the structural integrity of the Vt helical bundle fold.

f) The "hydrophobic hairpin" (TPWYQ) at the extreme C-terminus does not appear to be important for lipid insertion as previously proposed[26].

g) Release of the N-terminal strap of Vt facilitates higher affinity interactions with PIP_2 containing vesicles.

2. *Implications*

The tail domain of vinculin has been reported to bind acidic phospholipids, including phosphatidylserine (PS), phosphatidylinositol (PI), and phosphatidylinositol 4,5-bisphosphate (PIP_2)[18, 25, 26, 36]. Methods used to assess phospholipid binding have varied significantly, making comparative literature studies of Vt and mutant Vt lipid binding profiles difficult. We demonstrated that Vt exhibits minimal binding to mixed lipid vesicles containing 60% phosphatidylethanolamine (PE), 20% phosphatidylcholine (PC), and 20% phosphatidylserine (PS). The major components of eukaryotic membrane are PC, PE, PS, and PI[37]. Previous demonstrations of PS binding utilized pure PS vesicles, however PS is generally believed to constitute only 5-10% of the plasma membrane[37, 38]. The lack of Vt binding to mixed vesicles containing 20% PS suggests that the binding of PS may not

physiologically significant. In contrast, we demonstrated that Vt associates with mixed lipid vesicles in a PIP_2 concentration dependent manner, with significant association at 15% PIP_2. Although PIP_2 is a minor constituent of plasma membranes (0.1-5%), it is known to be enriched in focal adhesion[39, 40], and is known to directly regulate the actin cytoskeleton through modulating the activation and localization of cytoskeletal and regulatory proteins[41]. The specific affinity of Vt for PIP_2 suggests that this interaction may play a physiological role at sites of adhesion. One proposed function of the Vt-PIP_2 interaction is in the turnover of focal adhesions, a process critical to cellular motility.

Micelles have been used in studies of Vt lipid binding, however our data suggests that Vt interaction with micelles may not be physiologically relevant. In addition to a significant loss of tertiary structure upon interaction with micelles, Vt appears to loose all lipid specificity. Thus, lipid micelles may act as a detergent, unfolding Vt, and caution should be taking in interpreting reports of Vt-lipid binding based on methods utilizing lipid micelles.

As has been suggested previously, we found evidence that the C-terminal deletion mutant, VtΔC, exhibits a loss in tertiary structure and stability. Thus, the decrease in phospholipid binding observed with this mutant may be due to a loss in tertiary structure, rather than disruption of specific phospholipid interactions with the C-terminus. Moreover, the proposed role of the hydrophobic hairpin in membrane insertion (based on studies of VtΔC), does not appear to be correct. We demonstrated that the removal of the hydrophobic hairpin (VtΔC5) likely has minimal effects on the structure or conformation of Vt, while lipid binding is actually increased. These results suggest that insertion of the hydrophobic hairpin into lipid membranes is not a critical factor in lipid binding.

In addition to the hydrophobic hairpin in the C-terminus of Vt, two basic surfaces have been proposed as site of lipid interaction; the basic collar and the basic ladder[25, 26, 28]. Distinct from these two sites, we have identified the N-terminal strap of Vt as an important element in phospholipid binding. Our evidence indicates that the release of the strap from its interaction with the helix 1-2 interface enhances lipid binding, suggesting that a conformational change in the N-terminal strap of Vt may play a role in vinculin function. Although residues responsible for PIP_2 binding and specificity have not yet been conclusively identified, release of the strap may possibly increase the accessibility of K911 and K924, both residues postulated to be important for lipid binding[25, 35]. Interestingly, multiple ligand interaction sites, including those of vinexin, ponsin, and the Arp 2/3 complex, have been identified in the flexible neck region of vinculin, directly proceeding the strap of Vt[15]. The binding of ligand to the neck region of vinculin could affect the N-terminal strap of Vt, facilitation lipid binding, or conversely, Vt-lipid interaction could also cause a conformational change in the strap, facilitating ligand binding to the neck of vinculin.

3. *Current and Future Directions*

Although we have identified the N-terminal strap of Vt as an important factor in lipid binding, the mode and exact site of lipid interaction is still unclear. Multiple mutations have been identified that increase lipid binding, however Vt mutations which disrupt lipid binding, without significantly alter Vt structure, have not been identified. Basic collar residues and residues which would likely be exposed by release of the N-terminal strap of Vt can be mutated, and the effects of such mutations assessed. These residues may include R910, K911, and K924. Further complicating Vt lipid binding, it has been proposed that Vt may

undergo a significant conformational change upon interaction with lipids. Although we do not believe that the loss of tertiary structure seen upon interactions with lipid micelles is physiological, we have not been able to assess effects of interactions with lipid vesicles on the structure of Vt. If Vt undergoes a significant conformational change upon lipid binding, the site of PIP_2 interaction may not present in the crystal structure, complicating its identification. One method of assessing changes in the conformation of Vt upon lipid binding is the comparison of Vt's protease sensitivity in the presence or absence of lipid vesicles. Changes in the extent, or pattern of protease digestion could indicate whether a conformational change occurs upon phospholipid binding. In addition, mass spectrometry may aid in identification of sites of altered cleavage, which could indicate regions of Vt undergoing conformational changes.

E. Literature Cited

1. Geiger, B., et al., *Vinculin, an intracellular protein localized at specialized sites where microfilament bundles terminate at cell membranes.* Proc Natl Acad Sci U S A, 1980. **77**(7): p. 4127-31.

2. Belkin, A.M., et al., *Diversity of vinculin/meta-vinculin in human tissues and cultivated cells. Expression of muscle specific variants of vinculin in human aorta smooth muscle cells.* J Biol Chem, 1988. **263**(14): p. 6631-5.

3. Pardo, J.V., J.D. Siliciano, and S.W. Craig, *A vinculin-containing cortical lattice in skeletal muscle: transverse lattice elements ("costameres") mark sites of attachment between myofibrils and sarcolemma.* Proc Natl Acad Sci U S A, 1983. **80**(4): p. 1008-12.

4. Rudiger, M., et al., *Differential actin organization by vinculin isoforms: implications for cell type-specific microfilament anchorage.* FEBS Lett, 1998. **431**(1): p. 49-54.

5. Xu, W., H. Baribault, and E.D. Adamson, *Vinculin knockout results in heart and brain defects during embryonic development.* Development, 1998. **125**(2): p. 327-37.

6. Coll, J.L., et al., *Targeted disruption of vinculin genes in F9 and embryonic stem cells changes cell morphology, adhesion, and locomotion.* Proc Natl Acad Sci USA, 1995. **92**(20): p. 9161-5.

7. Goldmann, W.H. and D.E. Ingber, *Intact vinculin protein is required for control of cell shape, cell mechanics, and rac-dependent lamellipodia formation.* Biochem Biophys Res Commun, 2002. **290**(2): p. 749-55.

8. Rodriguez Fernandez, J.L., et al., *Suppression of vinculin expression by antisense transfection confers changes in cell morphology, motility, and anchorage-dependent growth of 3T3 cells.* J Cell Biol, 1993. **122**(6): p. 1285-94.

9. Subauste, M.C., et al., *Vinculin modulation of paxillin-FAK interactions regulates ERK to control survival and motility.* J Cell Biol, 2004. **165**(3): p. 371-81.

10. Xu, W., J.L. Coll, and E.D. Adamson, *Rescue of the mutant phenotype by reexpression of full-length vinculin in null F9 cells; effects on cell locomotion by domain deleted vinculin.* J Cell Sci, 1998. **111 (Pt 11)**: p. 1535-44.

11. Rodriguez Fernandez, J.L., et al., *Suppression of tumorigenicity in transformed cells after transfection with vinculin cDNA.* J Cell Biol, 1992. **119**(2): p. 427-38.

12. Vasile, V.C., et al., *Obstructive hypertrophic cardiomyopathy is associated with reduced expression of vinculin in the intercalated disc.* Biochem Biophys Res Commun, 2006. **349**(2): p. 709-15.

13. Vasile, V.C., et al., *A missense mutation in a ubiquitously expressed protein, vinculin, confers susceptibility to hypertrophic cardiomyopathy.* Biochem Biophys Res Commun, 2006. **345**(3): p. 998-1003.

14. Vasile, V.C., et al., *Identification of a metavinculin missense mutation, R975W, associated with both hypertrophic and dilated cardiomyopathy.* Mol Genet Metab, 2006. **87**(2): p. 169-74.

15. Ziegler, W.H., R.C. Liddington, and D.R. Critchley, *The structure and regulation of vinculin.* Trends Cell Biol, 2006. **16**(9): p. 453-60.

16. DeMali, K.A., C.A. Barlow, and K. Burridge, *Recruitment of the Arp2/3 complex to vinculin: coupling membrane protrusion to matrix adhesion.* J Cell Biol, 2002. **159**(5): p. 881-91.

17. Johnson, R.P. and S.W. Craig, *An intramolecular association between the head and tail domains of vinculin modulates talin binding.* J Biol Chem, 1994. **269**(17): p. 12611-9.

18. Johnson, R.P. and S.W. Craig, *The carboxy-terminal tail domain of vinculin contains a cryptic binding site for acidic phospholipids.* Biochem Biophys Res Commun, 1995. **210**(1): p. 159-64.

19. Johnson, R.P. and S.W. Craig, *F-actin binding site masked by the intramolecular association of vinculin head and tail domains.* Nature, 1995. **373**(6511): p. 261-4.

20. Miller, G.J., S.D. Dunn, and E.H. Ball, *Interaction of the N- and C-terminal domains of vinculin. Characterization and mapping studies.* J Biol Chem, 2001. **276**(15): p. 11729-34.

21. Weekes, J., S.T. Barry, and D.R. Critchley, *Acidic phospholipids inhibit the intramolecular association between the N- and C-terminal regions of vinculin, exposing actin-binding and protein kinase C phosphorylation sites.* Biochem J, 1996. **314**(Pt 3): p. 827-32.

22. Ziegler, W.H., et al., *A lipid-regulated docking site on vinculin for protein kinase C.* J Biol Chem, 2002. **277**(9): p. 7396-404.

23. Chen, H., D.M. Choudhury, and S.W. Craig, *Coincidence of actin filaments and talin is required to activate vinculin.* J Biol Chem, 2006. **281**(52): p. 40389-98.

24. Chen, H., et al., *Spatial distribution and functional significance of activated vinculin in living cells.* J Cell Biol, 2005. **169**(3): p. 459-70.

25. Bakolitsa, C., et al., *Structural basis for vinculin activation at sites of cell adhesion.* Nature, 2004. **430**(6999): p. 583-6.

26. Bakolitsa, C., et al., *Crystal structure of the vinculin tail suggests a pathway for activation.* Cell, 1999. **99**(6): p. 603-13.

27. Borgon, R.A., et al., *Crystal structure of human vinculin.* Structure (Camb), 2004. **12**(7): p. 1189-97.

28. Chandrasekar, I., et al., *Vinculin acts as a sensor in lipid regulation of adhesion-site turnover.* J Cell Sci, 2005. **118**(Pt 7): p. 1461-72.

29. Cohen, D.M., et al., *A conformational switch in vinculin drives formation and dynamics of a talin-vinculin complex at focal adhesions.* J Biol Chem, 2006. **281**(23): p. 16006-15.

30. Izard, T., et al., *Vinculin activation by talin through helical bundle conversion.* Nature, 2004. **427**(6970): p. 171-175.

31. Janssen, M.E., et al., *Three-dimensional structure of vinculin bound to actin filaments.* Mol Cell, 2006. **21**(2): p. 271-81.

32. Johnson, R.P. and S.W. Craig, *Actin activates a cryptic dimerization potential of the vinculin tail domain.* J Biol Chem, 2000. **275**(1): p. 95-105.

33. Miller, G.J. and E.H. Ball, *Conformational change in the vinculin C-terminal depends on a critical histidine residue (His-906).* J Biol Chem, 2001. **276**(31): p. 28829-34.

34. Huttelmaier, S., et al., *The interaction of the cell-contact proteins VASP and vinculin is regulated by phosphatidylinositol-4,5-bisphosphate.* Curr Biol, 1998. **8**(9): p. 479-88.

35. Saunders, R.M., et al., *Role of vinculin in regulating focal adhesion turnover.* Eur J Cell Biol, 2006. **85**(6): p. 487-500.

36. Johnson, R.P., et al., *A conserved motif in the tail domain of vinculin mediates association with and insertion into acidic phospholipid bilayers.* Biochemistry, 1998. **37**(28): p. 10211-22.

37. van Meer, G., D.R. Voelker, and G.W. Feigenson, *Membrane lipids: where they are and how they behave.* Nat Rev Mol Cell Biol, 2008. **9**(2): p. 112-24.

38. Vance, J.E. and R. Steenbergen, *Metabolism and functions of phosphatidylserine.* Prog Lipid Res, 2005. **44**(4): p. 207-34.

39. Marquez, M.G., et al., *Membrane Lipid Composition Plays a Central Role in the Maintenance of Epithelial Cell Adhesion to the Extracellular Matrix.* Lipids, 2008.

40. Raucher, D., et al., *Phosphatidylinositol 4,5-bisphosphate functions as a second messenger that regulates cytoskeleton-plasma membrane adhesion.* Cell, 2000. **100**(2): p. 221-8.

41. Yin, H.L. and P.A. Janmey, *Phosphoinositide regulation of the actin cytoskeleton.* Annu Rev Physiol, 2003. **65**: p. 761-89.